NOTE TO USERS

This reproduction is the best copy available.

uOttawa

L'Université canadienne
Canada's university

FACULTÉ DES ÉTUDES SUPÉRIEURES ET POSTOCTORALES

uOttawa

L'Université canadienne
Canada's university

FACULTY OF GRADUATE AND POSDOCTORAL STUDIES

Wendy Campbell

AUTEUR DE LA THÈSE / AUTHOR OF THESIS

M.Sc. (Chemistry)

GRADE / DEGREE

Department of Chemistry

FACULTÉ, ÉCOLE, DÉPARTEMENT / FACULTY, SCHOOL, DEPARTMENT

Novel Sulphur Linked AFGP Analogues:
Synthesis and Evaluation of Antifreeze Activity

TITRE DE LA THÈSE / TITLE OF THESIS

Robert Ben

DIRECTEUR (DIRECTRICE) DE LA THÈSE / THESIS SUPERVISOR

CO-DIRECTEUR (CO-DIRECTRICE) DE LA THÈSE / THESIS CO-SUPERVISOR

Christopher Boddy

John Pezacki

Gary W. Slater

Le Doyen de la Faculté des études supérieures et postdoctorales / Dean of the Faculty of Graduate and Postdoctoral Studies

Novel Sulphur-Linked AFGP Analogues:

Synthesis and Evaluation of Antifreeze Activity

By

Wendy Campbell

Thesis submitted to the

Faculty of Graduate and Postdoctoral Studies

University of Ottawa

In partial fulfillment of the requirements for the M.Sc degree

In the Ottawa-Carleton Chemistry Institute

Candidate	Supervisor
Wendy Campbell	Professor Robert Ben

Your file Votre référence
ISBN: 978-0-494-65524-5
Our file Notre référence
ISBN: 978-0-494-65524-5

Abstract

Antifreeze Glycoproteins (AFGPs) are peptide based compounds found in various organisms. They are a subclass of Biological antifreezes which are especially important for fish that live in polar waters; they inhibit the growth of ice and are thus keys to the survival of these organisms. The mechanism by which these compounds inhibit ice growth is regarded as absorption-inhibition at the macromolecular level. However the mechanism of action on the molecular level is widely debated among researchers.

The Ben lab has been designing AFGP analogues possessing enhanced chemical stability and biological activity for the purpose of structure activity studies. One of the most stable and potent analogues are the C-linked AFGP analogues. To improve our understanding of the effect of the nature of the atom at the anomeric position, a series of analogues possessing a sulphur atom at that position have been synthesized. The requisite glycosylated building blocks were synthesized via a modified protocol developed by Chi-Huey Wong and coworkers. The resulting building blocks were then assembled into antifreeze glycoprotein analogues using an automated solid phase synthesizer.

These analogues were evaluated for antifreeze-specific activity; recrystallization inhibition (RI), thermal hysteresis (TH) and dynamic ice shaping (DIS). None of the analogues showed thermal hysteresis activity and one showed weak dynamic ice shaping properties. The results from the IRI assay showed that the substitution of an electronegative atom at the anomeric position greatly reduces IRI activity. This follows a trend that was seen previously where the substitution of oxygen at the anomeric position also results in loss of activity. These results suggest that an anomeric carbon is necessary for optimal IRI activity within these systems and that is quite likely that the anomeric effect plays an important role in the loss of activity seen

when an electronegative atom is present. These results are outlined in this thesis and provide us with important information towards a unified understanding of the mechanism of action of these compounds.

Acknowledgements

First I would like to thank my supervisor Dr. Robert Ben for giving me this opportunity to further my studies. Thank you for your support and guidance you have given me over the past two years and for believing in my abilities when I was in doubt. Thank you for all the knowledge that you have imparted, I was very fortunate to have had you as a supervisor.

I would like to thank each and every member of the Ben-Fallis lab, you have all made my time here worthwhile. To Gloria and Sandy thanks for all the times spent studying in the library, doing problems and complaining about group meeting because we hate problem sets. Jenn I am forever indebted to you. Thank you for the time you took to tutor me. I will never forget the pKa session, I am pro now all because of you. To Matt, John,Pawel, Roger and Mike thanks for all the help with my chemistry. You guys were always there to answer any questions I may have had. To Taz, I really enjoyed sharing my fumehood with you over the summer, I had a blast; the things we would talk about! To Tal, my sister from another mother I loved our "itis" conversations my "armani" friend. To Liz, u always manage to make me smile, thanks for that and by the way the cd you got me for Christmas was very good. To Jackie, thank you for all the time and effort you invested into proof reading my thesis. I appreciate it very much. To Chantelle and Robyn I enjoyed having you guys in the lab. I will take a special memory of each and everyone one of you with me.

I am also thankful to my mother for believing in me and always encouraging. Special thanks to my forever friend Kemoye, always there for me no matter the circumstance. Without your love,support and help this would not have been possible.

Table of Contents

List of Figures

List of Schemes

List of Graphs

List of Tables

List of Abbreviations

Ac	Acetyl
AFPs	Antifreeze proteins
AFGPs	Antifreeze glycoproteins
Ala	Alanine
Asn	Asparagine
Boc	*tert*- Butyloxycarbonyl
d	doublet
DCM	Dichloromethane
dd	doublet of doublets
DIPEA	Diisopropylethylamine
DIS	Dynamic ice shaping
DMAP	4-Dimethylamino pyridine
DMF	*N.N*- Dimethyl formamide
dt	doublet of triplets
EDT	1,2 Ethanedithiol
ESI	Electrospray Ionisation
EtOAc	Ethylacetate
Et_2O	Diethyl ether
Fmoc	9-Fluorenylmethoxycarbonyl
Gal	Galactose
GalNHAc	*N*- Acetyl- galactosamine
Glc	Glucose
Gly	Glycine

HCTU	2 - (6 - Chloro - 1H - benzotriazole - 1 - yl) - 1,1,3,3 - tetramethylaminium hexafluorophosphate
Hz	Hertz
IR	Infrared
kDa	kiloDalton
Lys	Lysine
m	multiplet
M^+	Parent molecular ion
MALDI	Matrix-assisted laser desorption ionization
MeCN/ACN	Acetonitrile
MLGS	Mean Largest Grain Size
mOsmol	milliOsmolars
MS	Mass Spectrometry
PBS	Phosphate-buffered saline
ppm	Parts per million
Pro	Proline
RI	Recrystallization Inhibition
s	Singlet
SEM	Standard Error of Mean
SPPS	Solid Phase Peptide Synthesis
SAR	Structure Activity Relationship
t	Triplet
TFA	Trifluoroacetic Acid
TIS	Triisopropyl Silane

TH	Thermal Hysteresis
THF	Tetrahydrofuran

1.1 Biological Antifreezes

The ability of various organisms to exist in subzero temperatures without damage to their cells is an area of great interest in biology. Cold-blooded organisms such as fish are unable to modulate their internal temperature yet they are still able to survive in polar waters.[1] In 1953 Scholander and coworkers discovered that the bullhead fish (*Pagahenia borchgrevinki)* and the Antartic cold ice fish (*Dissostichus mawsonic);* fish that live in polar and subpolar areas of the ocean, have blood serum freezing temperature remarkably lower than the freezing temperatures of fish not adapted to the cold.[2,3] This was a bit surprising because the blood of marine fish is hypoosmotic relative to sea water so one would not expect fish to be able to survive at or near the freezing temperature of polar water. Even with the presence of colligative acting substances such as sodium chloride, urea and amino acids the observed magnitude of the freezing point depression is abnormally large.[4,5] These fish are able to lower their freezing temperature to approximately -2.1°C. Scholander found that the concentrations of the colligative acting substances in the fish serum are quite low, such that they would only contribute to a freezing point depression of approximately -0.86°C.[1] It was DeVries and coworkers that first attributed this additional -1°C difference to biological antifreezes (BAs).[6,7,8]

Biological antifreezes are not only found in fish but many other vertebrates, plants, fungi and bacteria.[9,10] These compounds are proteins (AFPs) and glycoproteins (AFGPs) that contribute very little to the osmotic pressure of the fish serum and lower the freezing temperature of fish serum in a non-colligative manner. Also as the freezing point is lowered the melting point remains unchanged. The antifreeze glycoproteins of polar fish are able to depress the freezing temperature of water about 500 times the amount that would have been expected based on the number of antifreeze glycoprotein molecules in solution.[11]

Initial comparative studies were done to compare the sole effect of a colligative solute; in this case sodium chloride, a biological antifreeze glycoprotein (AFGP), galactose and a protein (chicken lysozyme). The results are shown in the graph below. (Figure 1.1) [11] The graph illustrates that at low concentrations AFGP is slightly better than NaCl in lowering the freezing point of water. However when compared on a molar basis the activity of the AFGP is hundreds of times greater. This study suggests that AFGPs potent freezing point depression property is due to the unique glycopeptides structure as this property is absent when the carbohydrate and proteins are separated. The relationship between antifreeze activity and the concentration of the AFGPs seems to be non-linear, as the concentration of AFGP is increased so does its activity until a point of maximum activity is reached.

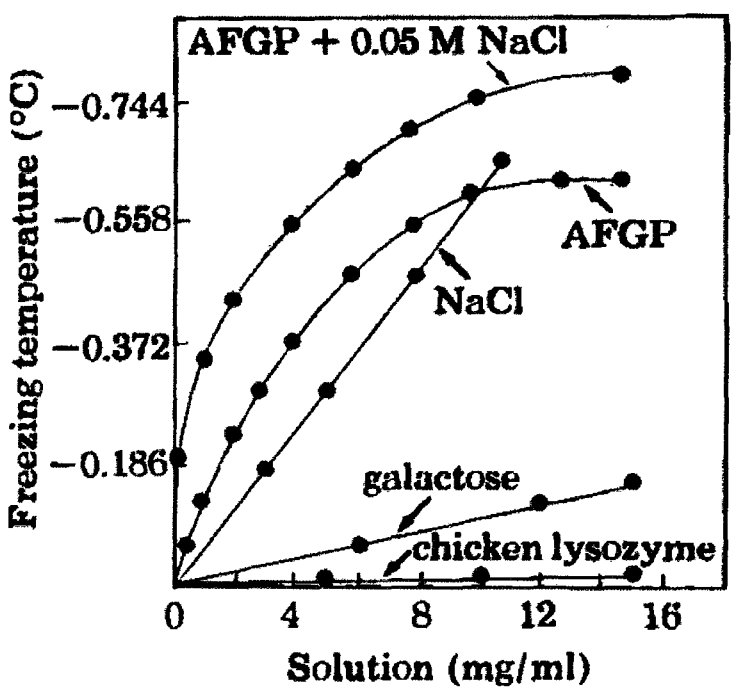

Figure 1.1 Illustration of freezing temperatures of chicken lysozyme, galactose, sodium, chloride, AFGPs and AFGP plus sodium chloride.

Finally the graph suggests that AFGPs and colligative acting substances such as sodium chloride do not function antagonistically but actually have an additive effect on the depression of freezing point.

1.2 Classification of Biological Antifreezes

Biological antifreezes are quite diverse in structure and are found in various organisms including fish, trees, plants and insects.[9,10,12] These compounds are usually found in the extracellular fluids of these organisms. In species of fish inhabiting polar regions biological antifreezes are synthesized in the liver, secreted into the blood and transported to all the fluid compartments within the fish except the brain and secretory vesicles.[13] In insects, biological antifreezes are located in the epidermal layer while in plants they are found in the xylem vessels, cell walls and intracellular spaces of tissues.[14] Even though biological antifreezes are found in such a diverse group of organisms and in varying locations, the biological function of the BAs is the same. BAs have been divided into two categories based upon their structures; and antifreeze proteins (AFPs) and carbohydrate containing antifreeze glycoproteins (AFGPs).

1.2.1 Antifreeze Proteins (AFPs)

Antifreeze proteins are biopolymers with diverse primary, secondary and tertiary structures and are divided into five subtypes. AFP Types I-IV are present in fish while Type V is found in insects. AFPs do not only come from various sources but differ in structure and size. (Figure 1.2)

Characteristic	Type I AFP	Type II AFP	Type III AFP	Type IV AFP	Type V AFP
Mass (kDa)	3.3 – 4.5	11.0-24.0	6.5-14.0	12.0	8.4-12.5
Properties	alanine rich, single α-helix	globular, random coil, cysteine rich	globular, β-sandwich 3° structure	glutamine rich, α-helical bundles	threonine and cysteine rich, disulfide bridges
Structure					
Source	Sculpin and right-eyed flounder 	sea raven, smelt, atlantic herring 	wolfish, eel pout and ocean pout 	longhorn sculpin 	yellow meal worm beetle 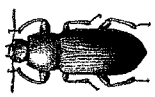

Figure 1.2 Characteristics of antifreeze proteins (adapted from Haymet).[15]

Type I AFPs were first reported by Duman and DeVries[16] and Hew and Yip[17]. The most extensively studied species comes from the winter flounder *Pseudopleuronectus americanus*. The molecular weight varies from 3.3 – 4.5 kDa. They consist of repeating amino acid sequences characterized by an alanine rich (65%) amphiphilic α-helix. Hew[17] has shown that the α-helix possesses a hydrophilic face with threonine hydroxyl functionalities oriented parallel to the longitudinal axis of the helix. It has been hypothesized that the hydrophilic face is involved in the binding of the protein to ice.[47,50]

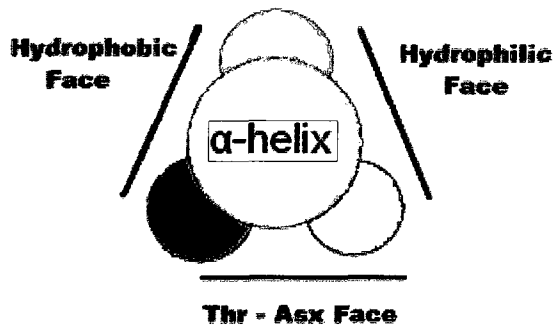

Figure 1.3 Cross-section of Type I AFP depicting the three faces of the α-helix; the threonine-aspartic acid/asparagine face, the hydrophobic face (consisting of alanine), and the hydrophilic face (comprised of threonine) which has been associated with ice binding.

Type II AFPs are found in Sea Raven, the Smelt and the Atlantic herring.[15] These AFPs are predominantly made of cysteine and alanine residues. They are globular proteins whose molecular weight ranges from 11.0 to 24.0 kDa.[18] The secondary structure of Type II AFPs is mainly random coil; however, other elements of the secondary structure include α-helices and β-pleated sheets. Sonnichsen has postulated that disulfide bridges between proximal cysteine residues are essential for antifreeze activity. These unique structural properties provide better TH activity than type I AFP.[19]

Type III AFPs have been isolated from ocean pout (*Macrozoarces americanus*) by Hew [20]*et al.* and are globular in structure. These proteins vary in size from 6.5-14.0 kDa and the primary structure is not dominated by any particular amino acid. The secondary structure of Type III AFPs consist of β-sheets arranged orthogonally, resulting in the formation of a 'β-sandwich' tertiary structure.[11]

Type IV AFPs were first isolated by Deng and coworkers from longhorn sculpin *(Myox ocephalus octodecimsponosis)*. These antifreezes are approximately 12 kDa and the tertiary structure of Type IV AFPs consists of a bundle of 4 α-helices.[21,22]

Type V AFPs have been isolated and characterized by Graham from the yellow meal-worm beetle *Tenebrio molitor.* These AFPs consist of 12 amino acid repeats with a cysteine moiety positioned at intervals no farther than 6 residues. These proteins vary in molecular weight from 8.4 kDa to 12.5 kDa.[23]

1.2.2 Antifreeze Glycoproteins (AFGPs)

AFGPs were first isolated and characterized by DeVries[24] in 1960 from the blood serum of Antarctic notothenioid *Pathogenia borchgrevinki* and *Dissostichus Mawsoni.* These compounds constitute a major fraction of the protein in the blood serum of the fish, and are also present in Arctic and north Atlantic cod. Unlike AFPs which are structurally diverse, AFGPs are structurally homologous. Each AFGP consists of a peptide backbone composed of alanine-alanine-threonine (Ala-Ala-Thr) repeats, with slight sequence variation, and a β-D-galactosyl-(1→3)-α-*N*-acetyl-D-galactosamine disaccharide fused to the threonine hydroxyl.[15] (Figure 1.3)

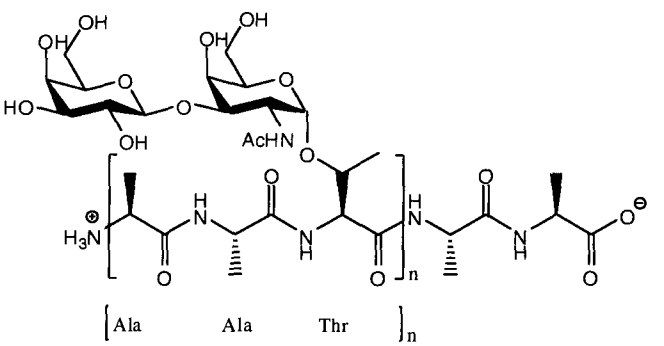

Figure 1.4: A typical structure of AFGP. The repeating unit (n) can vary from 4-50 AFGP8 is the smallest glycopeptide with n=4.

Notothenioid glycoproteins have been further divided into 8 classes (AFGP1-8) based upon their mobility in electrophoretic media (which is proportional to molecular weight).[25] The major difference is the number of tripeptide repeats which range from 4-50. The corresponding molecular weights range from 2.6kD to 33.7kD . On the basis of molecular weight, AFGP1-5 are classified as *large* while AFGP6-8 are classified as *small* (Figure 1.4)

Antifreeze	**Molecular Weight (kDa)**
AFGP1	33.7
AFGP2	28.8
AFGP3	21.5
AFGP4	15.5
AFGP5	10.5
AFGP6	5.0
AFGP7	3.8
AFGP8	**2.6**

Table 1.1 Classification of AFGPs on the basis of molecular weight

In some smaller AFGPs it has been found that some intermediate alanine residues can be substituted with proline (Figure 1.5a) and in *Eleginus gracilis* threonine can be replaced by L-arginine (Figure 1.5b)

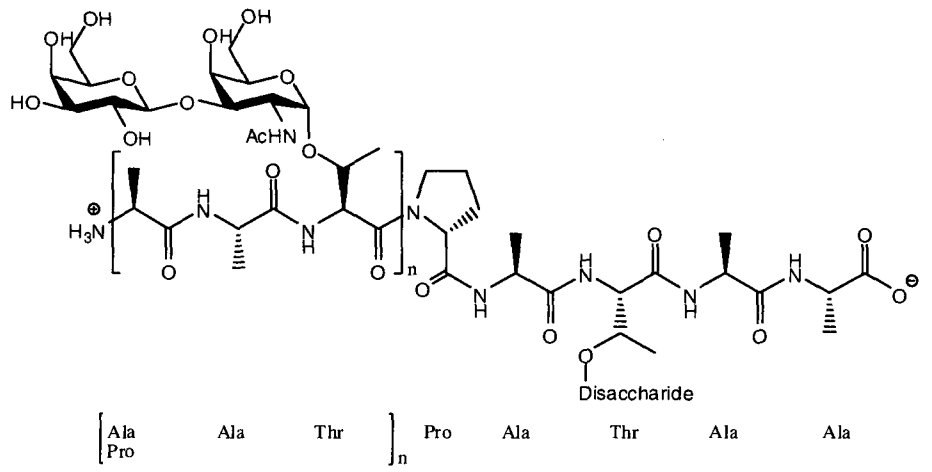

(a)

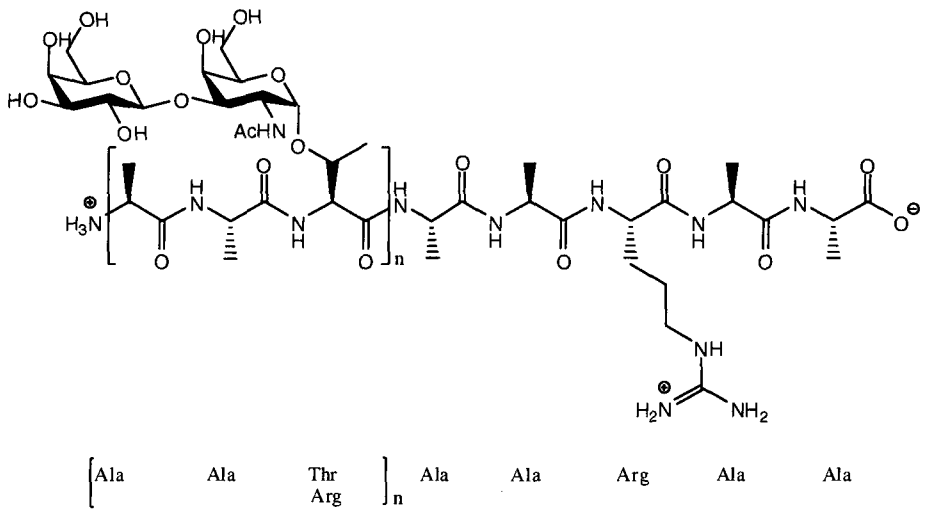

(b)

Figure 1.5: (a) AFGPs with L-proline that replaces L-alanine after L-threonine

(b) AFGPs with L-arginine that replaces L-threonine

It has been shown that each class of AFGPs comprises of multiple isoforms, for example class 6 AFGPs contains at least 14 different isoforms.[26] A protein isoform is a different form of

the same protein. These proteins are usually coded for by the same gene but alternate gene splicing or changes of single nucleotide bases within the gene.

Fletcher and colleagues have shown that larger AFGPs are more active in terms of antifreeze properties relative to the smaller molecules. However the most studied and synthesized AFGP is AFGP 8. This is mainly due to its small size and thus its relative ease of synthesis compared to its larger counterparts.

1.3 Antifreeze Properties

1.3.1 Thermal Hysteresis (TH)

It was mentioned earlier that biological antifreezes function in such a way as to depress the freezing temperature so as to prevent the freezing of the organism's plasma and subsequent death. However with the depression of freezing point there is no corresponding depression of melting point; the melting point remains the same.[15] The difference between the melting point (T_m) and the freezing temperature (T_f) is termed the thermal hysteretic gap. With pure water the freezing (T_f) and melting temperatures (T_m) are the same; 0°C. Also colligative acting substances such as salts do not exhibit this activity, salts such as sodium chloride depress the freezing temperature (T_f) and the melting point (T_m) to the same extent therefore no thermal hysteresis or thermal hysteretic gap.[27] The below graph (Figure 1.6)[11] illustrates that the melting temperature (T_m) is greater than the freezing temperature (T_f) in biological antifreezes whereas for sodium chloride and pure water there is no difference between the freezing temperature and the melting point.

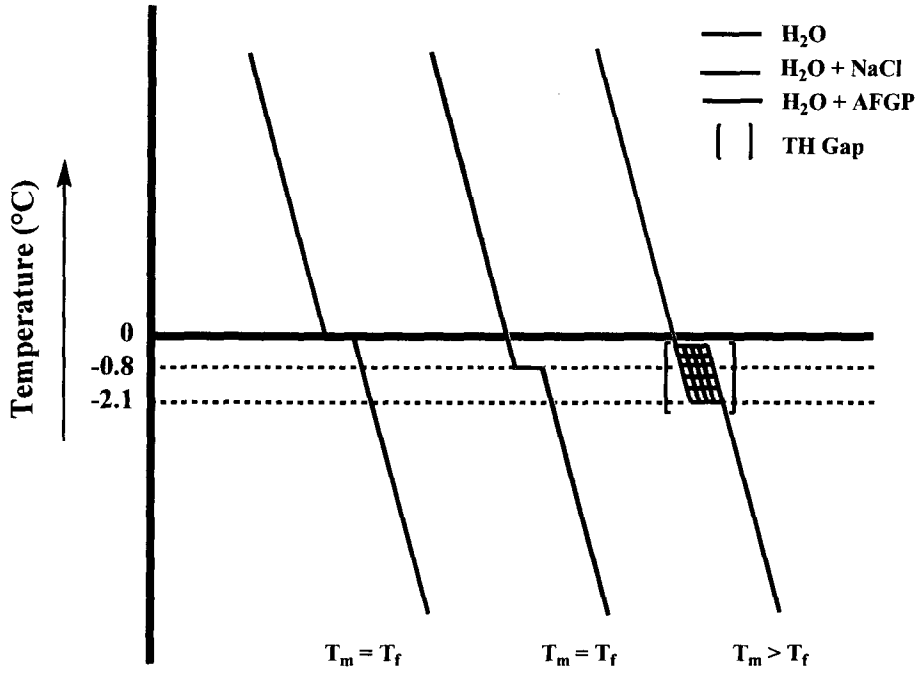

Figure 1.6: A schematic representation of thermal hysteresis. For reference, the profile of water is provided ($T_m = T_f = 0°C$).

Thermal hysteresis is not only indicative of antifreeze activity but can also be quantified. The magnitude of the TH gap is dependent upon the nature and concentration of the biological antifreeze. Higher molecular weight AFGPs (AFGP1-4) have been shown to exhibit greater TH activity than lower molecular weight AFGPs (AFGP6-8).[28] Also the magnitude of the TH gap varies from organism to organism. Generally speaking, AFPs exhibit greater TH activity than AFGPs.[29]

1.3.2 Dynamic Ice Shaping (DIS)

A second characteristic property of biological antifreezes is dynamic ice shaping. The growth of an ice crystal along certain planes is inhibited within the TH gap. This is a result of adsorption of biological antifreezes to specific prism faces of an ice crystal. Consequently, ice crystal habit or "morphology" is modified.[30] This change in the ice crystal's form is referred to as dynamic ice shaping.

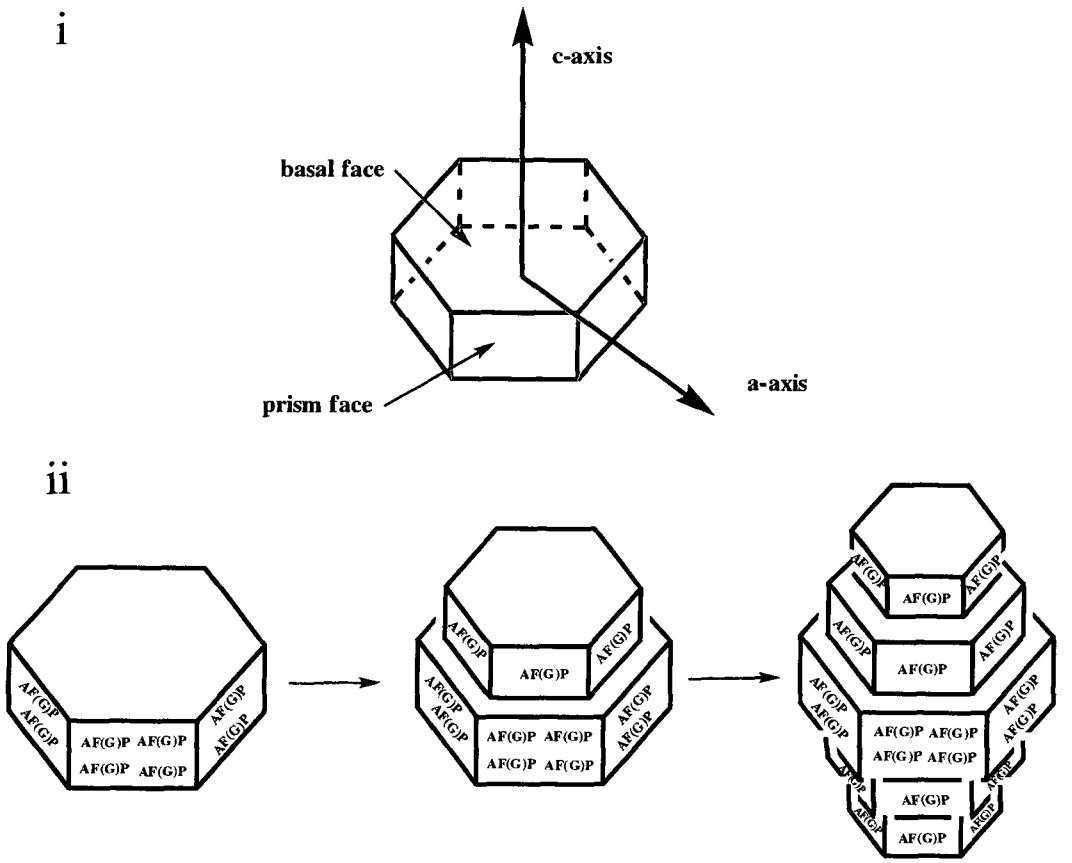

Figure 1.7 i) Hexagonal structure of an ice lattice unit and ii) Dynamic ice-shaping, resulting in the formation of a hexagonal bipyramidal crystal.[31]

In the absence of antifreezes, ice crystals grow perpendicular to the c-axis, enlarging the basal plane. In contrast, in the presence of biological antifreezes ice grows parallel to the c-axis (along the a-axis). The biological antifreezes selectively adsorb to the prism face preventing the normal perpendicular growth of ice crystals. The result is the growth of the crystals along the c-axis resulting in a hexagonal bipyramidal structure.[32,33,34,35] This occurs within the thermal hysteretic gap and is illustrated in the above diagram. (Figure 1.8)

As the temperature is decreased below the TH gap, the ice crystals begin to grow more rapidly and still along the c-axis resulting in the formation of ice spicules. These spicules are damaging to cells as they are able to puncture the cell membrane and lead to cell death. This property is attractive for applications such as cryosurgery.

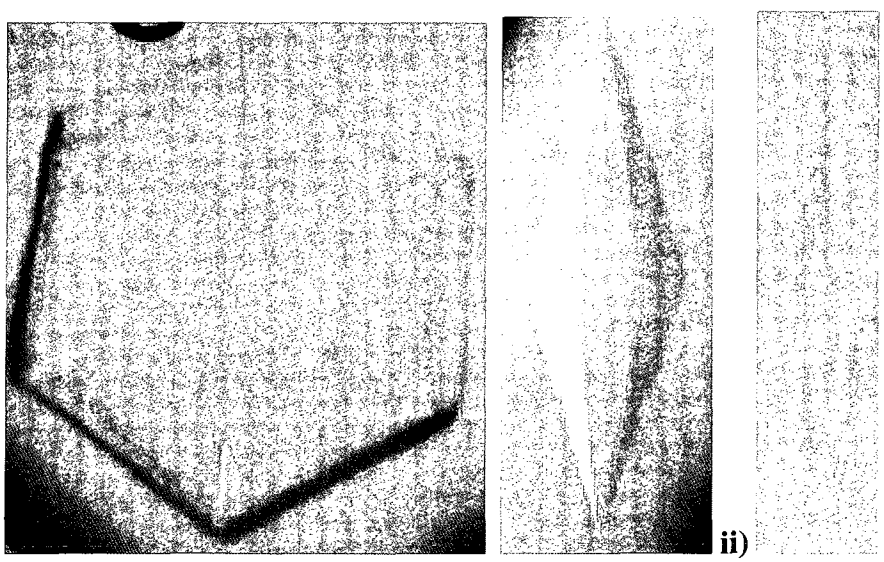

Figure 1.8: i) Ice crystals grown with AFP within the TH gap showing bipyramidal morphology (left; birds eye view, right; profile)[36,37] ii) Ice crystal grown with AFP below the TH gap, showing spiculation.[37]

1.3.3 Ice Recrystallization Inhibition (IRI)

In addition to thermal hysteresis (TH) and dynamic ice shaping (DIS), a third significant property of biological antifreezes is ice recrystallization inhibition (IRI). When a sample is frozen small ice crystals are generated. As the sample is warmed large ice crystals are formed at the expense of the smaller crystals. This phenomenon is referred to as ice recrystallization.[38] In this process, smaller grains are incorporated into larger grains to yield a sample with a larger mean grain size and fewer grains. This process is enthalpically driven as it minimizes the overall energy of the system.

There are two ways by which ice recrystallization can be inhibited; changing the boundary energy, or inhibiting the diffusion of water. AFGPs are thought to migrate to and adsorb to the surface of crystals at the ice/water interface and prevent ice boundary migration.[39] This can be seen when a solution of AFGP8 is frozen then thawed and the same is done for a PBS control solution. The solution containing AFGP8 shows crystals which are much smaller in size than those seen from the PBS control solution. AFGP8 prevents the formation of larger crystals from the smaller ones. Furthermore, biological antifreezes are able to achieve this at very low concentrations.[28,40]

Initially it was thought that both thermal hysteresis and ice recrystallization inhibition were due to the same process of adsorption onto the ice crystals.[41] Results from AFGP analogues synthesized in our lab and research published by Sidebottom[42] have demonstrated that the two properties are decoupled. Our lab is interested in the ice recrystallization inhibition property of biological antifreezes and not their thermal hysteretic properties.

1.4 Cell Membrane Stabilization

In addition to the above antifreeze properties biological antifreezes also posses the ability to stabilize cell membranes at low temperatures (non-freezing).[43,44] It has been reported that the phospholipid bilayer of cell membranes has a thermotropic phase transition as temperature is decreased. As the liquid-crystalline phase is converted into a gel phase the membrane becomes more permeable and cellular contents are leaked out.[45,46] Wu and Fletcher have suggested that biological antifreezes are able to bind to the cell membrane and prevent this leakage.[47]

1.5 Mechanism of Ice Growth Inhibition

1.5.1 At The Macroscopic Level:

Currently there are two mechanisms which have been theorized to explain the macroscopic mechanism of ice growth inhibition, a nucleation inhibition model and an adsorption-inhibition model. Freezing is the crystallisation of ice which occurs with super-cooled water. According to Hew and coworkers, in order for freezing to occur there has to be nucleation of an ice crystal. They theorize that the AFGPs lower the energy of the system by lowering the nucleation temperature. This increase in the nucleation barrier prevents the formation of a nucleus and thus prevents ice formation. [15, 48,49]

The second model is the adsorption-inhibition model advocated by Knight and DeVries[25.35] that suggests antifreezes bind to the growing ice surface preventing additional water molecules from adding to where the antifreeze has adsorbed. This results in ice growth between antifreeze adsorption sites only. As the temperature decreases the ice continues to grow but the ice front now has a high degree of surface curvature due to the binding of the biological antifreezes. The addition of water molecules to the now curved ice front is thermodynamically

unfavourable and this results in the freezing point depression. This phenomenon is known as the Kelvin Effect[50,51](Figure 1.11)

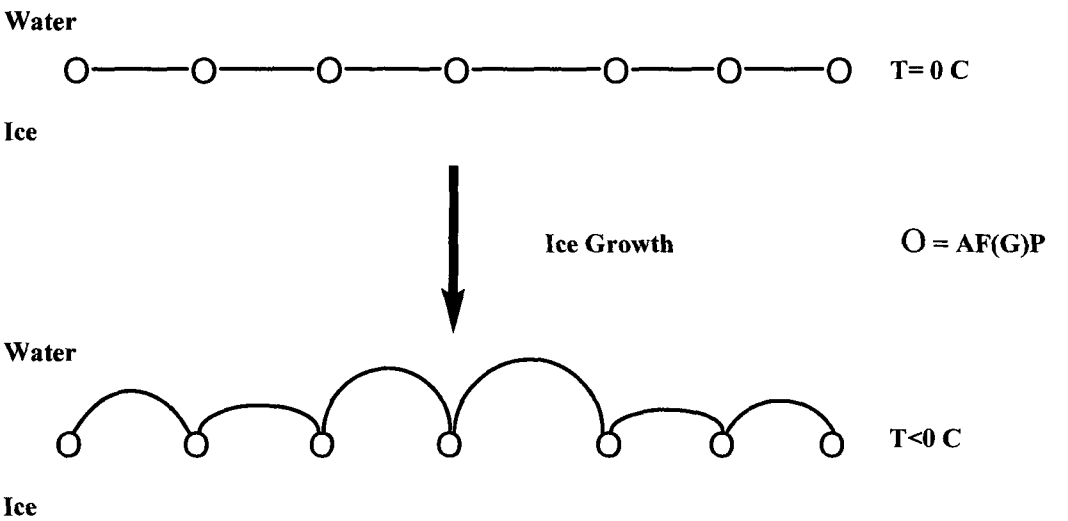

Figure 1.9 Schematic representation of the adsorption inhibition mechanism

Scientists have yet to agree on the driving force for the binding to ice in the adsorption-inhibition model. Knight and DeVries[35,44] are proponents of the irreversible binding concept which is supported by 3D models proposed by Knight. Kuroda[52] has suggested that this model is incorrect, and adsorption may be reversible. Wen and Laursen[53] have attempted to reconcile these conflicting views suggesting that antifreeze binding is concentration dependent. At low concentrations reversible adsorption occurs; however, at elevated glycoprotein concentrations, intermolecular interactions (van der Waals forces) between antifreezes dominate, resulting in greater binding affinity.

The two models described above seek to explain the ice binding affinity of AF(G)Ps on a macromolecular level and like the raging debate between the above two mechanisms there is also

a debate as to the mechanism at the molecular level.[37] Researchers are not agreed as to whether the AF(G)P- ice binding interaction is hydrophobic or hydrophilic.[54,55]

1.5.2 The Role of Hydrophilic Interactions in Binding to Ice

It was proposed that the hydroxyl groups of the disaccharide moiety are responsible for the ice-AFGP binding interaction by the formation of hydrogen bonds between AFGPs and the ice surface. Previous studies had shown that only two of the hydroxyl groups are in the correct conformation to form hydrogen bonds with the ice. So if each hydroxyl forms only one hydrogen bond with water then for an AFGP such as AFGP8, which consists of four glycosylated amino acid tripeptide units,only eight hydrogen bonds are possible, which is insufficient for the binding of the AFGP with the ice lattice.[35] A new revised mechanism was proposed by Knight and coworkers to account for the observed binding. They proposed that instead of the formation of one hydrogen bond with water, the hydroxyl groups of the disaccharide are actually incorporated within the ice lattice which would result in the ability of each AFGP 8 molecule to form a total of twenty-four hydrogen bonds. This model is more accepted than the previous hydrophilic model.[35] (Figure 1.12)

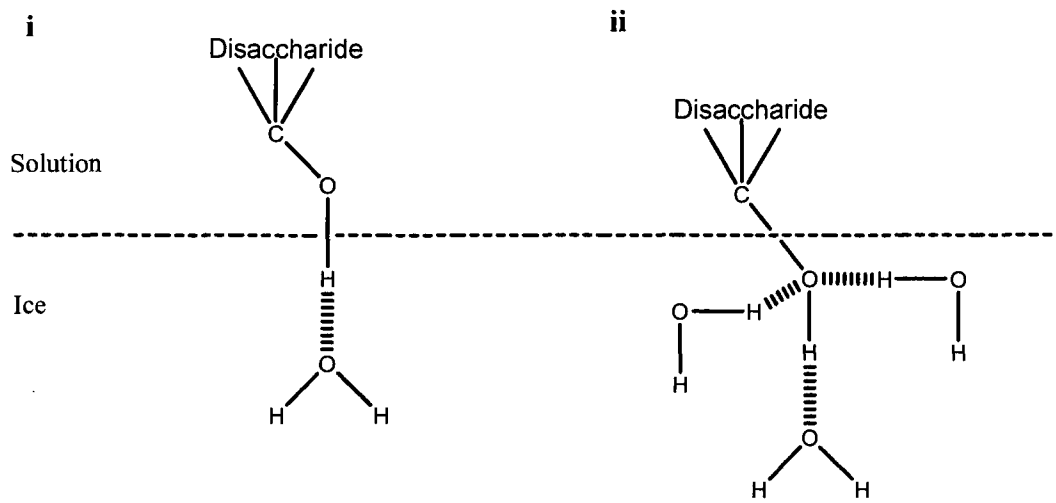

Figure 1.11: Hydrophilic interaction between the ice surface and AFGP8

(i)Hydrogen bonding with the ice surface

(ii)Hydrogen bonding interaction with the ice lattice

Devries[56] proposed a model explaining the binding of AFGP1. He proposed that the hydroxyl and carboxyl groups of various amino acids form hydrogen bonds with the prism face of ice crystals. This model was later revised by Wen and Laurensen[47] who suggested that the polar groups are within range of the oxygen atoms in the ice lattice and are therefore able to hydrogen bond. However this occurs at the pyramidal plane of the prism faces on the ice. (Figure 1.13)

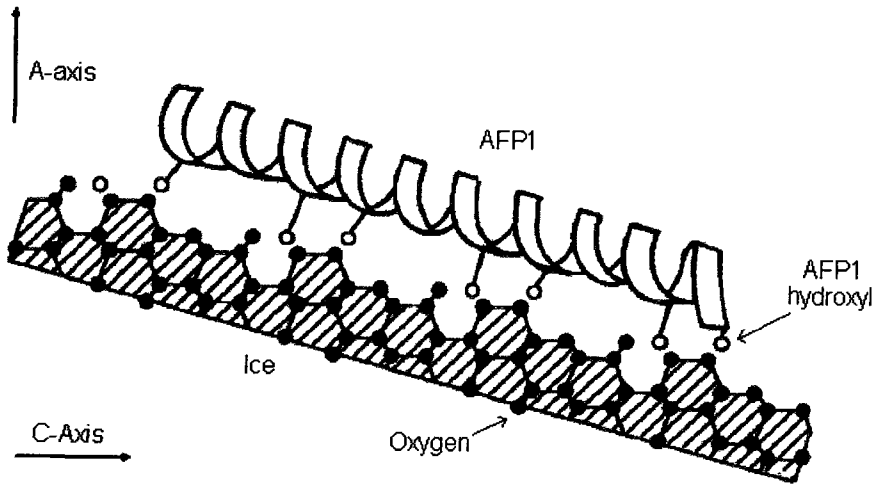

Figure 1.12 Revised model by Wen and Laurensen for hydrogen bonding for AFP1

This model is also supported by molecular modelling studies done by Madura and coworkers[57]. Their model suggests that polar groups of the amino acid side chains of AFP 1 are embedded in the ice crystal. (Figure 1.14)

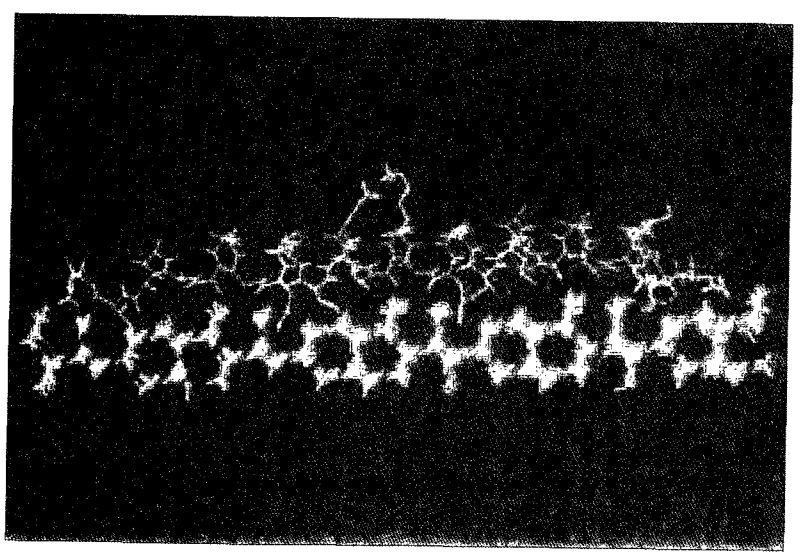

Figure 1.13 Molecular modeling by Madura of AFP1

1.5.3 The Proposed Role of the Hydrophobic Interactions in Binding to Ice

Structure activity studies were done on AFP 1 where the threonine residues were substituted with serine and valine. The results indicated that hydrophobic interactions do play some role in the binding of the AFP to ice.[39,47,58] For the analogue in which threonine was substituted with serine the TH activity was lost, meaning the interaction between the ice and the AFP was interrupted. Since serine has a hydroxyl group similar to that of threonine then the substitution would not disrupt any hydrogen bonds. Also for the analogue in which the threonine was substituted with valine there was only a small loss of TH activity. These results indicate the methyl group rather than the hydroxyl group is necessary for binding to ice and thus activity.

Structure activity relationship studies were also done by Nishimura [59]on AFGP8 and similar results were shown. When the threonine residues in AFGP8 were substituted by serine the result was a total loss of TH activity. Therefore one can conclude that the methyl group is quite important for binding and thus TH activity.

Structure activity relationship and molecular modelling seem to show that both hydrophobic and hydrophilic interactions are necessary for biological antifreeze and ice binding. However a unified molecular mechanism has yet to be proposed.

1.6 Applications of Biological Antifreezes

Biological antifreezes have unique properties that may potentially be important for use in many aspects of our lives.

One of the many potential applications of BAs involves using these compounds as cryopreservatives. Cryopreservation of cells and tissue has long been a challenge for scientists. The challenge lies in maintaining the quality and viability of cells and tissues during the freezing and eventual thawing processes. During the freezing process cells are damaged by intracellular ice formation which crushes the cells and creates an osmotic imbalance. Organs are not frozen to prevent this mechanical stress and cell death but are kept viable by hypothermic storage.[60] Cryopreservants such as DMSO and glycerol are able to keep cells in a super cooled state but do little to prevent the physical stress to cells caused by ice formation.[61] Vitrification is a possible solution to this problem. In this technique a concentrated solution of cryoprotectants is added to the sample prior to cooling, these cryoprotectants lower the freezing point and increase the viscosity of the sample. As the sample is cooled no crystallization occurs but an amorphous solid is formed.[62] One of the main disadvantages of this technique is the high concentration of cryopreservant that is used. These have toxic effects on the cells. Additionally vitrification does not work well with large volumes but is more suitable for small samples since the cooling rate is not uniform for large volumes[63]. So a way to overcome the above problems could be the use biological antifreezes or analogues of these compounds as cryoprotectants as these will protect and stabilize the cell membrane during cooling, inhibit ice growth during freezing and prevent ice recrystallization when thawing.[64]

Another potential but opposite application of biological antifreezes is their use in cryosurgery. Rubinsky and coworkers[56] found that freezing red blood cells in the presence of 40μg/ml of AFGps reduced cell survival. They surmised that this cell death is the result of the formation of the needle shaped ice crystals, which occurs when the temperature is lowered below the TH gap. The crystal spicules puncture the cell membranes causing the cells to die.

Cryosurgery is a procedure that takes advantage of the destructive effect that freezing has on cells. Rubinsky utilized this property along with the destructive effects of biological antifreezes to perform non-invasive ultrasound mediated cryosurgery.[56] In vivo testing was done using a solution of AFGP1. It was shown that when the solution was injected in a solid tumour almost 100% of the cancer cells were killed.[65,66] This is potentially one of the least invasive and cost effective methods for destroying cancer cells within the body.

A third application of the use of biological antifreezes is their use in the frozen food industry. Many foods are perishable and need to be frozen in order to maintain viability. However the freezing of foods such as meats and ice cream result in a loss of taste and texture. Goff and Regand[67] have shown that the addition of AFPs from winter wheat extract causes ice cream to retain its texture after being frozen. The use of biological antifreezes in food products has been approved by the American Food and Drug Administration.[68] This has been applied commercially by companies such as Breyers. These are placed in ice cream bars to maintain the texture of the product after freezing.

Biological antifreezes are a diverse class of molecules with varying properties and potential applications. The mechanism of action of these compounds has been a challenge for various researchers including members of the Ben lab. The Ben lab is interested in the cryoprotective properties of BAs. Over the years we have made great strides in the synthesis of these compounds and analogues. We have gained meaning and important information regarding how the structure of these compounds relates to their antifreeze activity. We are still lacking understanding in many areas so as we continue many new analogues will be synthesized and numerous structure activity relationship studies have been and will continue to be undertaken in hopes of elucidating the mechanism of action of these compounds. This work will help to realize

the many commercial, medical and industrial applications of rationally designed biological antifreezes.

References

[1] Scholander, P. F., VanDam, 1., Kanwisher, J. W., Hammel, H. T., Gordon, M. S. *J. Cell. Comp. Physiol.* **1957** 49:524

[2] Gordon, M. S., Amdur, B. H., Scholander, P. F. *Biol. Bull.* **1962** 122:52

[3] Scholander, P. F., Flagg, W., Walters, V., Irving, L. *Physiol. Zool.* **1953** 26:67

[4] DeVries, A. L., Wohlschlag, D. E. *Science* **1969** 163:1073

[5] Feeney, R. E.. *Am. Sci.* **1974** 62:712

[6] DeVries, A. L., Komatsu, S. K., Feeney,R. E. *J. Biol. Chem.* **1970** 245:2901

[7] Duman, J. G.. *Cryobiology* **1982** 19:613

[8] Tomchaney, A. P., Morris, J. P., Kang, S.H., Duman, J. G. *Biochemistry* **1982** 21:716

[9] Feeny, R.E., T.S. Burcham and Y. Yen . *Annu. Rev. Biophys. Biophys. Chem.* **1986** 15:59-78

[10] Tsvetkova, N. M., et. al. *Biophysical Journal.* **2002** 82:464-473

[11] Yeh, Y., Feeny, R. *Chem Rev.* **1996** 96:601

[12] Ben, R.N. *Chem BioChem.* **2001** 2:161-166

[13] O'Grady, S.M., Schrag, J.D., Raymond, J.A., Devries, A.L. *Exp. Zool.* **1982** 224:177

[14] Duman, J.G., Howarth, K.L., Tomchney, A., Patterson, J.L. *J. Comp. Biochem. Physiol.* **1982** 73: 543

[15] Harding, M.M., Anderberg, P.I., Haymet, A.D. *J. Eur. J. Biochem.* **2003** 270: 1381-1392

[16] Duman, J.G., Devries, A.L. *Nature* **1974** 247:237

[17] Hew, C. L., Yip, C.C. *Biochem. Biophys. Res. Commum.* **1976** 71:845

[18] Ewart, K. V., Fletcher, G. L. *Can. J. Zool.* **1990** 68:1652

[19] Sonnichsen, F.D., Sykes, B.D., Davies, P.L. *Protein Sci.* **1995** 4:460

[20] Hew, C.L., Slaughter, D.., Joshi, S.B., Fletcher, G.L., Annanthnarayanan, V.S. *J. Comp. Biochem Physiol* **1984** 155B:81

[21] Deng, G.J., Andrews, D.W. and Laursen, R.A. *FEBS Lett.* **1997** 402:17–20

[22] Deng, G. J. and Laursen, R. A. *Biochim. Biophys. Acta.* **1998** 1388:305–314

[23] Graham, L.A., Liou, Y-C., Walker, V. K. and Davies, P.L. *Nature.* **1997** 21:727-729

[24] DeVries, A. L., Komatsu, S.K., Feeny, R.E. *J. Biol Chem.* **1970** 245:2901-2908

[25] Raymond, J. A., DeVries, A. L., *Cryobiology* **1972** 9:541

[26] . Wu,Y., Banoub, J., Goddard, S.V., Kao, M.H. and Fletcher, G.L. *Comp. Biochem. Physiol. B.* **2001** 128: 265–273

[27]Fletcher, G. L., Hew. C.L., Devries, P. L. *Ann. Rev. Physiol.* **2001** 63:359

[28] Knight, C.A., DeVries, A.L. and Oolman, L.D. *Nature.* **1984** 308:295–296

[29] Kao, M.H., Fletcher, G.L., Wang, N.C., and Hew, C.L. *Can. J. Zool.* **1986** 64:578–582

[30] Yang, D. S., Sax, M., Chakarbartty, A., Hew, C. L. *Nature* **1988** 333:232-237

[31] Tomimatsu, Y., Schere, J., Yeh, Y., Feeny, R.E. *J Biol Chem.* **1976** 251:2290-2298

[32] DeVries, A.L., *Science*, **1971** 172:1152-1155

[33] Hew, C.L., Yang, S.C.D. *Eur. J. Biochem.* **1992** 203:42

[34] Knight, C.A., Cheng, C.C., and DeVries, A.L. *J. Biophys.***1991** 59:409-418

[35] Knight, C.A., Driggers, E., and DeVries, A.L. *J. Biophys.* **1993** 64:252-259

[36] Wathen, B., Kuiper, M.J., Walker, V.K. and Jia, Z. *Can. J. Phys.* **2003** 81:39-45

[37] Haymet, A.D.J., Ward, L.G. and Harding, M.M. *FEBS Lett.* **2001** 491:285-288

[38] Kuiper, M.J., Davies, P.L., Walker, V.K. *Biophys. J.* **2001** 81:3560-3565

[39] Knight, C.A., Wen, D.-Y. and Laursen, R.A. *Cryobiology.* **1995** *32*:23-34

[40] Knight, C.A., Hallet, J. and DeVries, A.L. *Cryobiology.* **1988** 25:55-60

[41] Knight, C.A.; *Nature* **2000** 406:250

[42] Sidebottom, C., Buckley, S., Twigg, S., Telford, J., Warrall, D., Hubbard, R., Lillford, P., Holt, C., McArthur, A. Jarman, C., and Pudney, S.P. *Nature.* **2000** 406:256-258

[43] Rubinsky, B.A., Arav, A., Mattiolo, M., Devries, A.L. *Biophys. Res. Comm.* **1990** 173:1369-1374

[44] Tablin, F., Oliver, A. E., Walker, N.J., Crown, L.M., Crown, J.H. *J Cell Physiol.* **1996** 168:305-318

[45] Quinn, P.J. *Cryobiology.* **1985** 22:128

[46] Clerc, S.G., Thompson, T.E. *Biophys. J.* **1995** 68:2323

[47] Wu, Y.' Fletcher, G.L. *Biochem. Biophys. Acta* **2000**:11:1524

[48] Wilson, P. W., Leader, J. P. *Biophys. J.* **1995** *68*:2098

[49] Hall, D.G., Lips, A. *Langmuir.* **1999** 15:1905

[50] Bouvet, V., Ben, R. *Cell Biochemistry and Biophysics.* **2003** 39:133

[51] Wilson, P.W. *Cryoletters.* **1993** 14:31-36

[52] Kuroda, T. *Proc. 4th Topical Conference on Crystal Growth Mechanism. Hokkaido Press.* **1991** p157

[53] Wen, D. and Laursen, R.A. *J. Biophys.* **1992** *63*1659.

[54] Chao, H., Houston, M.E., Hodges, R.S., Key, C.M., Sykes, B.D., Loewen, M.C., Davies, P.L., Sonnichsen, F.D. *Biochemistry.* **1997** 36:14652-14660

[55] Wierzbicki, A., Taylor, M.S., Knight, C.A., Madura, J.D, Harrington, C.S., Sikes, C.S. *Biophys. J.* **1996** 71:8-18

[56] DeVries, A.L. *Rev. Physiol.* **1983** 45:245-260

[57] Madura, J.D., et al. *J. Am. Chem. Soc.* **1994** 116:417-418

[58] Zhang, W. & Laurensen, R. A. *J. Biol. Chem.* **1998** 273:34806-34812

[59] Nishimura, *Angew. Chem Intl. Ed.* **2004** 21: 856-862

[60] Peg, D.E. *Semin Reprod. Med.* **2002** 20:5-13

[61] Baust, J.M., van Buskirk, R., *In Vitro Cell Dev. Biol.* **2000**: 36:262

[62] Meryman, H.T. *Crobiology.* **1984** 21:407-426

[63] Rubinski, B., Arav, B.A., DeVries, A.L. *Cryoletters.* **1991** 12:93-106

[64] Wang, J.H. *Cryobiology.* **2000** 41:1-9

[65] Koushafar, H., Rubinsky, B. *Urology.* **1997** 49:421

[66] Pham, L., Dahiya, R., Rubinsky, B. *Cryosurgery.* **1999** 38:169

[67] Goff, H.D. and Regand, A. *Journal of Dairy Science.* **2006** 89:49-57

[68] Rulis, A.M. *Agency Response Letter.* U.S. Food and Drug Administration, Centre for Food Safety and Applied Nutritions, Office of Food Additive Safety. **2003**. available from; http://www.cfsan.fda.gov/~rdb/opa-g117.html

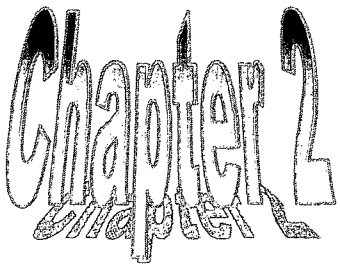

2.1 Synthesis of AFGPs and AFGP analogues

Glycopeptides are important molecules for both chemists and biologists. For chemists they are challenging and interesting synthetic targets while for biologists they are secondary metabolites with diverse structures and functions.[1] Determination of glycopeptide structure and conformation is particularly challenging and it is often very difficult to understand how the structure of a glycopeptide relates to its particular function in vivo. Glycoproteins have been shown to have numerous and diverse functions including the ability to function as modulators for cell-cell communication which is necessary in processes such as intra- and intercellular trafficking, receptor binding and signalling.[2,3] Naturally occurring glycopeptides are usually linked by an N or O-glycosidic linkage between the carbohydrate and polypeptide backbone.[4] The structure of native antifreeze glycoprotein falls into the latter category where an L-threonine amino acid is O-linked to a dissacharide moiety.

As mentioned in the previous chapter, antifreeze glycoproteins are naturally found in the plasma of teleost fish that live in subzero temperatures.[5] The isolation and purification of these proteins are quite time and cost intensive; as a result the synthesis of these compounds and perhaps simpler analogues would be far more suited for subsequent commercial applications of these antifreeze glycoproteins. There are several isoforms of AFGPs with the smallest being AFGP 8 where n=4. The structure is shown below in (Figure 2.1).

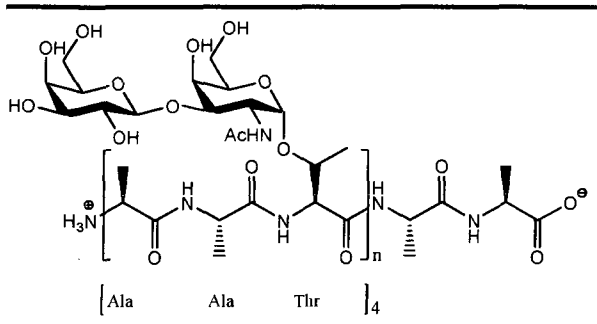

Figure 2.1: A typical structure of AFGP. The repeating unit (n) can vary from 4-55. AFGP8 is the smallest glycopeptide with n=4.

The native AFGP consists of three main domains; the carbohydrate moiety, the side chain linker and finally the peptide backbone. The Ben group has synthesized and tested numerous analogues possessing modifications in one or more of these regions. These analogues have been tested for the three properties that antifreeze glygoproteins usually exhibit, namely; thermal hysteresis (TH), dynamic ice shaping (DIS) and ice recrystallization-inhibition (IRI). These three properties were extensively explained in the previous chapter. If one recalls thermal hysteresis and dynamic ice shaping have a destructive effect on cells and are best suited for applications such as cryosurgery.[6,7,8] The third property, ice recrystallization inhibition actually has a protective effect. It allows for the formation of smaller ice crystals at the expense of larger ones which results in the protection and increased viability of cells when frozen and kept at low temperatures.[9,10] We in the Ben lab are interested in the cryoprotective properties of biological antifreezes rather than their possible destructive effect on living cells.

2.1.1 Second Generation C-linked Analogues

One of our most potent analogues; an analogue that showed marked ice recrystallization inhibition activity but no thermal hysteresis or dynamic ice shaping properties was the C-serine analogue (**2a**). There are several structural features of this analogue that differ greatly from the native structure. (Figure 2.2) Firstly, a galactose moiety replaces the native disaccharide sub unit. Secondly, the linker region is changed from an O to a C-glycosidic linkage. Finally, the peptide backbone is changed to $[Ser\text{-}Gly\text{-}Gly]_4$. Figure 2.2 is a schematic representation of these differences.

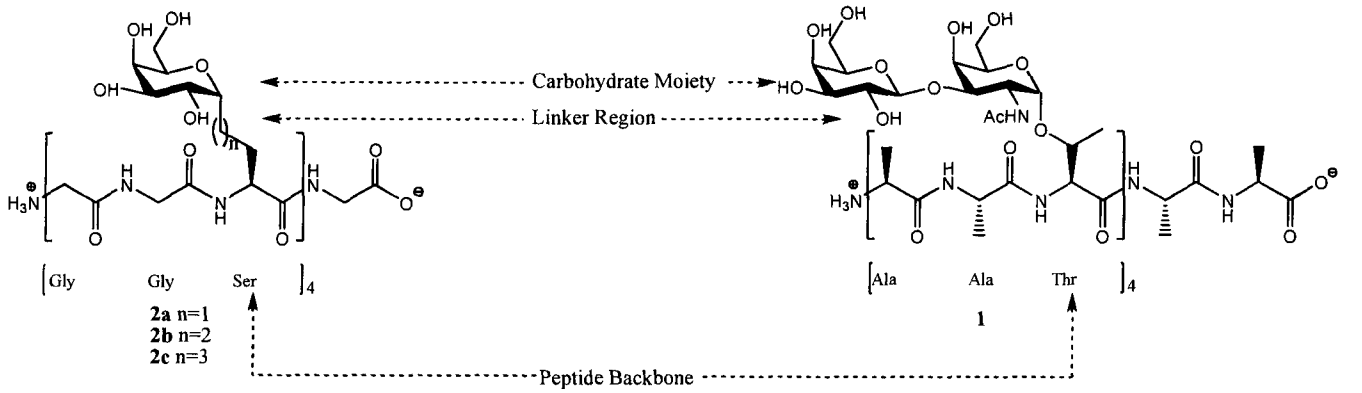

Figure 2.2: Several of our second generation C-linked analogues

Analogues **2a, 2b** and **2c** differ in the number of methylene units in the linker region. Analogue **2a** has two methylene units, **2b** has three and **2c** has four. However only the C-Serine analogue **2a** showed potent recrystallization inhibition activity and remains our best analogue to date.[11]

It was concluded from these results that the linker length is very important and has an optimum length of two methylene units from the peptide backbone to the sugar moiety. Extending the linker modifies the orientation of the sugar which results in a marked decrease in ice recrystallization inhibition activity. (Graph 2.1)

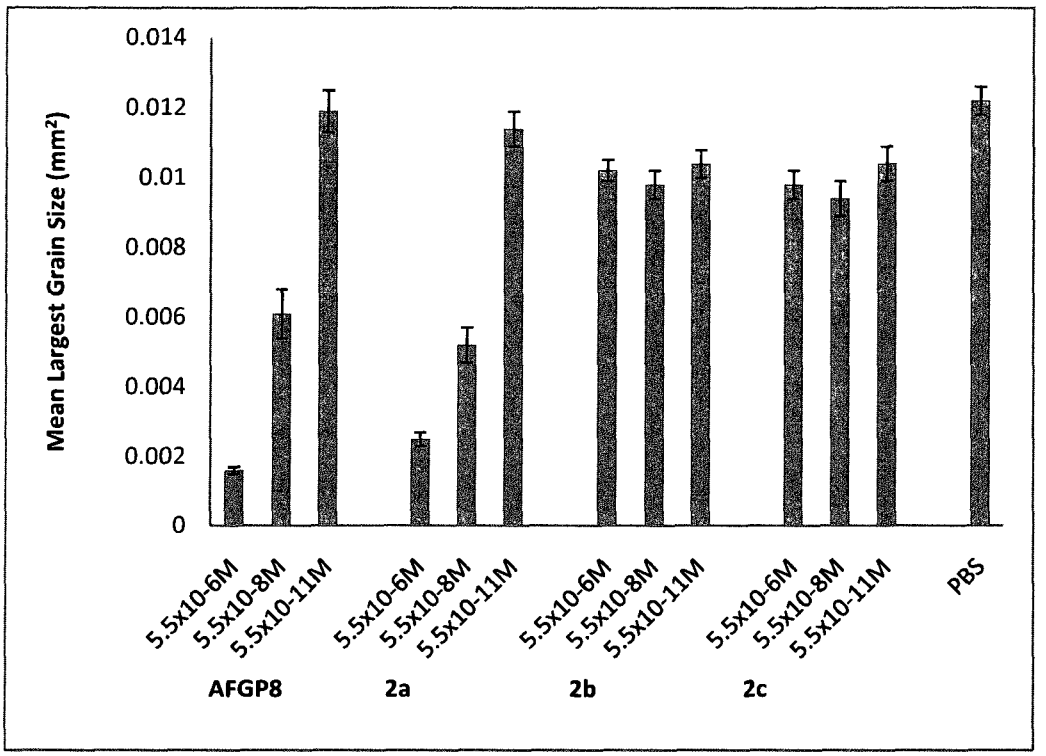

Graph 2.1: Ice recrystallization inhibition activities of 2nd generation C-linked analogues.

Previous SAR studies conducted by Nishimura et al. have indicated that an *N*-acetyl at the C-2 position of O-linked analogues was important for antifreeze activity namely thermal hysteresis; these analogues were not tested for ice recrystallization inhibition.[12] Therefore a C-serine analogue linked to a galactose moiety with an *N*-acetyl group at C-2 (**2d**) was synthesized and tested for TH, DIS and IRI. It was observed that analogue **2d** had reduced IRI activity, 31% less relative to the activity shown by the C-serine analogue (**2a**), and this analogue displayed dynamic ice shaping but no thermal hysteresis activity. [11]

2.1.2 O-Linked Analogues

O-Glycosidic bonds are known to be sensitive under enzymatic, acidic and basic conditions. Under acidic conditions the oxygen on the serine side chain is protonated which then drives the

formation of an oxocarbenium ion and thus the dissociation of the glycosidic bond. The O-glycosidic bond is also cleaved under basic conditions. In this reaction sequence the α-hydrogen is deprotonated resulting in the formation of the alkene and the cleavage of the glycosidic bond. (Scheme 2.1)[13,14]

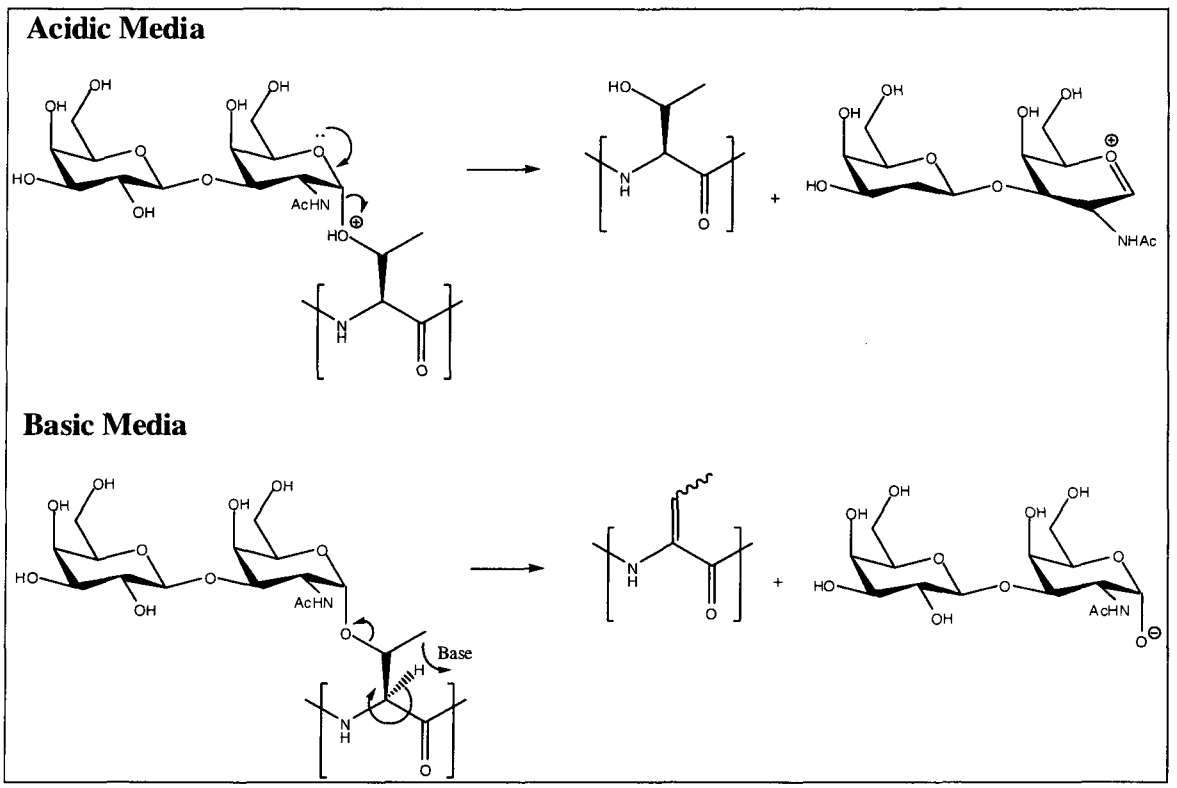

Scheme2.1: Hydrolysis of O-Glycosidic bonds under acidic and basic conditions

Our lab was able to synthesize various O-linked analogues through a mild synthetic strategy that prevented the hydrolysis of the glycosidic bond. Various analogues were synthesized including **3a** and **4a.** These analogues were tested for antifreeze activity and the results from analogue **3a** were compared to those from the C-linked analogue **2a**. No dynamic ice shaping or thermal hysteresis were observed for either analogue, however there was a marked loss of ice recrystallization inhibition for **3a** compared to the C-linked counterpart **2a**. Figure 2.3 compares the ice recrystallization inhibition of analogues **2a** and **3a.**[15]

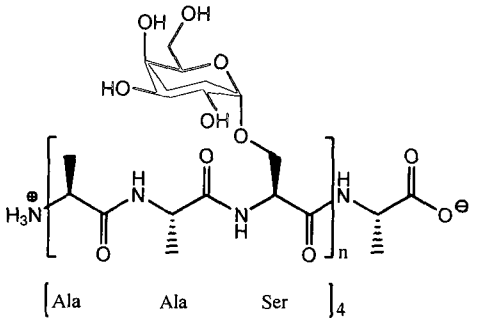

3a

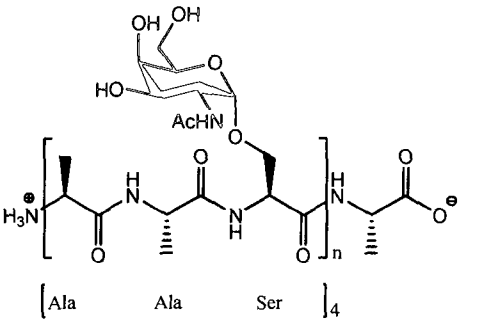

4a

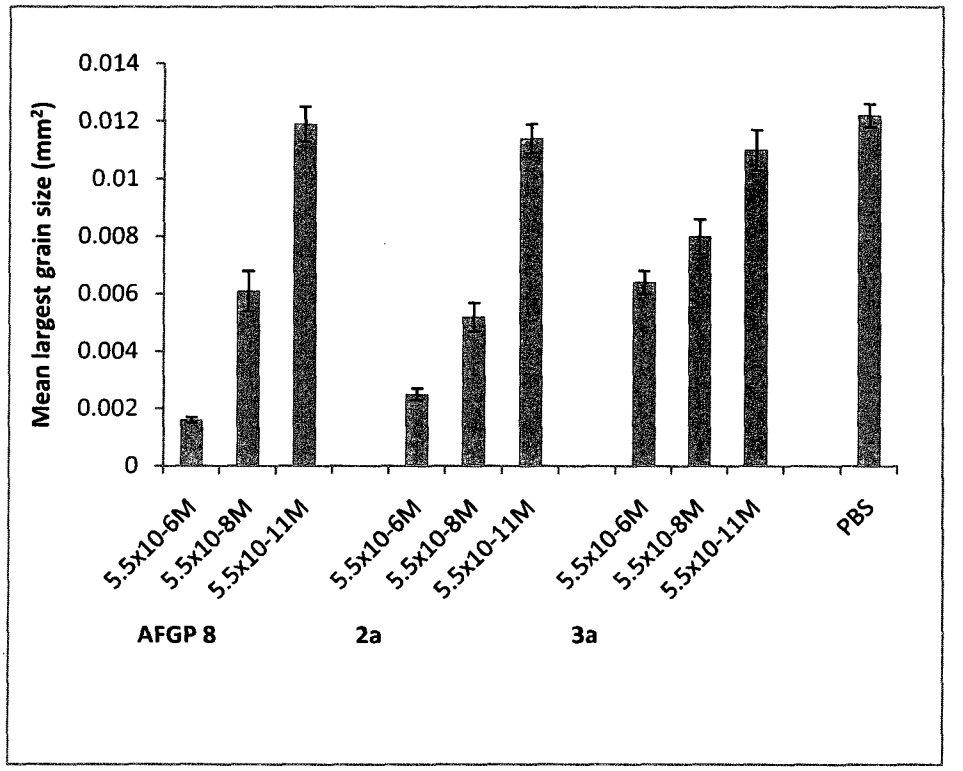

Figure 2.3: Structures of the O-linked analogues and comparison of IRI of a pair of O and C-linked analogues

It was hypothesized that the difference in activity may have been as a result of an electronegative atom at the anomeric position as this is the only structural difference between the two analogues. It would seem that this causes the glycoprotein to exist in a different relative conformation than its C-linked counterpart. The effect of an electronegative atom may also be as a result of stereoelectronics due to the orbitals on oxygen. The resulting conformation results in these analogues conferring reduced ice

recrystallization inhibition properties.

The term anomeric effect was first coined in 1958 by Edward and Lemieux,[16,17] describes the tendency of heteroatomic substituents adjacent to the heteroatom within a pyranose ring to prefer the axial orientation instead of the less hindered equatorial orientation that would be expected from steric considerations. Several explanations for the anomeric effect have been proposed. The simplest explanation involves dipoles; in the equatorial configuration the dipoles involving both heteroatoms are partially aligned and thus repel each other. However the axial configuration has the dipoles opposing; this is the more stable and lower energy state.[14]

A second and more widely accepted explanation is the stereoelectronic effect. There is a stabilizing interaction between the unshared electron pair on the heteroatom within the pyranose ring and the low lying σ* orbital of the axial C-X bond. These two orbitals are able to overlap and electron density from the oxygen within the ring can be donated into the σ* orbital resulting in a lower energy configuration. This orbital overlap is absent if the C-X bond is in an equatorial configuration.[14]

In the C-linked analogue the anomeric effect does not contribute as much to the conformation of the polymer and to its activity. We believe that the existence of this electronegative atom at the anomeric position greatly changes the activity of the analogue; analogues show reduced ice recrystallization ability.

2.2 Research Goals and Objectives

The main goal of my research is to determine the effect of replacing the linker atom at the anomeric position with sulphur. Sulphur is more electronegative than carbon and is much larger than both carbon and oxygen. Synthesis of S-linked serine analogues **65-67** will provide meaningful information about the influence of an electronegative atom at the anomeric position. Additional information that can be gained from this set of analogues is; the effect of the *N*-acetyl group at C-2 and

the effect of an increased hydrophobic backbone on antifreeze activity.

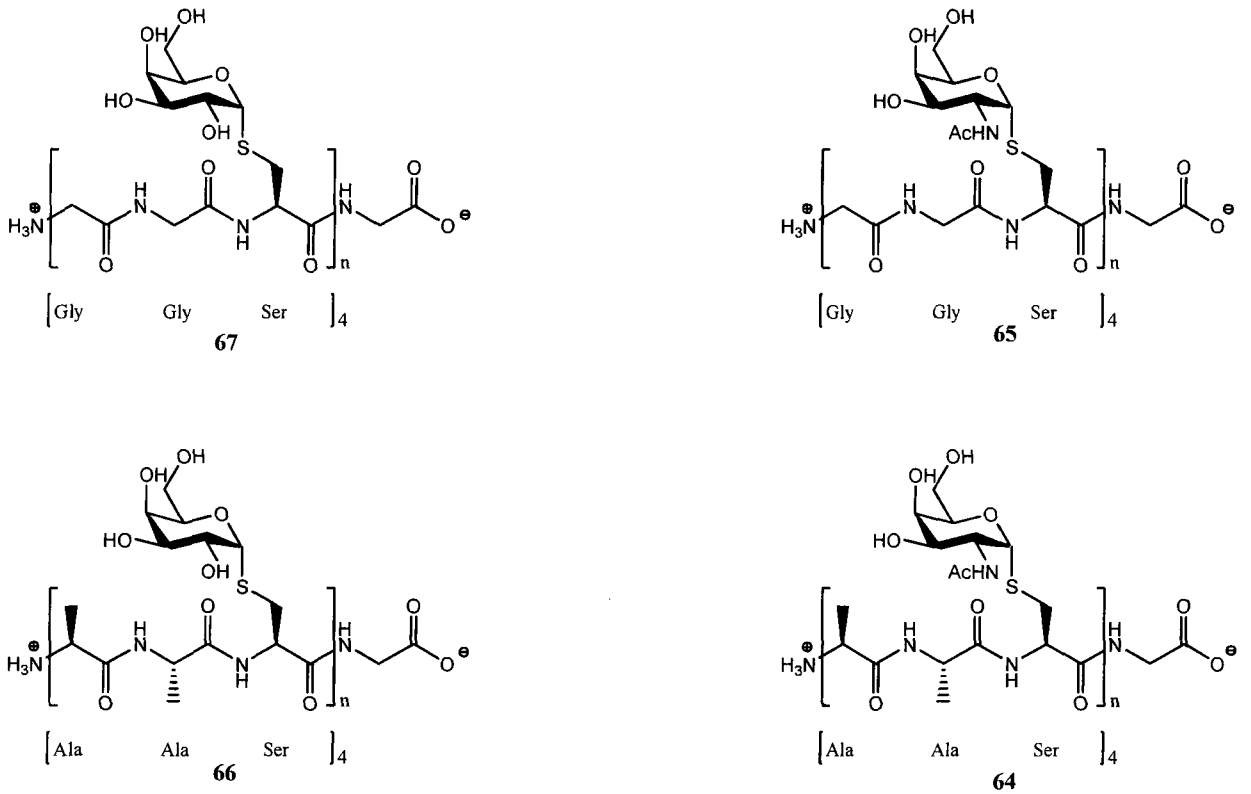

Figure 2.4: Synthetic targets

Replacing the anomeric oxygen or nitrogen in oligosaccharides with sulphur has become quite common in the literature and has led to an important class of compounds; thioglycosides.[18] These compounds have been used as glycosyl donors[19], enzyme inhibitors[20], enzyme resistant scaffolds[21] and synthetic vaccines[22]. Organosulphur chemistry is quite versatile and this is reflected in the number of ways that exist for the preparation of thioglycosides. The anomeric C-S bond is more stable than C-O as S-linked glycosidic bonds have been shown to be resistant to enzymatic hydrolysis and to be more stable under acidic and basic conditions than their O-linked counterparts.

In comparing analogues **2a** and **3a** it would seem that the presence of an electronegative atom

at the anomeric position acts in such a way that results in reduced IRI activity. The same effect is likely to be seen for the thioglycoconjugates. Substitution of a more electronegative atom (O instead of C) at the anomeric position results in loss of IRI activity.[15] Therefore substituting sulphur would have that same effect; the thioglycoconjugate **67** will have reduced IRI activity relative to analogue **2a**.

Our lab has previously synthesized O-linked analogue pairs with the presence or absence of the *N*-acetyl group at C-2 being the only structural difference; [Thr-Gly-Gly α (Gal)]$_4$: **6a** and [Thr-Gly-Gly α GalNHAc]$_4$: **6b.**[15] These were tested for dynamic ice shaping, thermal hysteresis and ice recrystallization inhibition. While these analogues failed to demonstrate thermal hysteresis, analogue **6a** showed dynamic ice shaping and **6b** was shown to be 12% more active relative to **6a** with regards to IRI. Interestingly this is the opposite of what was seen with C-linked analogue pairs **2a** and **2d**. It would seem that the effect of the presence of an *N*-acetyl group at C-2 is dependent on the electronegativity of the atom at the anomeric position. For the C-serine *N*-acetyl derivative the ice recrystallization inhibition activity decreased quite dramatically, 31% relative to the C- serine analogue. While for the O-linked analogue pair **6a** and **6b** the presence of the *N*-acetyl group results in improved IRI activity. The S-linked analogue pairs will most likely have similar relative IRI activity to the O-linked analogue pairs due to the electronegative linker atom.

2.3 Synthetic Strategies for the Preparation if S-Linked Glycoconjugates

To accomplish our goal, our first objective was to develop a synthetic strategy for the synthesis of S-linked building blocks. The most common synthetic approach to the synthesis of S-linked glycopeptides is to employ an anomeric thiolate nucleophile that reacts with an alanine derivative which has a leaving group. A major drawback of this approach is the possibility of the formation of diastereomers at the α-carbon resulting from β-elimination and subsequent Michael addition.[23](Scheme 2.2)

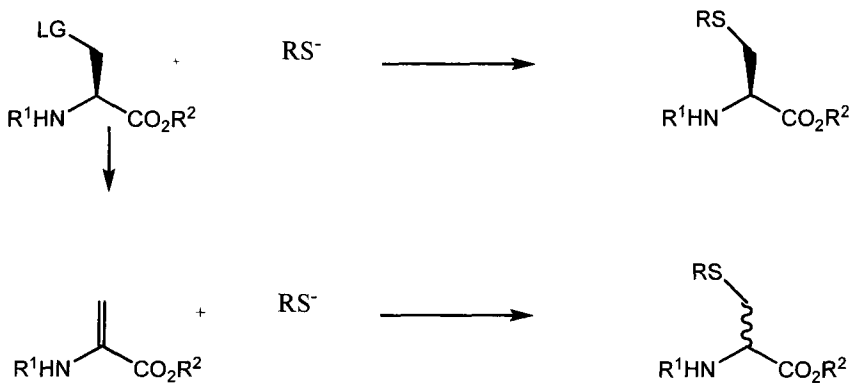

Scheme 2.2: The common synthetic approach used in the synthesis of S-linked glycoconjugates

Schmidt and co-workers were able to overcome this problem quite successfully using a method in which the reaction occurred in an ethyl acetate/water biphasic system with tetra-*n*-butylammonium hydrogen sulphate (TBAHS) and $NaHCO_3$. This protocol however has its own disadvantage; it is not compatible with the direct synthesis of S-linked Fmoc-glycosyl modified amino acids. The Fmoc protected compounds can only be obtained indirectly from the S-linked Boc-modified glycosyl amino acids because the reaction is so basic. [24,25,26]

Chi-Huey Wong and co-workers then explored alternate reaction conditions that would allow for the direct synthesis of not only S-linked Boc protected compounds but also Fmoc protected compounds. The ideal reaction conditions should allow for selective generation of the thiolate ion *in situ* while preventing β-elimination. Secondly a solvent such as dimethyl formamide (DMF) is needed as it is able to dissolve peptides. Thirdly the reaction condition should allow for the direct synthesis of glycoconjugates that have amino acid derivatives with different protecting groups.[23]

The resulting optimized reaction condition is a simple "two-step one-pot" reaction scheme; selective deprotection of the sulphur atom with NaOH in dry methanol (pH~7.5), the solvent is then

removed and the resulting thiolate sodium salt is subjected to nucleophilic substitution with bromoalanine in dry DMF. A slightly modified approach of the above protocol was employed in the syntheses of the building blocks for analogues **65-67**. Retrosynthetic analyses of both glycopeptide building blocks are shown below. The glycopeptides building block for analogues **66** and **67** are the same as the two analogues only differ in the amino acids that comprise the peptide backbone. The same is seen for the glycopeptide building block for analogues **64** and **65**.

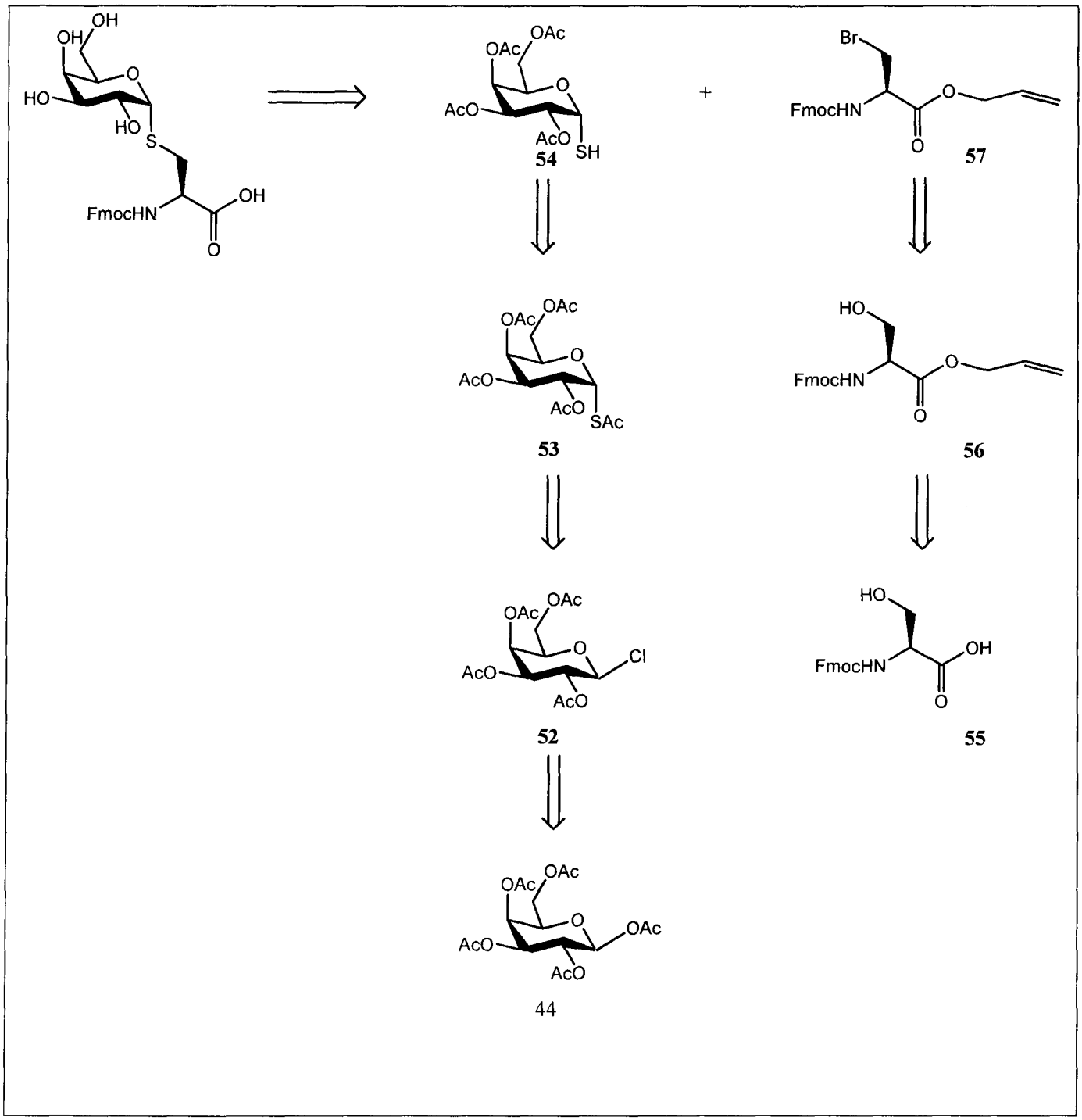

Scheme 2.3 : Retrosynthetic Analyses of analogues 66 and 67

Thiolate salts can be obtained from the deprotonation of thiols such as 2,3,4,6-Tetra-*O*-acetyl-1-thio-α-D-galactopyranose **(54).** It is important that reactions such as these are carefully monitored as side reactions are common. Thiols are generated from the selective deacetylation of peracetylated sugar 2,3,4,6-Tetra-*O*-acetyl-1-α-*S*-acetyl-1-thio-D-galactopyranose **(53)**. This reaction has been shown

in the literature and is accomplished at -25°C using NaOMe in MeOH. 2,3,4,6-Tetra-*O*-acetyl-1-α-*S*-acetyl-1-thio-D-galactopyranose **(53)** is generated via the displacement of the chloride from 2,3,4,6-tetra-*O*-acetyl-β-D-galactopyranosyl chloride **(52).** The synthesis of β-halide sugars are quite common in the literature even though they are quite unstable they are easily obtained from commercially available material β-D-Galactose pentacetate **(44).**

The bromoalanine **(57)** portion of the building block is obtainable from commercially available Fmoc protected serine **(55)**. The carboxy terminal is protected with a suitable protecting group and the primary alcohol brominated using the Appel reaction.

The retrosynthesis for the building block necessary for the solid phase synthesis of analogues **5b** and **5c** is different from the above due to the existence of the C-2 *N*-acetyl group. However the amino acid component is the same and is not shown in the below diagram. In this proposed synthesis the synthesis starts with the commercially available galactosamine hydrochloride **(45).** The nitrogen is protected with a bulky protecting group such as anisaldehyde to promote the synthesis of the β-acetyl derivative. The Schiff base is further acetylated followed by nitrogen deprotection resulting in the amine which is then acetylated to form 2-acetamido-2-deoxy-1,3,4,6-tetra-*O*-acetyl-β-D-galactopyranose **(49)**. The resulting amide converts to a thioamide with Lawesson's reagent [2,4-bis(4-methyoxyphenyl)-1,3-dithia-2,4-diphosphetane-2,4-disulfide] in hot toluene. The resulting thioamide cyclises to produce the GALNAc-thiazoline **(50)** which is hydrolysed to generate the thiol **(51).** Deprotonation of the thiol then produces the thiolate salt. The thiolate salt would then react with the bromoalanine derivative to produce the necessary building block. The full retrosynthesis of this carbohydrate moiety is shown below.

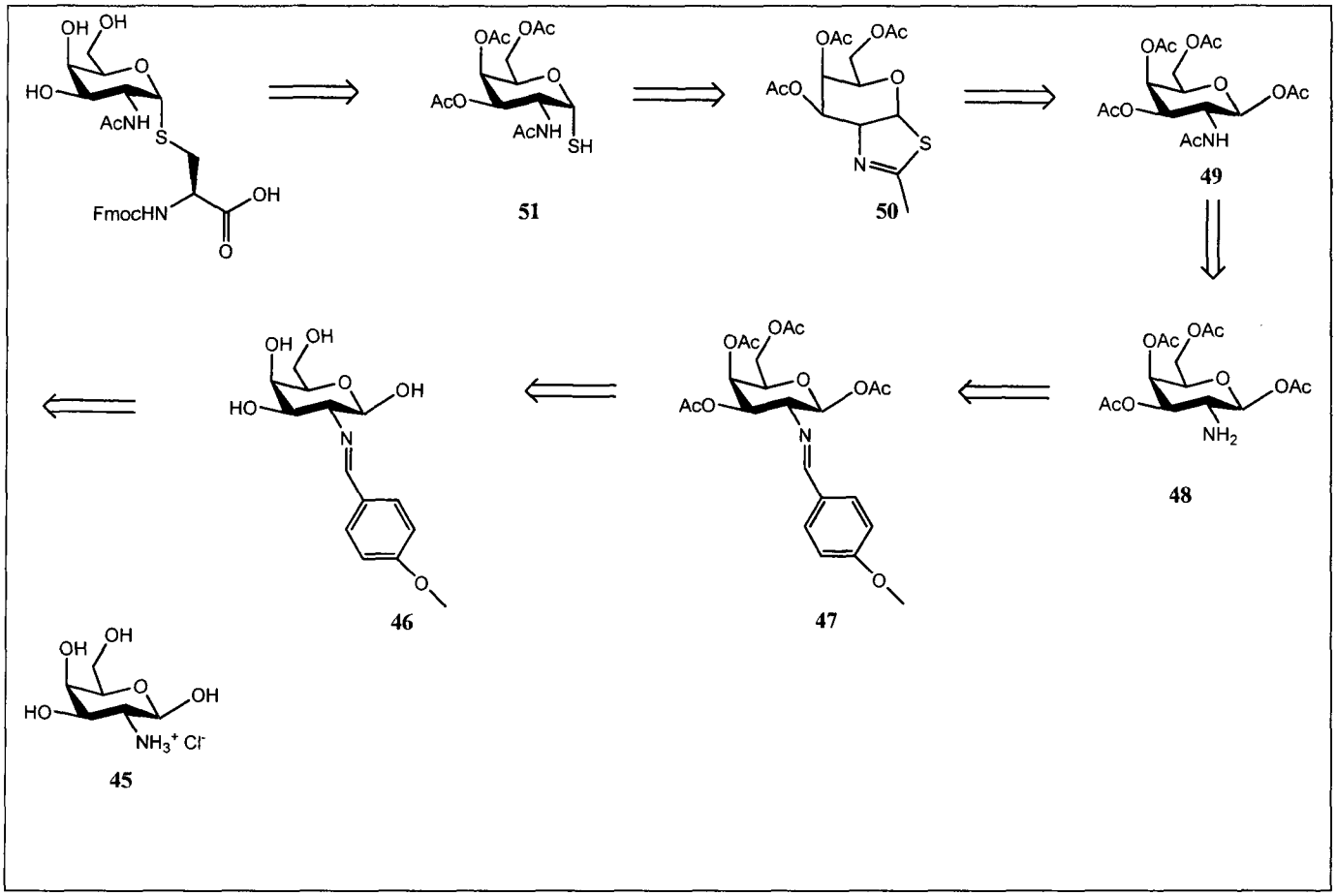

Scheme 2.4: Retrosynthetic Analysis of the carbohydrate potion of analogues 64 and 65

2.4 Summary

In conclusion four new AFGP analogues will be synthesized.

- Most importantly, structure-activity studies will be undertaken to test the hypothesis that substitution of a sulphur atom for a carbon at the anomeric position will result in reduced activity similar to that seen for the an oxygen.
- Information will also be gleaned on the effect of the *N*-acetyl group at C-2 on antifreeze activity. Two sets of analogues will be compared here; using this new information will be compared to our previous results, in the hopes of eventually determining a generalized model for an IRI structure activity relationship.

- Finally these analogues will increase our understanding on the effect of an increased hydrophobic peptide backbone on antifreeze activity.

References

[1] Marcaurelle, L.A., Bertozzi. C. *Chem. Eur. J.* **1999** 5:1384

[2] Dwek. R.A. *Chem Rev.* **1996** 96: 683

[3] Varki, A. *Glycobiology.* **1993** 3:97

[4] Capon, B. *Chem Rev.* **1969** 69:407

[5] O'Grady, S.M., Schrag, J.D., Raymond, J.A., Devries, A.L. *Exp. Zool.* **1982** 224:177

[6] Rubinski, B., Arav, B.A., DeVries, A.L. *Cryoletters.* **1991** 12:93-106

[7] Koushafar, H., Rubinsky, B. *Urology.* **1997** 49: 421

[8] , L., Dahiya, R., Rubinsky, B. *Cryosurgery.* **1999** 38:169

[9] Peg, D.E. *Semin Reprod. Med.* **2002** 20:5-13

[10] Wang, J.H. *Cryobiology.* **2000** 41:1-9

[11] S. Liu, Ph. D. Thesis, Univeristy of Ottawa **2006**

[12] Nishimura, et *al. Angew. Chem Intl. Ed. 2004 43: 856-862*

[13] T.Bar, R., Schmidt, R. *Liebigs Ann. Chem.* **1991** 185

[14] Sparks, M.A., Williams, K.W., Whitesides, G..M. *J. Med. Chem.* **1993** 36:78

[15] Bouvet, V., Ph. D. Thesis, University of Ottawa **2005**

[16] Fabian, M.A.; Armstrong, K.B.; Perrin, C.L. *J. Am. Chem. Soc.* **1994** 116:715-722

[17] Salzner, U.. *J.Org. Chem.* **1995** 60:986-995

[18] Horton, D.; Wander, J. D. In *The Carbohydrates. Chemistry and Biochemistry*; Pigman, W., Horton, D., Eds.; Academic Press: New York, **1980** IB: 799-842

[19] Crich, D.; Smith, M. *J. Am. Chem. Soc.* **2001** *123*:9015-9020

[20] Driguez, H. *Chembiochem* **2001**, *2*, 311-318. Driguez, H. *Top. Curr. Chem.* **1997** *187*:85-116

[21] Roy, R.; Hernandez-Mateo, F.; Santoyo-Gonzales, F. *J. Org.Chem.* **2000** *65*:8743-8746

[22] Bousquet, E.; Spadaro, A.; Pappalardo, M. S.; Bernardini, R.; Romeo, R.; Panza, L.; Ronisvalle, G. *J. Carbohydr. Chem.* **2000** *19*:527-541

[23] Chi-Huey Wong, et al. *Angew. Chem. Intl. Ed.* **2005** 44:4596-4599

[24] Zhu, X.M., Schmidt, R.R. *Chem. Eur. J.* **2004** 10:875.

[25] Zhu, X.M., Schmidt, R.R. *Tetrahedron Lett.* **2003** 44:6063.

[26] Zhu, X.M., Pachamuthu, K., Schmidt, R.R. *Org.Lett.* **2004** 6:1083

Chapter 3

3.1 Synthesis of S-linked AFGP Analogues

Glycosylation of peptides is one of the most complex postranslational modifications that occur in living organisms. The study of postranslational modification of peptides is necessary to understand the functions of glycans and their involvement in numerous biological processes. [1] There are various methods mentioned in the literature for the synthesis of natural and modified glycopeptides.[2,3] Naturally occurring glycopeptides are most commonly linked by O- or N-glycosidic linkage between the sugar moiety and the appropriate amino acid residue. Modified glycopeptides that replace the anomeric oxygen or nitrogen with sulphur have been previously synthesized. S-linked glycopeptides are more chemically stable and more resistant to the action of glycosidases.[4] Most importantly this change is tolerated by most biological systems.[5,6] Various synthetic strategies can be found in the literature. The required building blocks for Fmoc solid phase synthesis were prepared by modifying a convergent strategy first reported by by Chi-Huey Wong and coworkers.[1] The carbohydrate and amino acid derivatives were coupled together via a simple SN2 reaction to give the corresponding building blocks and the polypeptides were then assembled using automated solid phase peptide synthesis (SPPS).

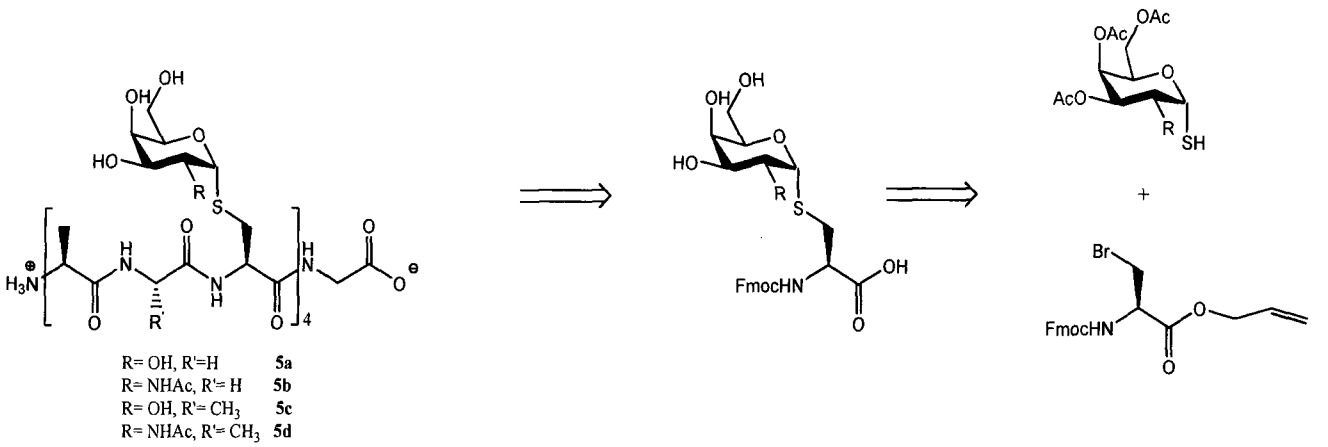

Figure 3.1: General retrosynthetic analysis of target analogues

3.2 Preparation of the Carbohydrate Components

Previous structure activity relationships carried out in our lab suggested that D-galactose is the best monosaccharide for antifreeze activity. In the synthesis of these analogues the galactose for the sugar component was again utilized and a second sugar component was also synthesized; the GalNHAc moiety, both with thiol groups at the anomeric positions.

3.2.1 Synthesis of 2-Acetamido-2-deoxy-2,3,4-tri-*O*-acetyl-1-thio-α-D-galactopyranose (51)

Initially an attempt was made to synthesise this carbohydrate moiety from the commercially available β-D-galactose pentacetate **40** as outlined in the following reaction scheme. The scheme shows the synthesis of 2-Acetamidotetra-O-acetyl-2-deoxy-D-galactopyranose **49**; an important intermediate in the synthetic strategy of 2-Acetamido-2-deoxy-2,3,4-tri-*O*-acetyl-1-thio-α-D-galactopyranose **51**.

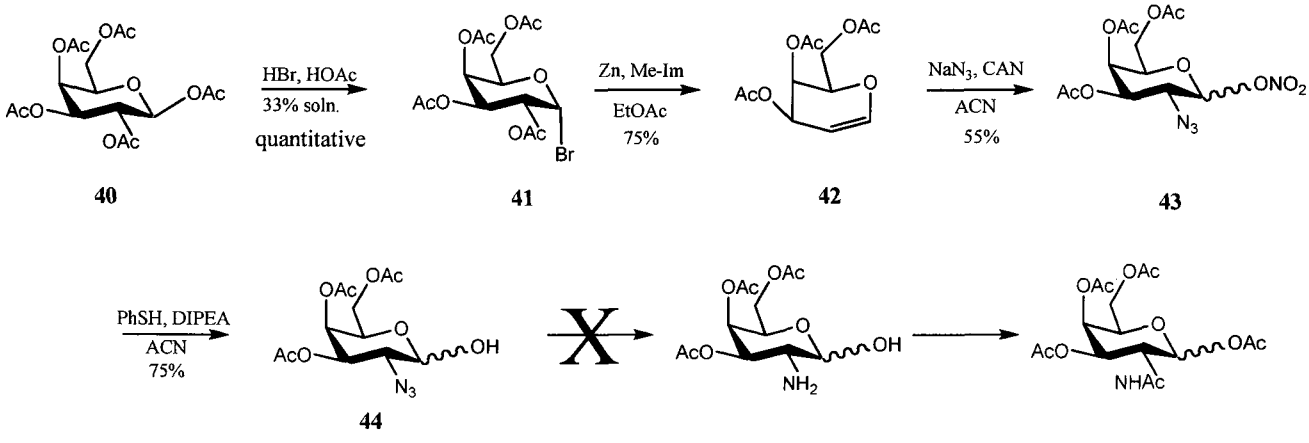

Scheme: 3.1: Attempted synthesis compound 49

This attempt was unsuccessful and was therefore abandoned after attempts to reduce the azide at C-2 failed. Numerous approaches were employed including attempts to carry out the

reduction with a combination of $SnCl_2$, PhSH and Et_3N; this was also unsuccessful. Reduction with $NiCl_2$, $NaBH_4$ and boric acid in ethanol was equally unsuccessful. Moreover a one pot reduction and acetylation was attempted using Zn bore no results. Consequently it was decided to employ an alternate approach starting with the commercially available material that already had an amino moiety at C-2; D-galactosamine hydrochloride **45**.

Initially I attempted to directly acetylate the entire sugar molecule by stirring with acetic anhydride, pyridine and DMAP. This was successful but produced a 2:1 α/β mixture in low yield. The β-anomer is required for the synthesis of the GalNHAc thiol **51**, but attempts to separate this diastereomeric mixture proved unsuccessful. As a result of the combination of inseparable disastereomers and low reaction yield this approach was abandoned and the synthetic strategy reported by Kim and Davidson[7] was employed to synthesize the desired β- anomer (Scheme 3.2) .

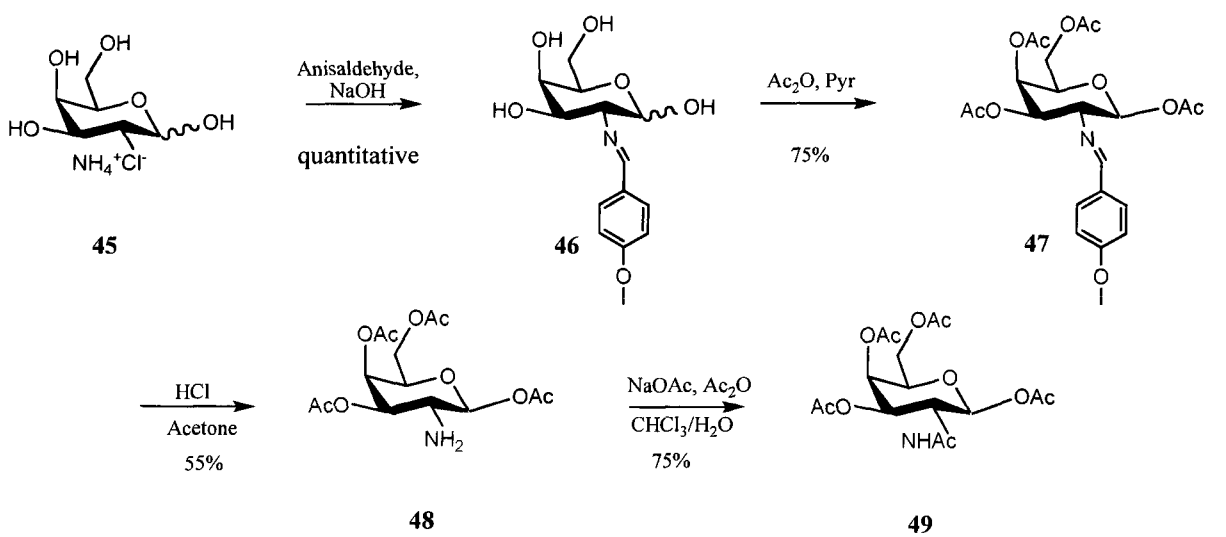

Scheme 3.2: Actually synthesis of compound 49

D-galactosamine hydrochloride **45** was neutralised with one molar equivalent of NaOH which also acted as the solvent. Anisaldehyde was added which resulted in the formation of a Schiff base **46** in quantitative yield. The Schiff base was then acetylated using acetic anhydride and pyridine to furnish **47** in 75% yield. This acetylation results solely in the production of the β-anomer. In general, acetylation of hexoses usually results in a mixture of acetylated products with the α-anomer being the most predominant due to the anomeric effect. However in this particular reaction that is not the case, only the β-anomer is formed, there was no trace of the α disatereomer. The imine **47** was then hydrolyzed to the amine **48** using 5N hydrochloric acid in acetone. **49** was furnished by the acetylation of **48** with anhydrous sodium acetate and acetic anhydride in 75% yield.

Following a two step protocol developed by Knapp and Myers, 2-Acetamido-2-deoxy-2,3,4-tri-*O*-acetyl-1-thio-α-D-galactopyranose **51** was synthesized from 2-Acetamidotetra-O-acetyl-2-deoxy-D-galactopyranose **49.** Treatment of **49** with Lawessons' reagent [2,4-bis(4-methoxyphenyl)-1,3-dithia-2,4-diphosphetane-2,4-disulfide] in toluene at 80°C results in the conversion of the amide to a thioamide and then cyclization of the thiocarbonyl group with the anomeric center produced the the GalNHAc-thiazoline **50** in a yield of 90%. The thiazoline ring of **50** underwent acidic hydrolysis with cleavage of the imine C-S bond (rather than the anomeric C-S bond) to give the desired compound 2-Acetamido-2-deoxy-2,3,4-tri-*O*-acetyl-1-thio-α-D-galactopyranose **51**. The scheme is shown below.

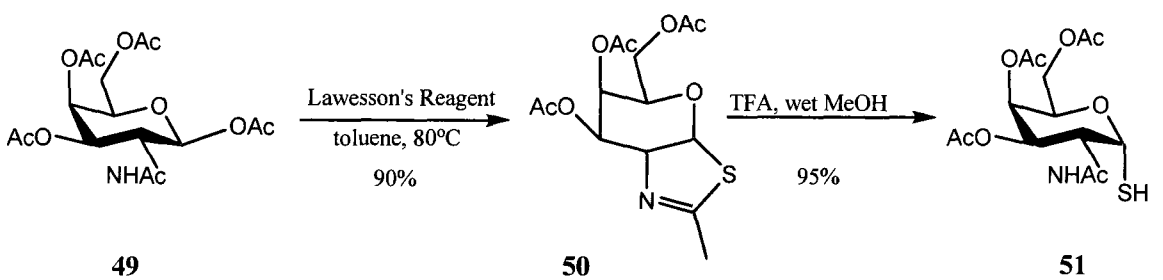

49 **50** **51**

Scheme 3.3: Completion of the synthesis of the first carbohydrate component

3.2.2 Synthesis of 2,3,4,6-tetra-*O*-acetyl-1-thio-α-D-galactopyranose 54

A second carbohydrate moiety was synthesized in an analogous manner as describe above. The starting material for this synthesis was commercially available β-D-galactose pentacetate **40.** Following a protocol developed by Ibatullin and Selivanov the peracetylated starting material was converted to the thermodynamically unstable glycosyl chloride; 2,3,4,6-tetra-O-acetyl-β-Dgalactopyranosyl **52.** This was accomplished using a slight excess of phosphorous pentachloride in the presence of a catalytic amount of boron trifluoride etherate in dichloromethane. This reaction is mildly exothermic and is fully completed within ten minutes with quantitative yield of the β-sugar. **52** is relatively unstable but is easily recrystallised from diethyl ether to give a pure white powder. Thioacetate **53** was prepared by simple nucleophilic displacement of the anomeric β-chloride of **52** by a thioacetate. DMF was used as the solvent and the potassium thioacetate was generated by mixing thioacetic acid and potassium *tert*-butoxide, leading to exclusive formation of 2,3,4,6-tetra-*O*-acetyl-1-S-acetyl-1-thio-α-D-galactopyranose **53.** In the final step the sulphur of **53** was selectively deacetylated to give the corresponding thiol. Chi-Huey Wong[1] and coworkers recommend that one uses drops of 1N NaOH in dry methanol at a pH of 7.0-7.5 to deacetylate the sulphur and form the thiolate salt which is the ideal coupling partner. However this protocol resulted in various deacetylated

products where one or more of the acetyl groups were cleaved. Even though the desired salt was present (confirmed by mass spectrometry), it was not isolatable. Alternate reaction conditions were tried. These are summaurized in the below table.

Entry	SM	Products	Reagents	Temperatures	Yield
1	**53**	**54**	NaOH in dry MeOH	RT	Mixture
2	**53**	**54**	Hydrazine hydrate acetonitrile	RT	30%
3	**53**	**54**	$TiCl_4$, Zn in DCM	0°C	0
4	**53**	**54**	NaSMe, MeOH	-20°C to RT	Mixture
5	**53**	**54**	NaOH, $NH_2OH{\cdot}HCl$	0°C	Mixture
6	**53**	**54**	NaOMe, MeOH	-25°C	90%

Table: 3.1: Summary of the various reaction conditions used and yields obtained

The sixth reaction condition worked very well and I was able to obtain and isolate pure **55** via column chromatography. Granted this is not the thiolate salt however the thiolate was easily obtained by deprotonation. The overall scheme for the synthesis of this second carbohydrate coupling partner is shown below.

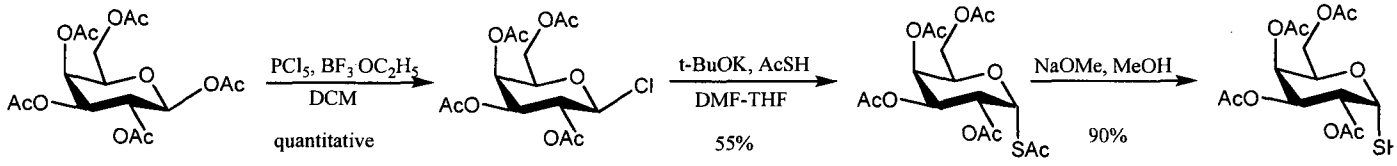

Scheme 3.4: Synthesis of the second carbohydrate component, compound 54

3.3 Preparation of the Amino Acid Component

Our most potent analogue is the C-serine analogue that has a serine amino acid component with a carbon linker to the sugar component. For my analogues I have also used a serine amino acid component. The amino acid coupling partner is the same for all the analogues and is a variation of L-serine; it has a bromine atom instead of a hydroxyl group. This bromine is a an excellent leaving group and is necessary for the SN_2 coupling reaction between the sugar and amino acid component.

3.3.1 Synthesis of Fmoc-β-bromo-L-Alanine-OAllyl (57)

Commercially available Fmoc-L-serine-OH, **55** was added to a solution of HBTU, DIPEA and allyl alcohol in DCM. The allyl ester of serine **56** was produced in a yield of 60%. Literature precedent suggested that the bromoalanine is quite unstable and should not be purified via column chromatography. Initially following a protocol used for Chi-Huey Wong[1] and coworkers bromination of the allylated serine was attempted with Ph_3P bound resin and CBr_4 which does not require column purification. This reaction requires high temperatures and the resulting product is usually obtained by filtration to remove the resin. The product was indeed

obtained but was not pure enough, coupling of this with the carbohydrate components resulted in trace amounts of the glycosylated building blocks.

A second approach was undertaken to synthesize **57** by reacting **56** with Ph_3P and CBr_4 at low temperature followed by flash chromatography. The yield was relatively low (40%) but the result was a pure white powder which was successfully able to be coupled with the thiolate to produce the glycosylated building blocks.

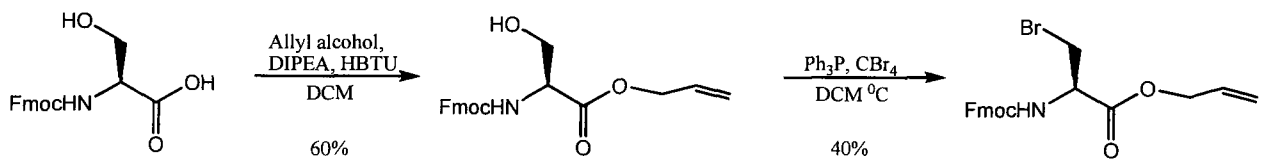

55 **56** **57**

Scheme 3.5: Synthesis of bromoalanine

3.4 Preparation of the Glycosylated Building Blocks

With both the carbohydrate and the amino acid components synthesized, coupling reactions were performed to prepare the glycosylated building blocks. Both carbohydrate components have a thiol functional group, it was necessary to deprotonate the thiol and form a thiolate salt resulting in increased nucleophilicity of the sulphur.

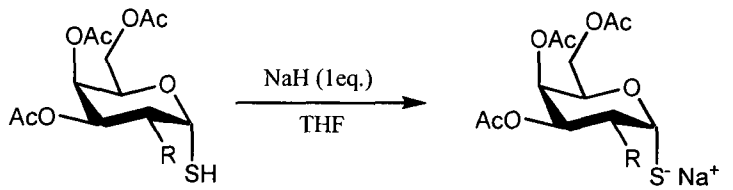

R= NHAc **51**

R=OAc **54**

R= NHAc **58**

R=OAc **59**

Scheme 3.6: Selective deprotonation of the thiol resulting in the thiolate salt

3.4.1 Synthesis of Glycosylated Amino Acids

The thiolate salts **58** and **59** were coupled with the bromoalanine in DMF at -78°C. The reaction proceeded for three hours at room temperature and completion was confirmed via TLC. The glycosylated products were obtained in 67% yield for compound **60** and 60% yield for compound **61.**

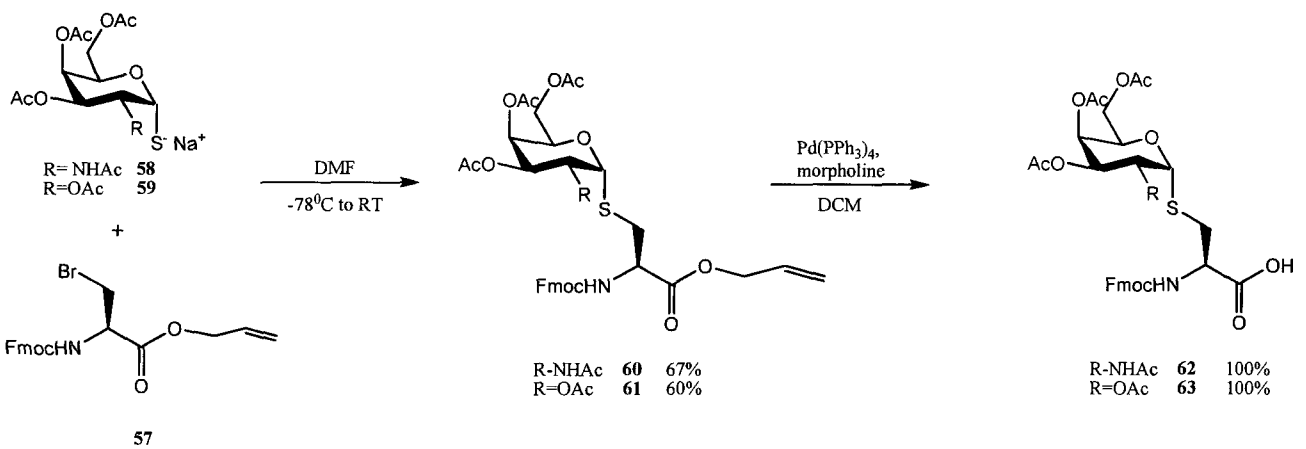

R-NHAc **60** 67%
R=OAc **61** 60%

R-NHAc **62** 100%
R=OAc **63** 100%

Sheme 3.7: Synthesis of the glysosylated building blocks

The deallylation of compounds **60** and **61** was performed in the presence of tetrakis(triphenyphosphine) palladium catalyst and morpholine in dichloromethane to give the Fmoc building blocks **62** and **63** in quantitative yields

3.5 Solid Phase Synthesis

Solid phase synthesis as the name suggests, involves synthesis on a solid supported resin. This chemistry was first reported almost fifty years ago with the work of Merrifield[8] This approach has been used in various areas including the synthesis of biopolymers, polypeptides, polysaccharides and glycopolymers. Solid phase peptide synthesis has various advantages over solution phase chemistry one of the major ones being that the coupling steps are quite high yielding due to minimization of physical losses as the peptide remains attached to the solid support throughout the synthesis. Also separation of intermediate peptides from excess reagents is effected by filtration, purification after each step involves washing off of excess reagents with common solvents such as DMF, DCM and MeOH. This prepares the insoluble solid support for the next step in the synthesis.

3.5.1 General Strategy for Solid Phase Peptide Synthesis (SPPS)

The first point of consideration in solid phase peptide synthesis is the solid support resin. Several resins are commercially available, our lab has always employed the use of Fmoc-glycine pre-loaded Wang resin for the synthesis of our glycopeptides polymers. Wang resin consists of cross-linked polystyrene matrix and is functionalized with a *p*-benzyloxy benzylalcohol linker which allows for the loading of the first amino acid by the C-terminus. This is an acid-labile bond.

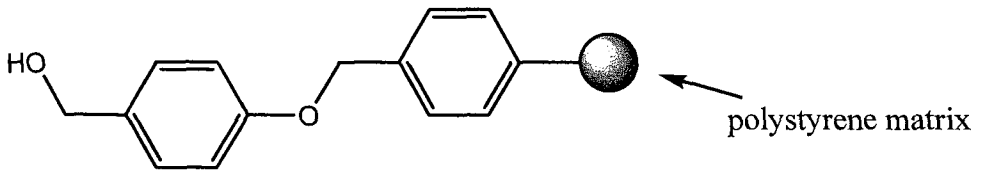

Figure: 3.2: p-benzyloxy benzylalcohol (Wang) resin

The beads are activated by soaking in dry DMF for about an hour which allows for them to become swollen. The glycopeptides are assembled using an Fmoc synthetic strategy; the assembly is done using an automated APEX instrument. The basic principle of Fmoc involves the removal of the Fmoc protecting group at the α-terminus of the amino acid with a base such as piperidine to provide a free site for coupling to the next activated, Fmoc protected amino acid. Amino acid activation is pre done using 1.1 equivalents of the activating agent 1H-Benzotriazolium 1-[bis(dimethylamino)methylene]-5chloro-,hexafluorophosphate (1-),3-oxide (HCTU). Immediately prior to the coupling 2.5 equivalents of diisopropylethylamine (DIPEA) is added. All equivalents are calculated with respect to the amino acid with is in turn calculated in terms of resin loading. Resin loading varies but the Wang resin that is used for these syntheses has a loading capacity of 0.6mmol/g. The first amide bond is formed between the deprotected glycine residue that is found on the resin and the new activated amino acid. The coupling times are determined by the number of equivalents of amino acid that is used. Excess reagents are washed off with N,N-dimethylformamide (DMF) after each Fmoc deprotection and amino acid coupling step. The growth of the polymer chain is accomplished by the sequential Fmoc deprotection and coupling of new amino acid until the desired length of the polymer has been synthesized in the required sequence. After deprotection of the last Fmoc protecting group,

the polymer is cleaved from the resin and remains in solution. It is then precipitated from ether as a solid product. Deacetylation is achieved in basic conditions and the product is neutralized with acid exchange resin. The final AFGP analogues are obtained after purification by reverse phase HPLC and lyophilisation. A summary for general solid phase synthesis is outlined below;

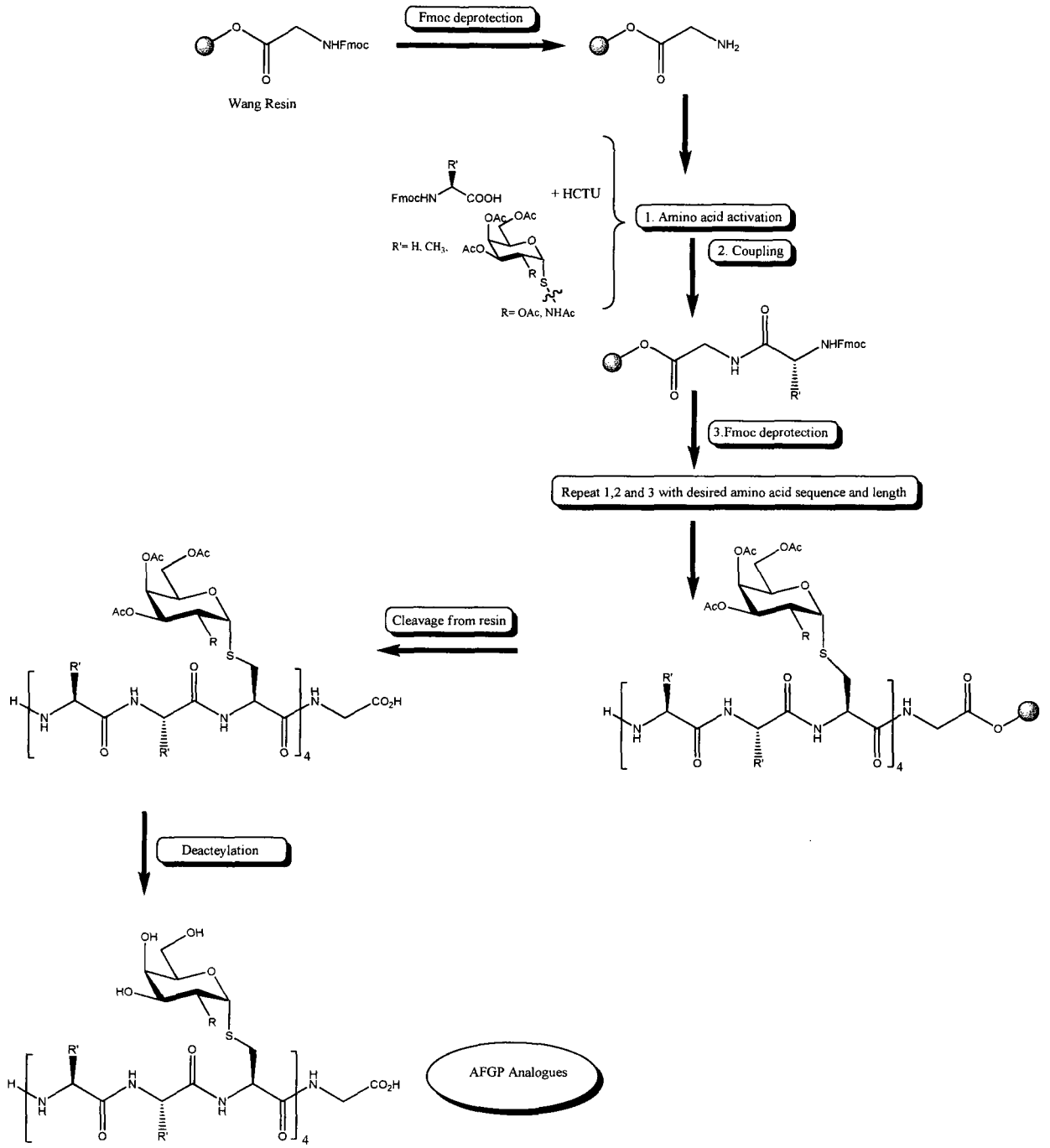

Scheme 3.8: General Strategy for solid phase synthesis

3.5.2 Solid Phase Assembly of the new Analogues

All of the new AFGP analogues were assembled via automated solid phase synthesis on the APEX ChemAdvantec automatic solid phase synthesizer. All the syntheses were the same general method, the only differences being the amino acid or building block used. I will outline the detailed synthesis of one analogue.

3.5.2.1 Synthesis of [S-Ser(α-D-GalNHAc)-Ala-Ala]$_4$-Gly (64)

The Fmoc-glycine pre-loaded Wang resin with a loading capacity of 0.6mmol/g was activated by swelling with dry DMF for two 30 minute sessions. The resin bound amino acid Fmoc deprotection was accomplished by treatment with 20% piperidine in dry DMF. This suspension was shaken for two 30 minute periods to ensure all the Fmoc groups were removed. Excess reagents were washed off with DMF (3 x 4mL). The first amino acid coupling with the free amine bound to the resin was performed with commercial available alanine (5 equivalents with respect to the resin) pre-mixed with HCTU (1 equivalent with respect to the amino acid) in DMF in the presence of DIPEA (2.5 equivalents with respect to the amino acid). This solution was gently shaken for one hour and this coupling was repeated a second time. Once this amino acid was added the Fmoc protecting group was removed using 20% piperidine/DMF. The whole process is repeated for the addition of the second amino acid, alanine and its subsequent deprotection. The third coupling was performed with building block **61** to complete the tripeptide. Building block coupling was done with 1.5 equivalent of the building block with respect to the resin with the reagents having the same ratio of equivalents as the previous couplings. The entire sequence of tripeptide formation was repeated three more times to get four tripeptide repeat units. The building block coupling reaction required longer coupling times (25

hours) due to the reduced number of equivalents used. After final deprotection of the Fmoc protecting group, the resin was washed successively with DMF, DCM and methanol. The desired product was cleaved using a specially prepared cleavage cocktail. This acidic cocktail is usually used for sulphur containing polymers, it consisted of TFA:water:phenol:thioanisole:EDT 82.5:5:5:5:2.5. Evaporation and precipitation with diethyl ether yielded the protected polymer in 70% yield.

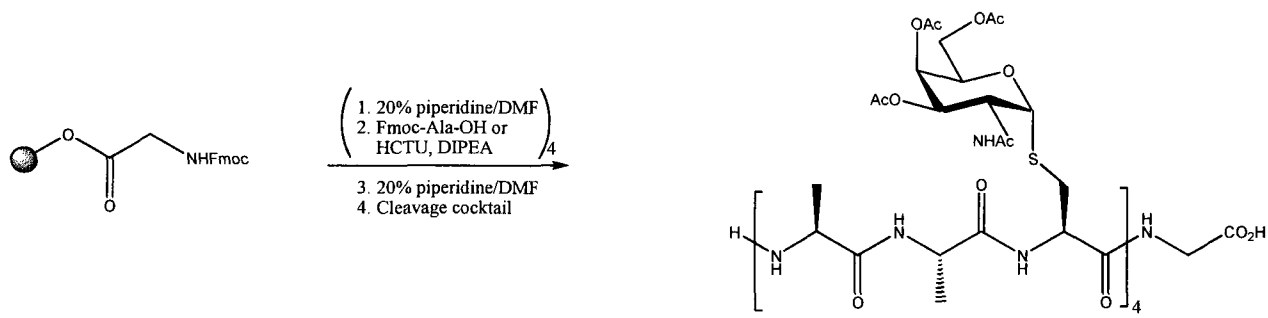

Scheme 3.9: Solid Phase assembly of [S-Ser(D-GalNHAc)-Ala-Ala]$_4$-Gly

Deacetylation was performed in basic conditions in the presence of hydrazine hydrate [hydrazine hydrate, 55 %:methanol (1:7)]. The reaction mixture was neutralized with acidic Amberlite IR-120 resin, filtered and concentrated. The resulting mixture was dissolved in water and washed successively with hexanes, chloroform, EtOAc and ethanol. The product was lyophilized and purified on sephadex column.

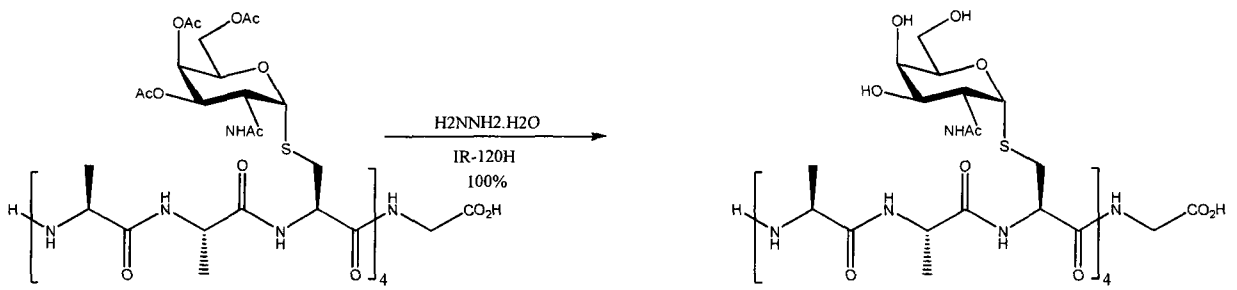

Scheme: 3.11:Deacetylation of polymer obtained from solid phase synthesis

All four analogues were synthesized via this reaction sequence. The results from solid phase synthesis were confirmed with MALDI spectrometry and are summarized below;

New S-Linked AFGP Analogues		**Crude Yield**
[Ala-Ala-S-Ser(α-D-GalNHAc)]$_4$-Gly	**64**	**70%**
[Gly-Gly-S-Ser(α-D-GalNHAc)]$_4$- Gly	**65**	**67%**
[Ala-Ala-S-Ser(α-D-Gal)]$_4$-Gly	**66**	**85%**
[Gly-Gly-S-Ser(α-D-Gal)]$_4$-Gly	**67**	**90%**

Table3.2: Summary of new AFGP analogues prepared via automated solid phase synthesis

The use of automated solid phase synthesis has been shown to be an efficient method to synthesize S-linked AFGP analogues. The syntheses were reproducible and required very little purification.

3.6 Antifreeze Activity of the S-Linked AFGP Analogues

The antifreeze activity of AFGPs both natural and synthetic analogues has been assessed by utilizing their unique properties: thermal hysteresis (TH), recrystallization inhibition (RI) and dynamic ice shaping (DIS).

3.7 Assessing Thermal Hysteresis Activity and Dynamic Ice Shaping of Analogues 64, 65, 66 and 67

Thermal hysteresis analysis was performed using a nanoliter osmometer. This technique is regarded as the "golden standard" for assessing thermal hysteresis and is one of the most important tests to quantify antifreeze activity of biological antifreezes. This technique not only allows for the measurement of the TH gap but it is also used to observe any change in ice morphology, dynamic ice shaping. To perform the assay the sample was prepared by dissolving 10mg/mL of the analogues in doubly distilled water. A sample holder containing nanoholes was loaded with paraffin oil. A nanoliter droplet of analyte was then submerged in the pre-cooled oil in the holder and flash frozen to -40°C. The temperature was increased gradually until the sample was melted back to a single crystal. The melting and freezing points were determined and the thermal hysteretic gap was calculated as the difference between the freezing and melting points. Each sample was tested twice and the results of the assay of the S-linked analogues are presented in the following table. All of the S-linked analogues were devoid of thermal hysteretic activity. The melting and freezing points of each analogue were the same. The table also includes this colligative value. Interestingly analogue **65** does show weak dynamic ice shaping seen from its hexagonal pyramidal shaped crystal. The other analogues all showed spherically shaped crystals, no change in the ice morphology.

Analogues	Ice Shaping	TH M.P/F.P(°C)
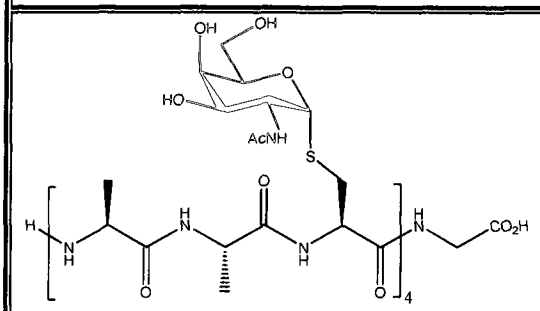 **64**	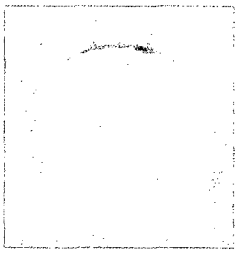	NO TH -0.39
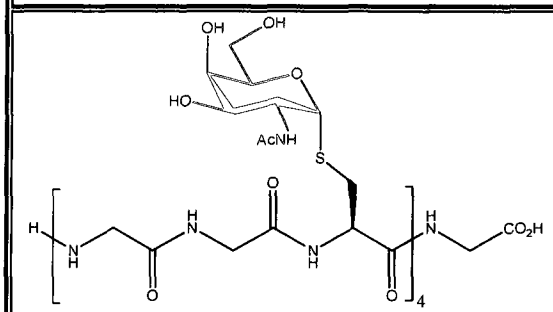 **65**		NO TH -0.46
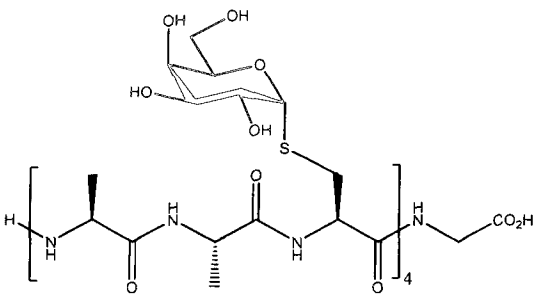 **66**	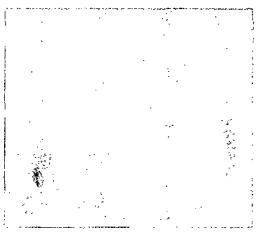	NO TH -0.21

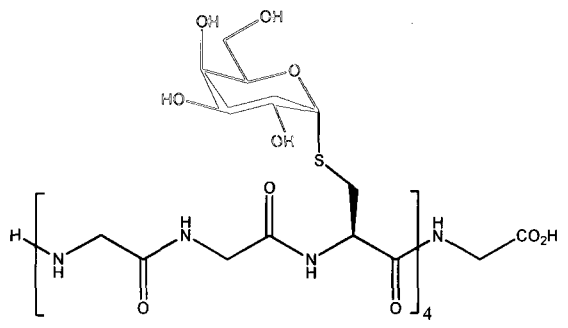 67	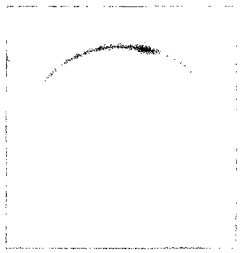	NO TH -0.22

Table 3.3: Thermal Hysteresis and Dynamic Ice Shaping Results

3.8 Assessing Ice Recrystallization Inhibition (IRI) Activity of Analogues 64, 65, 66 and 67

Another technique to quantify antifreeze activity of biological antifreezes is the ice recrystallization inhibition assay. This technique can detect antifreeze activity at very low sample concentrations compared to that required for thermal hysteresis. To perform the IRI assay, solutions of AFGPs of concentrations 5.54 x 10^{-6}, 5.54 x 10^{-8} and 5.54 x 10^{-8} M were made. They were dissolved in a phosphate-buffered saline (PBS) solution at pH 7.4. A 10μL droplet of the solution was dropped from a height of three meters onto a pre-cooled aluminum block at -78°C. The droplet instantly freezes as a very thin wafer and is immediately transferred to a microscope stage where the temperature is maintained at -6.6°C. The wafer was then allowed to anneal for 30 minutes to recrystallize. Photographs were taken at three different areas of the wafer for each concentration that was analyzed.

Domain recognition software, specifically designed for this purpose was used to calculate the surface area of twelve crystals in each photo. The average value was standardized relative to

a known value of the size of PBS crystals (0.01286mm^2), PBS served as the negative control. The error in calculation was propagated in terms of standard error of mean (SEM). The mean largest grain size was plotted against the different concentrations of analogues. The results are given below.

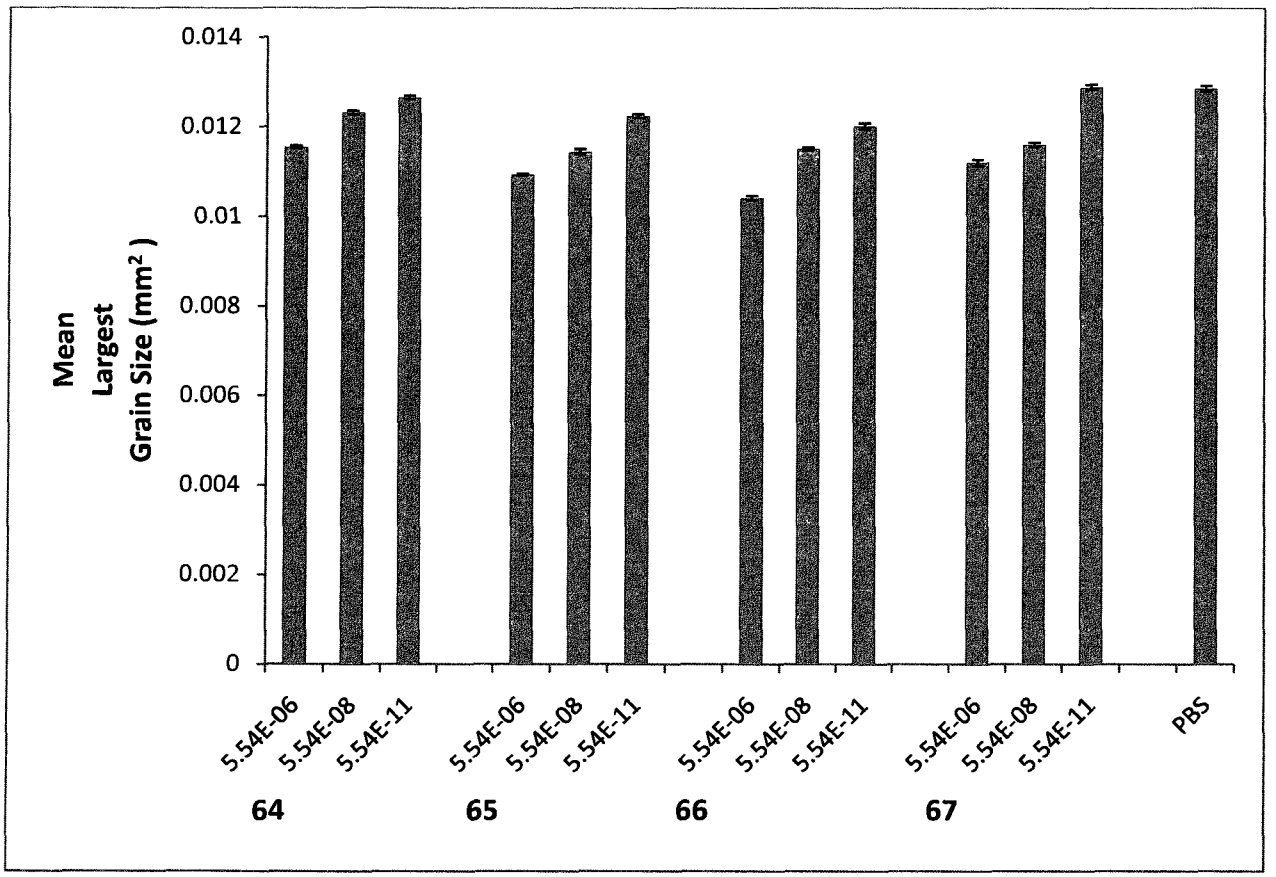

Graph 3.1: IRI data for S-Linked Analogues

Conc. (M)	**64** [Ala-Ala-S-Ser(α-D-GalNHAc)]$_4$-Gly	**65** [Gly-Gly-S-Ser(α-D-GalNHAc)]$_4$-Gly	**PBS**
5.54E-06	0.01154±0.00003	0.01093±0.00002	
5.54E-08	0.01231±0.00004	0.01141±0.00006	0.01286±0.0002
5.54E-11	0.01265±0.00004	0.01224±0.00004	

Conc. (M)	**66** [Ala-Ala-S-Ser(α-D-Gal)]$_4$-Gly	**67** [Gly-Gly-S-Ser(α-D-Gal)]$_4$-Gly	**PBS**
5.54E-06	0.01041±0.00005	0.01121±0.00007	
5.54E-08	0.01151±0.00003	0.01160±0.00005	0.01286±0.0002
5.54E-11	0.01201±0.00007	0.01289±0.00006	

Table: 3.4: MLGS of S-linked analogues and PBS (mm^2)

3.9 Discussion of Results:

As can be seen from the above results none of the S-linked AFGPs synthesized showed thermal hysteresis activity and only one analogue **(65)** exhibited weak dynamic ice shaping. The absence of thermal hysteretic activity is not surprising as we have previously shown in our lab that thermal hysteresis and ice recrystallization inhibition are decoupled. In addition to that many of our analogues do not show thermal hysteretic activity. The C and O-linked counterparts of these new S-linked analogues do not show any thermal thermal hysteresis activity. The change in ice morphology that is exhibited by analogue **65** means that this analogue is having some interaction with the ice. The AFGP is binding to the prism face of the ice crystals

preventing its growth along the a-axis. Growth then occurs along the c-axis resulting in this hexagonal bipyramidal shape. Even though no DIS is seen for any of the previous analogues there may still be some minimal interaction of the analogues with ice.

All of these analogues demonstrated very minimal IRI activity relative the negative control PBS. For all these analogues the IRI activity increased in a non-colligative manner. In comparing these new analogues it is seen that analogue **66** is the most active of the four followed by **65**, **64** and then **67**.

Graph 3.2 shows a comparison between the IRI activities of analogue **67** [Gly-Gly-S-Ser(α-D-Gal)]$_4$-Gly, the previously synthesized analogue **2a** [Ala-Ala-C-Ser(α-D-Gal)]$_4$-Gly and **3a** [Ala-Ala-O-Ser(α-D-Gal)]$_4$-Gly.

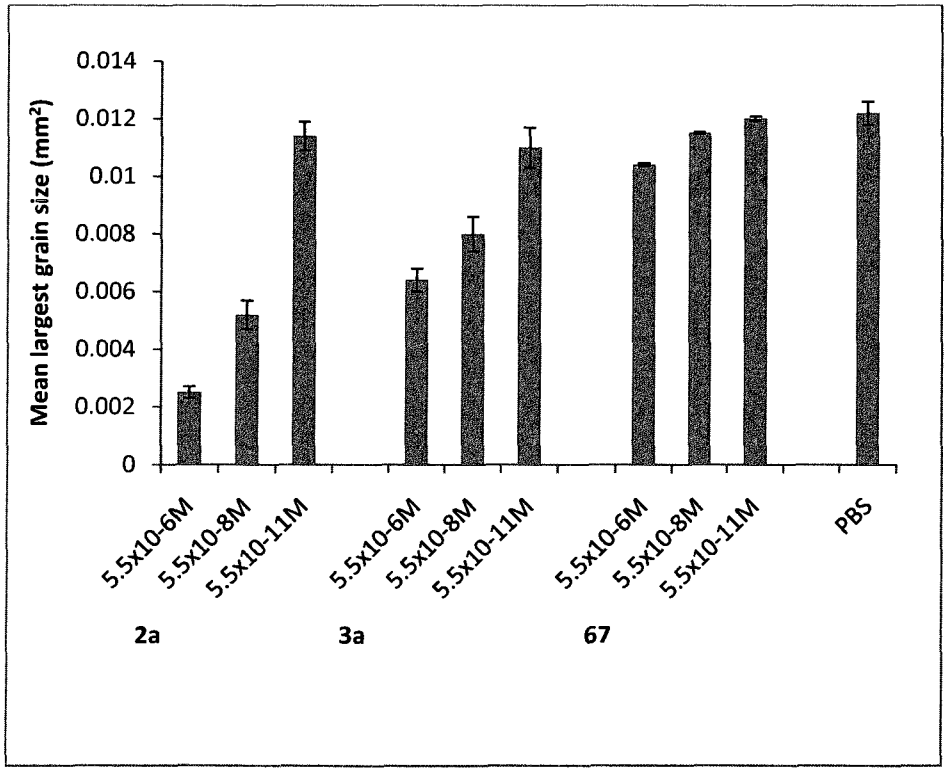

Graph 3.2: Comparison of IRI activity of C-, O- and S-linked AFGPs

Literature precedent has shown that the conformations in solution of *O*- and C-linked glycosides are very similar, and that the binding affinity to a particular receptor is not usually affected.[9] However, previous data provided by the Ben lab has demonstrated that this is not the case concerning our analogues. AFGP **2a** is our most potent analogue; studies have shown that substituting an oxygen atom for the carbon at the anomeric position reduces IRI activity. Results from the studies of S-linked analogues demonstrate that the substitution of a sulphur atom in place of a carbon at the anomeric position also reduces the IRI activity. Since the only difference between the analogues is the linker atom (differences due to peptide backbone is minimal) it can be concluded that the presence of an electronegative linker atom at the anomeric position has a significant effect on IRI activity. One explanation for this might be that the anomeric effect. The anomeric effect plays an important role in conformation of the O- and S-linked glycoconjugates. Perhaps this has an effect upon the presentation or the orientation of the carbohydrates on the glycoconjugates and thus their IRI activity. It may be that the C-linked system is able to adopt a novel carbohydrate presentation that allows for improved IRI activity. However due to the anomeric effect on the other systems they are unable to adopt this conformation and thus show a marked decrease in activity. A recent study performed by our lab shows that an anomeric carbon is necessary for IRI activity. Detailed molecular modelling simulations of a potent 1st generation C-linked analogues indicate that the increased IRI activity is the result of the creation of a hydrophobic pocket between the carbohydrate and the peptide backbone. Therefore the presence of an atom other than carbon would not allow for the hydrophobic pocket to form.[10] One may question the validity of this claim since the native structure which has remarkable IRI activity has an oxygen linker atom. However it is important to note that even though there are many structural differences between the two systems and it is

Preparation of 2,3,4,6-tetra-*O*-acetyl-1-thio-α-D-galactopyranose (54)

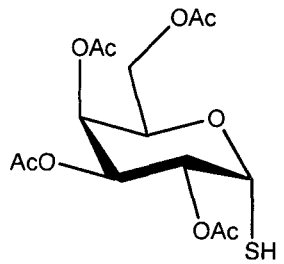

Compound **53** (0.140g, 0.344mmol) was dissolved in 20mL of methanol under argon. The solution was brought to -25°C and 1 molar equivalent of NaOMe is added. The solution was stirred for 30min at -25°C. Amberlite resin was added to neutralize the reaction mixture and this was stirred for another 25mins. The resin was filtered and the solution was concentrated and purified via column chromatography on silica gel with 6:4 Pet. Ether/EtOAc as eluant. A light yellow oil was produced in 90% yield.

^{1}H NMR (400 MHz, $CDCl_3$): δ 5.97(t, J = 5.0, Hz 1H), 5.41(dd, J = 3, 1.3 Hz, 1H), 5.21(m, 2H), 4.57(m, 1H), 4.06(m,2H), 2.10,2.04,2.01, 1.96 (s x 4, 12H, 3OAc), 1.78(d, J =5.1Hz, 1H, SH)

MS (ESI-TOF high-acc) calcd for $C_{14}H_{20}O_8S$(M+) 348.3688, found: 371.7453.

Allyl N-(9-Fluorenylmethoxycarbonyl)-L-Serine (56)

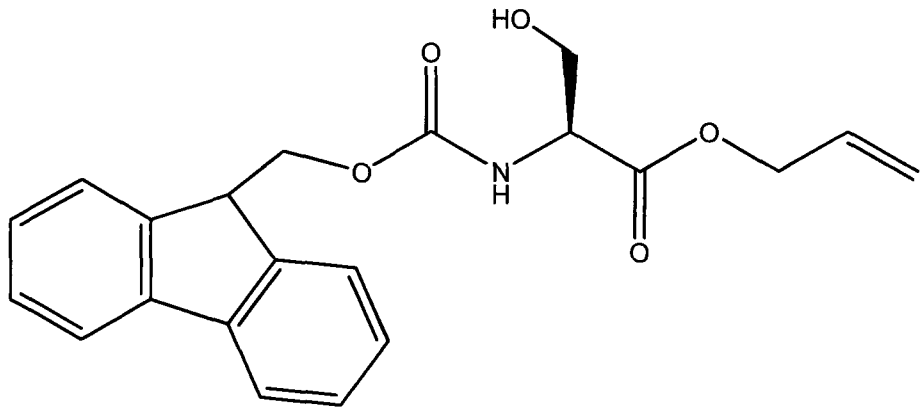

To a stirred suspension of HBTU (1.27g, 3.36mmol), allyl alcohol (1.3mL) and DIPEA (3.01mL) in DCM a solution of commercially available L-serine **55** (1.0g, 3.06mmol) in DCM was added drop wise over a period of half an hr. The reaction was monitored by TLC ~45mins. After the disappearance of starting material the resulting solution was washed with H_2O and Brine. The organic layer was dried over magnesium sulphate, concentrated under vacuum and purifies via flash chromatography 6:4 Hexanes/EtOAc to produce a yellow solid.(0.787g, 60%). Characterization data are in accordance to published ones.

Allyl N-(9-fluorenylmethoxycarbonyl)-β-Bromo-L-Alaninate (57)

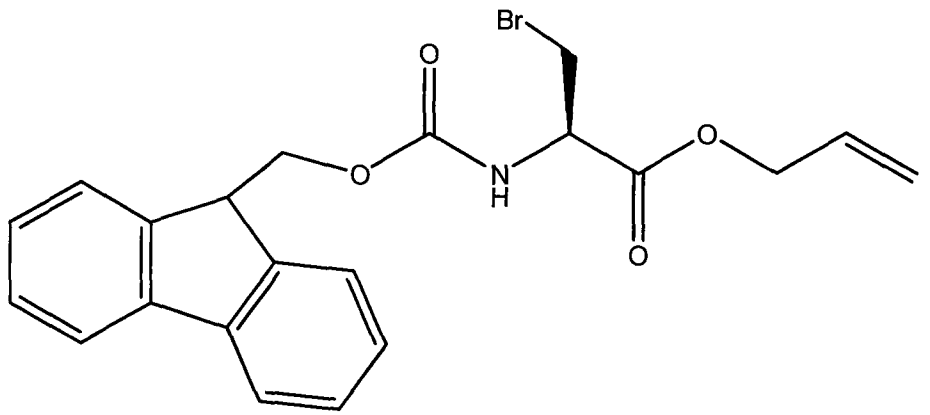

Ph_3P (2.14 g, 8.17 mmol) was added portionwise to a solution of **56** (1.50g, 4.08 mmol) and CBr_4 (2.71 g, 8.17 mmol) in dry CH2Cl2 (20 mL) at 0°C.The mixture was stirred at 0°C for 20 min and was then concentrated under reduced pressure at room temperature. The residue was purified by flash-column chromatography (petroleum ether/EtOAc 3:1) to give 1 (0.820g , 40%) as a white solid.

^{1}H NMR (400 MHz, $CDCl_3$): δ7.75 – 7.30 (m, 8H), 5.93 (ddd, 1H, J = 22.1, 10.6, 4.8 Hz, 1H), 5.73 (d, J = 7.6 Hz, 1H), 5.37 (d, J = 17.3Hz, 1H), 5.30 (d, J = 10.5 Hz, 1H), 4.84 (m, 1H), 4.71(m, 1H), 4.41 (dd, J = 7.6, 2.6 Hz, 1H), 4.24 (t, J = 7.3 Hz, 1H), 3.86 (dd, J = 10.6, 3.2 Hz, 1H), 3.76 (dd,1H, J = 10.6, 3.5 Hz, 1H)

^{13}C NMR (400 MHz, $CDCl_3$): δ168.3, 155.8, 143.9, 143.8, 141.5, 131.3, 128.0, 127.3, 125.3, 120.3, 119.7, 67.6, 67.1, 54.6, 47.3, 33.9

MS (ESI-TOF high-acc) calcd for $C_{21}H_{20}BrNO_4$ ($M+Na^+$) 452.0468, found: 452.0453.

N-(9-Fluorenylmethoxycarbonyl)-S-(3,4,6-tri-*O*-acetyl-2-acetamido-2-deoxy-α-D-galactoopyranosyl)-L-Cysteinyl-Allyl Ester (60)

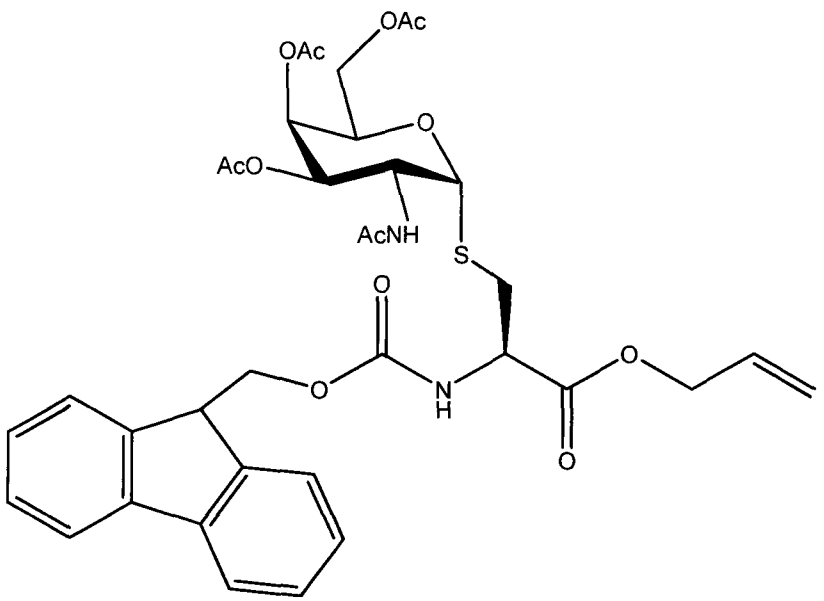

Compound **51** (0.200g, 0.550mmol) was dissolved in THF, exactly 1 equiv. of NaH was added, the solution was stirred until no more hydrogen was produced. The solvent was evaporated at room temperature to give the solid thiolate salt. The salt was then dissolved in dry DMF under argon and cooled to -78°C. A solution of **57** (0.236g, 0.550mmol) in DMF is added dropwise to the solution of the thiolate salt. The reaction is allowed to proceed for 3hrs at room temperature and monitored by TLC. The mixture was diluted with EtOAc, washed with H_2O. The organic layer was dried over magnesium sulphate and concentrated under vacuum. The resulting oil was purified via flash chromatography on silica gel with 50-80% EtOAc/Hexanes to give **60** in 67% yield.

^{1}H NMR (400 MHz, $CDCl_3$): δ 7.78–7.25 (m, 8H), 6.18 (d, J = 8.0 Hz, 1H), 5.90 (ddd,

J = 5.9, 11.0, 23.0 Hz 1H), 5.63 (d, J = 8.9), 5.36 (s, 2H), 5.34 (d, J= 16.9 Hz, 1H), 5,28 (d, J = 11.2 Hz, 1H), 4.95 (dd, , J= 3.1, 11. Hz, 1H), 4.80 (m, 1H), 4.72 (m, 1H), 4.66 (d, J = 5.0, Hz, 1H), 4.47 (dd, *J* = 7.1, 10.6 Hz 1H), 4.42 (dd, J = 6.5, 10.9, 2H), 4.22 (t, J = 6.6, Hz, 1H), 4.18 (dd, J = 5.2, 11.4 Hz, 1H), 4.06 (t, J = 6.7Hz, 1H), 3.99 (dd, J = 7.5, 11.4Hz, 1H), 3.34 (dd, J = 5.2, 14.6 Hz, 1H), 3.02 (dd, J = 3.4, 14.5 Hz, 1H), 2.19, 2.03, 1.98, 1.97 (s x 4, 12H)

^{13}C NMR (400 MHz, $CDCl_3$): δ 170.9, 170,4, 170.1,170.0, 155.7, 143.8, 143.6, 141.4, 141.3, 131.2, 128.2, 127.7, 127.1, 126.9, 125.0, 120.0, 119.3, 87.4, 69.2, 68.2, 67.3, 66.8, 66.7, 66.4, 62.1, 61.3, 54.2, 48.3, 47.1, 36.0, 29.7,23.3, 20.7, 20.5

MS (ESI-TOF high-acc) calcd for $C_{35}H_{40}N_2O_{12}S$ ($M+H_+$) 713.2375, found: 713.2376.

N-(9-Fluorenylmethoxycarbonyl)-S-(2,3,4,6-tri-*O*-acetyl-2-α-D-galactoopyranosyl)-L-Cysteinyl- Allyl Ester (61)

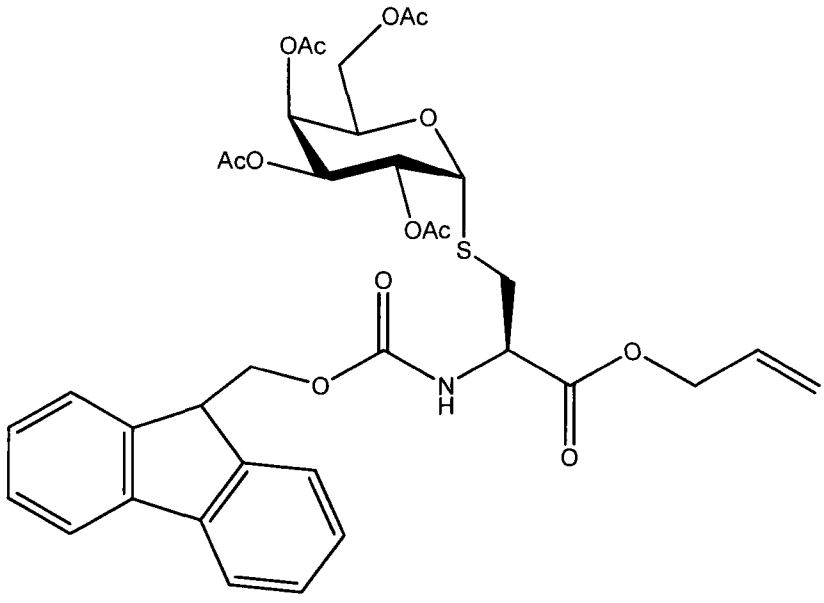

Compound **61** was made via the same protocol employed for compound **60.** For this reaction **54** and **57** were used to produce the desired compound on **67**% yield.

^{1}H NMR (400 MHz, $CDCl_3$): δ 7.77–7.20 (m, 8H, aromatic), 6.00 (d, J = 8.3 Hz, 1H), 5.84 (ddd,J = 6.0, 11.1, 22.7 Hz, 1H), 5.57 (d, J = 5.6 Hz, 1H), 5.24 – 5.37 (m, 4H), 5.06 (dd, J = 3.2, 11.0, 2H), 4.58 (m, 3H), 4.38 (m, 3H), 4.16 (t, 1H,*J* = 6.7Hz, 1H), 4.03 (m, 3H), 3.19 (dd, J = 5.6, 14.4 Hz, 1H), 2.92 (dd, J= 4.0, 14.8 Hz, 1H), 2.10, 2.02, 1.98, 1.93 (s x 4, 12H)

^{13}C NMR (400 MHz, $CDCl_3$): δ 170.6, 170.3, 170.3, 170.0, 155.9, 144.0, 141.5, 131.5, 128.3, 128.3, 127.9,125.2, 120.3, 120.2, 119.6, 84.8, 68.0, 67.9, 67.9, 67.6, 67.2, 66.7, 62.1, 54.4, 47.3, 34.9, 21.0, 20.8, 20.7, 20.6

MS (ESI, MeOH) calcd for $C_{35}H_{39}NO_{13}S$ ($M+H^+$) 714.2215, found: 714.2208.

IR: 1751, 1655

N-(9-Fluorenylmethoxycarbonyl)-S-(3,4,6-tri-*O*-acetyl-2-acetamido-2-deoxy-α-D-galactoopyranosyl)-L-Cysteinyl (62)

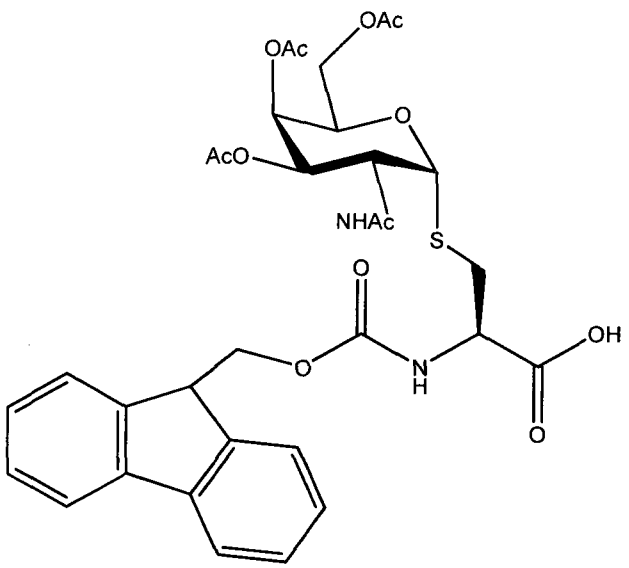

S-linked glycosyl amino acid **60** (0.270g, 0.378) was treated with tetrakis(triphenylphosphine)palladium(0) catalyst and morpholine (10equiv.) in dichloromethane to give the Fmoc-modified building block **62** swiftly (100%).

^{1}H NMR (400 MHz, $CDCl_3$): δ(400 MHz, $CDCl_3$): δ 7.78–7.25 (m, 8H), 6.18 (d, *J* = 8.0 Hz, 1H), 5.63 (d, J = 8.9), 5.36 (s, 2H), 5.34 (d, J= 16.9 Hz, 1H), 5,28 (d, J =11.2 Hz, 1H), 4.95 (dd, , J= 3.1, 11. Hz, 1H), 4.72 (m, 1H), 4.66 (d, J = 5.0, Hz, 1H), 4.42 (dd, J = 6.5, 10.9, 2H), 4.22 (t, J = 6.6, Hz, 1H), 4.06 (t, J = 6.7Hz, 1H), 3.34 (dd, J = 5.2, 14.6 Hz, 1H), 3.02 (dd, J = 3.4, 14.5 Hz, 1H), 2.19, 2.03, 1.98, 1.97 (s x 4, 12H)

^{13}C NMR (400 MHz, $CDCl_3$): δ 170.9, 170,4, 170.1,170.0, 155.7, 143.8, 143.6, 141.4, 131.2, 128.2, 127.7, 127.1, 126.9, 125.0, 120.0, 87.4, 69.2, 68.2, 67.3, 66.8, 66.7.

MS (ESI, MeOH) calcd for $C_{32}H_{32}N_2O_{12}S$ ($M+H^+$) 673. 6842, found: 673.8753.

N-(9-Fluorenylmethoxycarbonyl)-S-(2,3,4,6-tri-*O*-acetyl-2-α-D-galactoopyranosyl)-L-Cysteinyl- Allyl Ester (63)

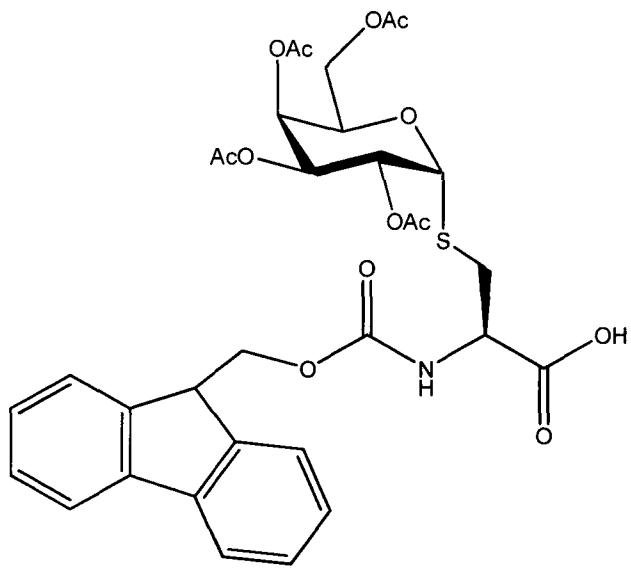

Compound **63** was synthesized from **61** using the same protocol as **62.**

^{1}H NMR (400 MHz, $CDCl_3$): δ 7.77–7.20 (m, 8H, aromatic), 6.00 (d, J = 8.3 Hz, 1H), 5.57 (d, J = 5.6 Hz, 1H), 5.24 – 5.37 (m, 2H), 5.06 (dd, J = 3.2, 11.0, 2H), 4.58 (m, 3H), 4.38 (m, 2H), 4.16 (t, 1H,*J* = 6.7Hz, 1H), 4.03 (m, 2H), 3.19 (dd, J = 5.6, 14.4 Hz, 1H), 2.92 (dd, J= 4.0, 14.8 Hz, 1H), 2.10, 2.02, 1.98, 1.93 (s x 4, 12H)

^{13}C NMR (400 MHz, $CDCl_3$): δ 170.6, 170.3, 170.3, 170.0, 155.9, 144.0, 131.5, 128.3, 128.3, 127.9,125.2, 120.3, 120.2,, 84.8, 68.0, 67.9, 67.9, 67.6, 67.2, 62.1, 54.4, 47.3, 34.9, 21.0, 20.8, 20.7, 20.6

MS (ESI, MeOH) calcd for $C_{35}H_{39}NO_{13}S$ ($M+H^+$) 674. 6842, found: 674.8753

[Ala-Ala-S-Ser(α-D-GalNHAc)]$_4$-Gly (64)

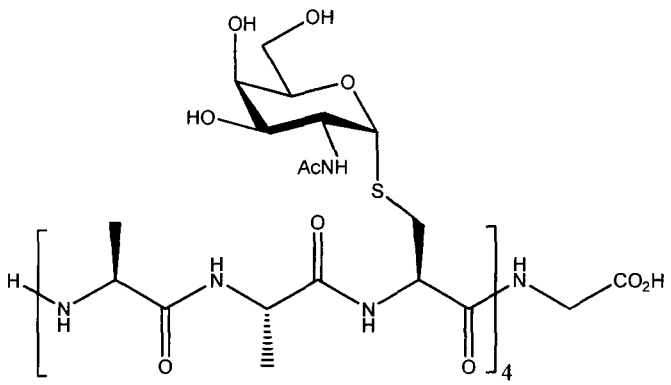

Following automated solid phase peptide synthesis the acetylated compound **64** and was cleaved off the beads using cleavage cocktail comprising of TFA:water:phenol:thioanisole:EDT 82.5:5:5:5:2. The acetylated product was readily deacetylated using hydrazine hydrate in MeOH to give compound **64.** This was confirmed by MALDI. Unfortunately time constraints prevented the HPLC purification of this analogue. However preliminary purification on sephadex column was done.. For all the ananlogues it was very difficult to obtain carbon spectra due to small amounts produced.

(MALDI, MeOH, negative ion) m/z calcd for $C_{70}H_{117}N_{17}O_{34}S_4$ (M^-Na^+) 1890.6832, found 1890.0367.

[Gly-Gly-S-Ser(α-D-GalNHAc)]$_4$- Gly (65)

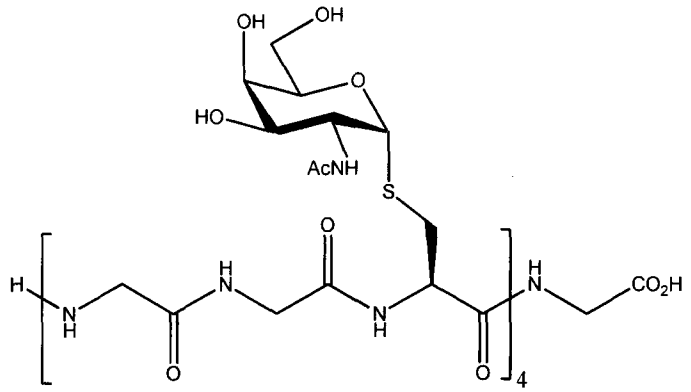

Crude compound **65** was obtained in the same way as **64.**

(MALDI, MeOH, negative ion) m/z calcd for $C_{62}H_{101}N_{17}O_{34}S_4$ (M^-Na^+) 1775.558, found 1776.7865

[Ala-Ala-S-Ser(α-D-Gal)]$_4$-Gly (66)

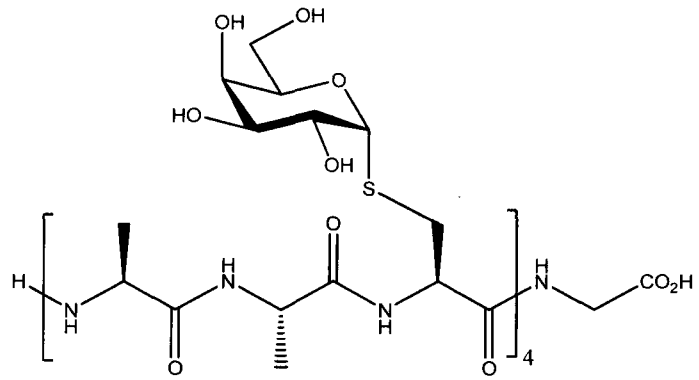

Following automated solid phase peptide synthesis the acetylated compound **66** and was cleaved off the beads using cleavage cocktail comprising of TFA:water:phenol:thioanisole:EDT 82.5:5:5:5:2. The acetylated product was readily deacetylated using hydrazine hydrate in MeOH to give compound **66.** This was confirmed by MALDI. Unfortunately time constraints prevented the HPLC purification of this analogue. However preliminary purification on sephadex column was done.

(MALDI, MeOH, negative ion) m/z calcd for $C_{62}H_{105}N_{13}O_{34}S_4$ (M^-Na^+) 1726.5770, found 1730.6578

[Gly-Gly-S-Ser(α-D-Gal)]$_4$-Gly (67)

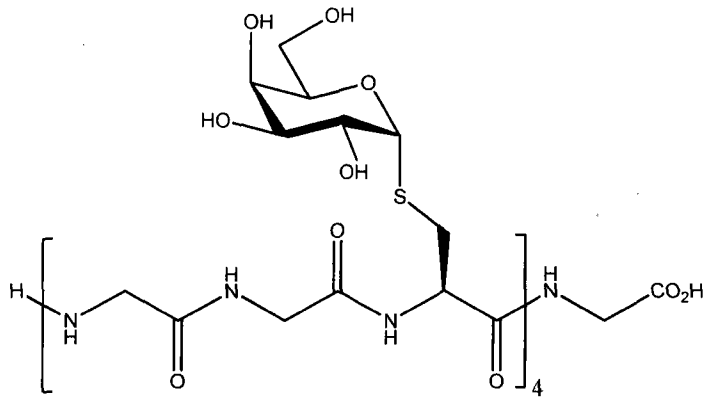

Following automated solid phase peptide synthesis the acetylated compound **64** and was cleaved off the beads using cleavage cocktail comprising of TFA:water:phenol:thioanisole:EDT 82.5:5:5:5:2. The acetylated product was readily deacetylated using hydrazine hydrate in MeOH to give compound **64.** This was confirmed by MALDI. Unfortunately time constraints prevented the HPLC purification of this analogue. However preliminary purification on sephadex column was done.

(MALDI, MeOH, negative ion) m/z calcd for $C_{54}H_{89}N_{13}O_{34}S_4$ (M^-Na^+) 1614.4518, found 1614.9816

^{1}H and ^{13}C Spectra

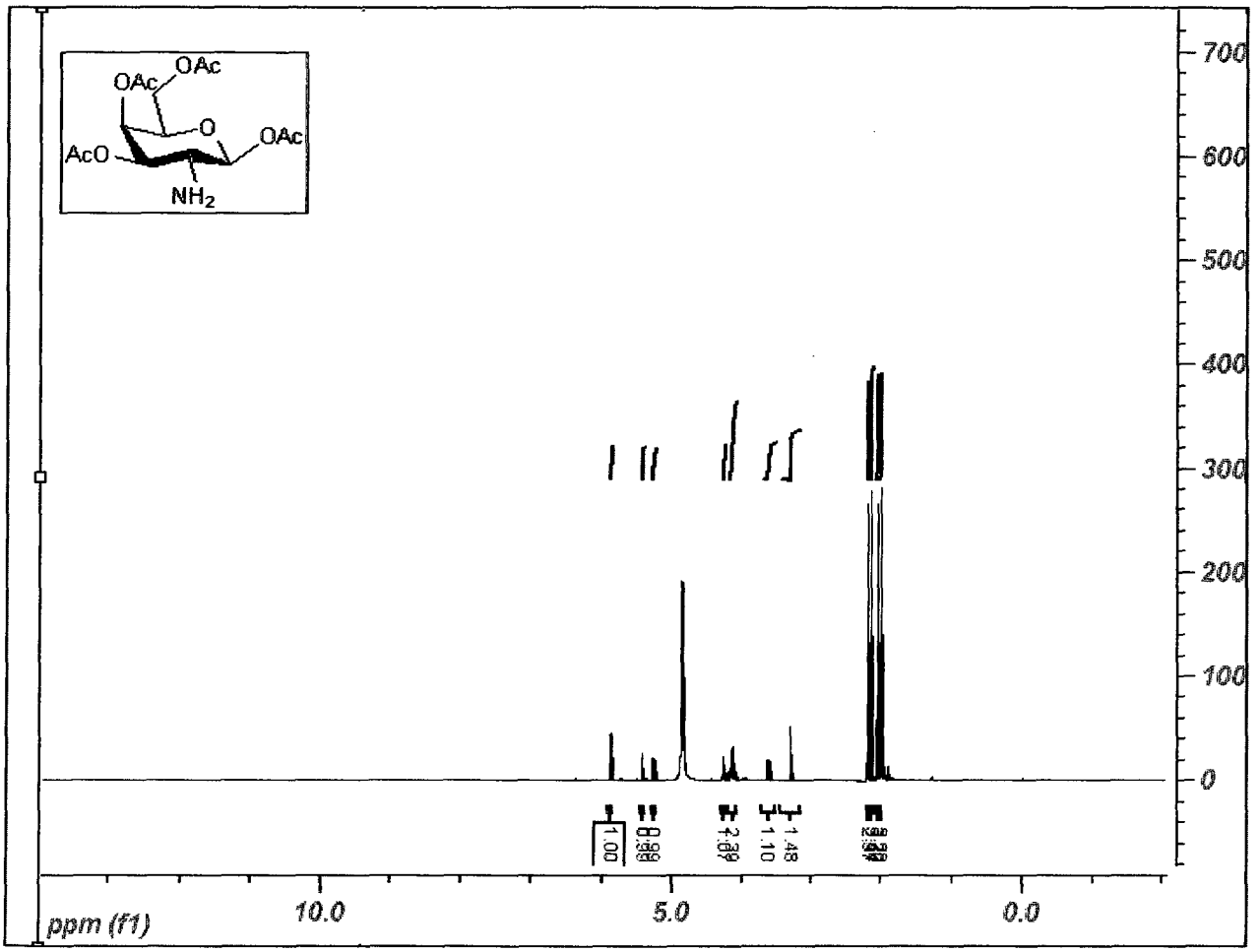
OAc
OAc
O
OAc
AcO
NH2
700
600
500
400
300
200
100
0
1.00
0.99
2.09
1.48
1.10
10.0
5.0
0.0
ppm (f1)

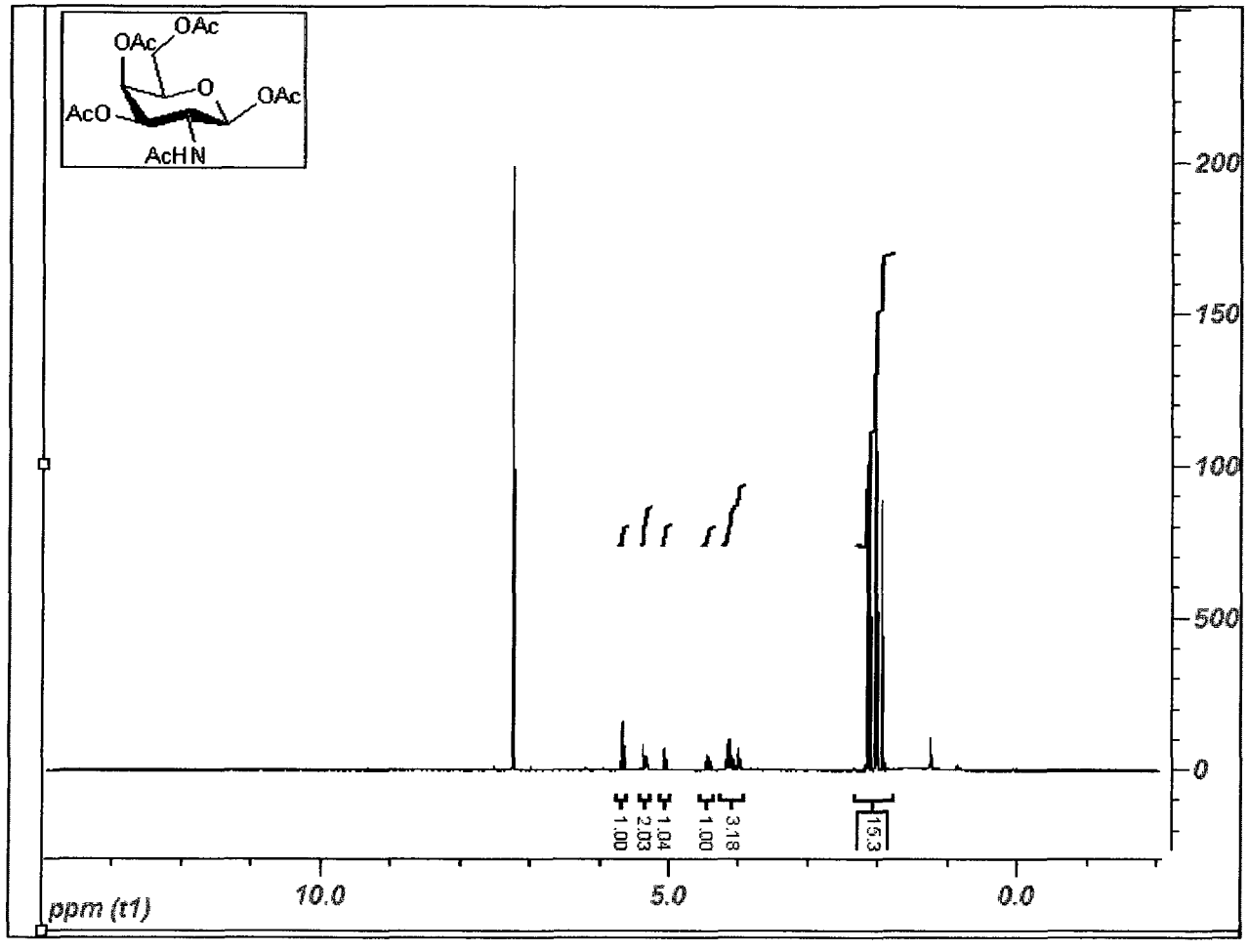
OAc
OAc
O
OAc
AcO
AcHN
200
150
100
500
0
1.00
2.03
1.04
1.00
3.18
15.3
ppm (t1)
10.0
5.0
0.0

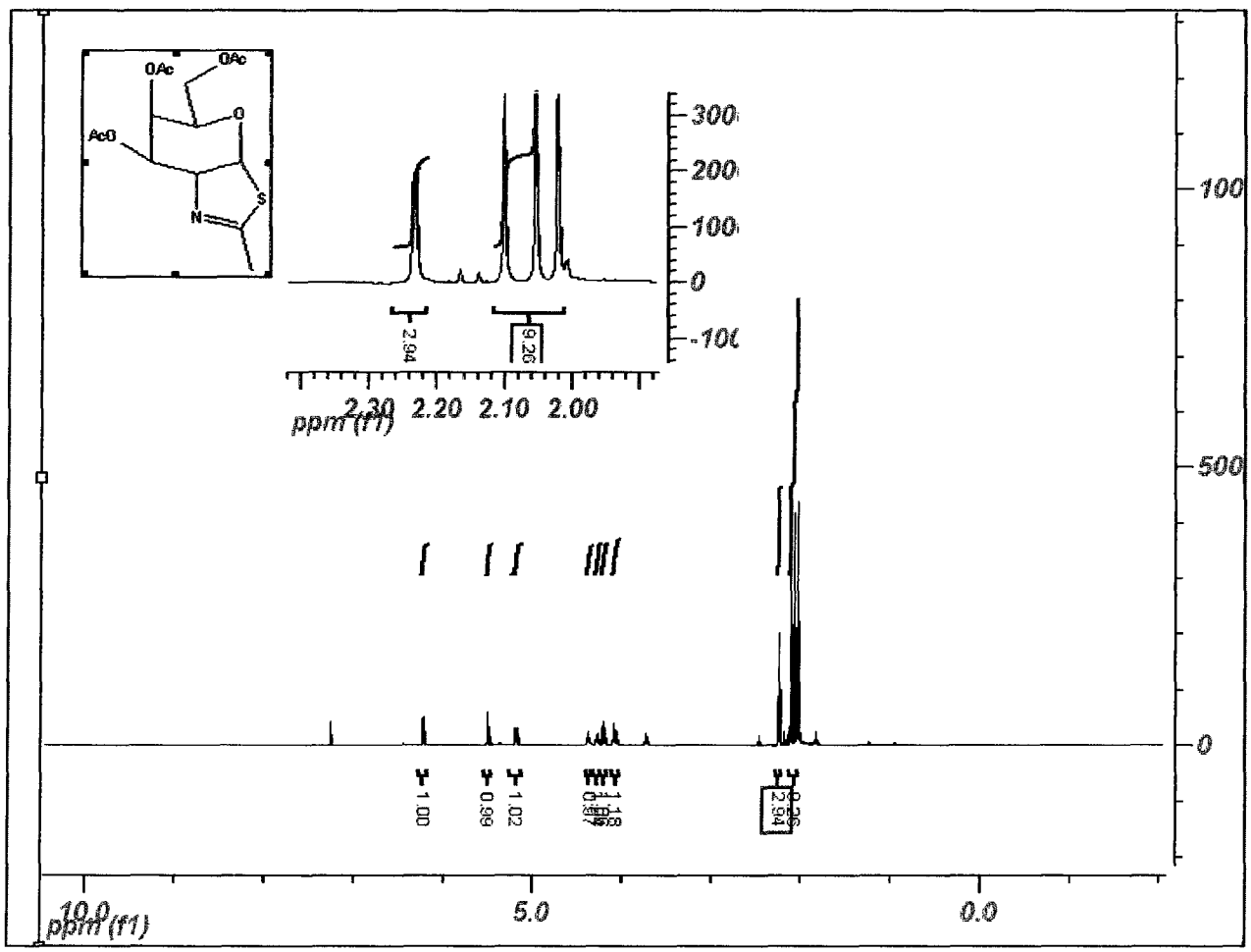
OAc
OAc
AcO
O
N
S
300
200
100
0
-100
2.94
9.26
2.30
2.20
2.10
2.00
ppm (f1)
100
500
0
1.00
0.99
1.02
1.18
0.87
2.94
10.0
5.0
0.0
ppm (f1)

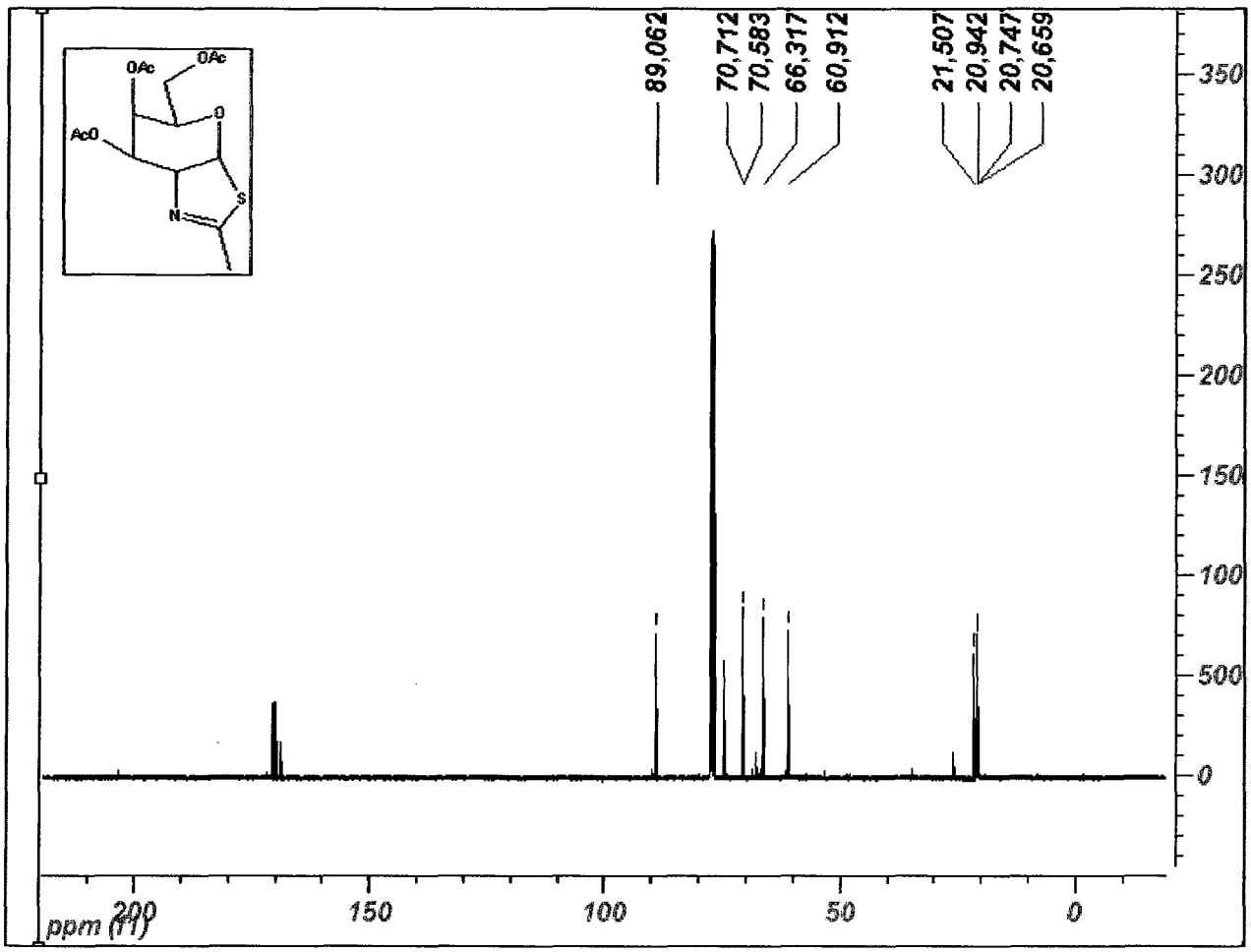
89,062
70,712
70,583
66,317
60,912
21,507
20,942
20,747
20,659
OAc
OAc
AcO
O
S
N
350
300
250
200
150
100
500
0
ppm (f1)
200
150
100
50
0

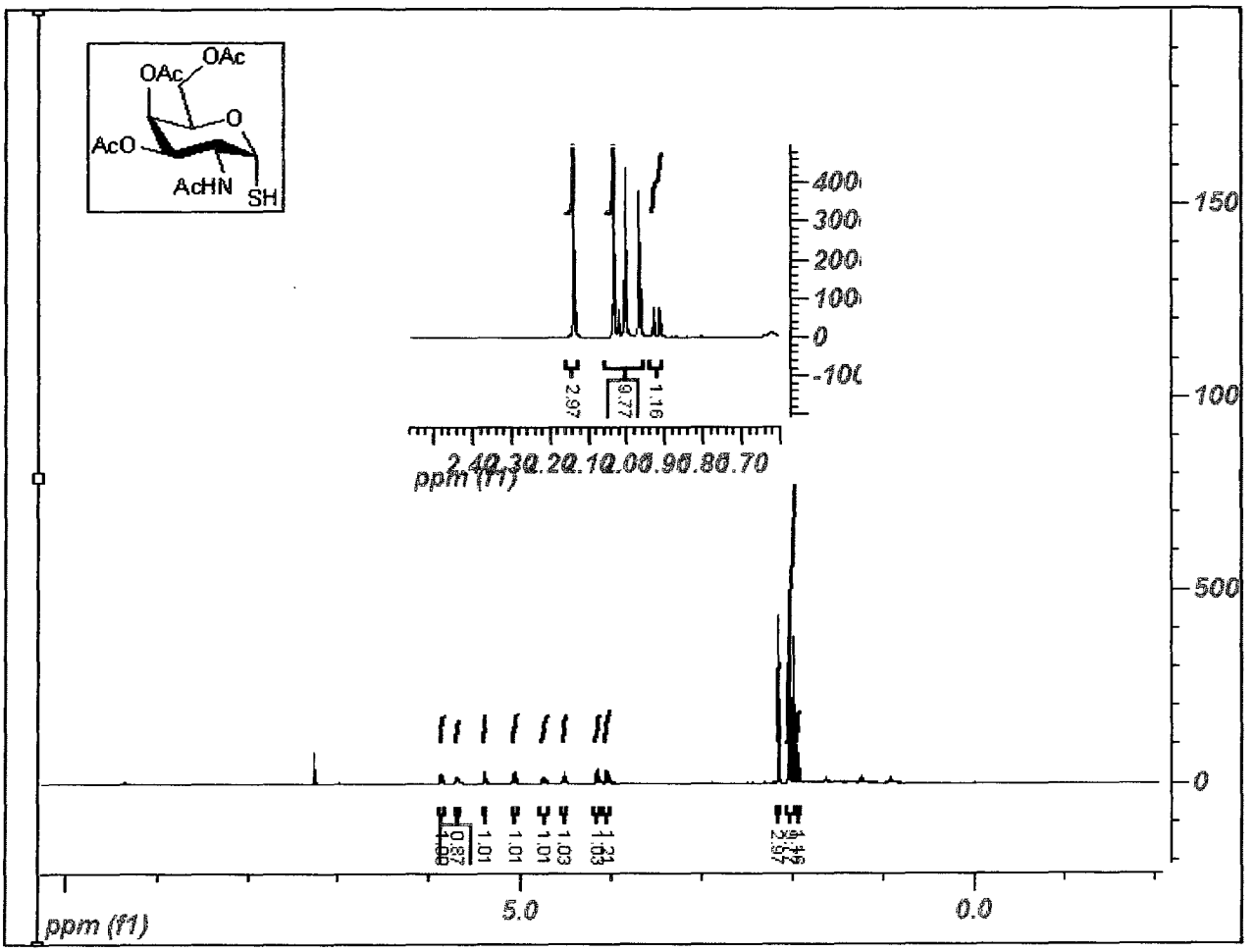
OAc
OAc
O
AcO
AcHN
SH
ppm (f1)
5.0
0.0

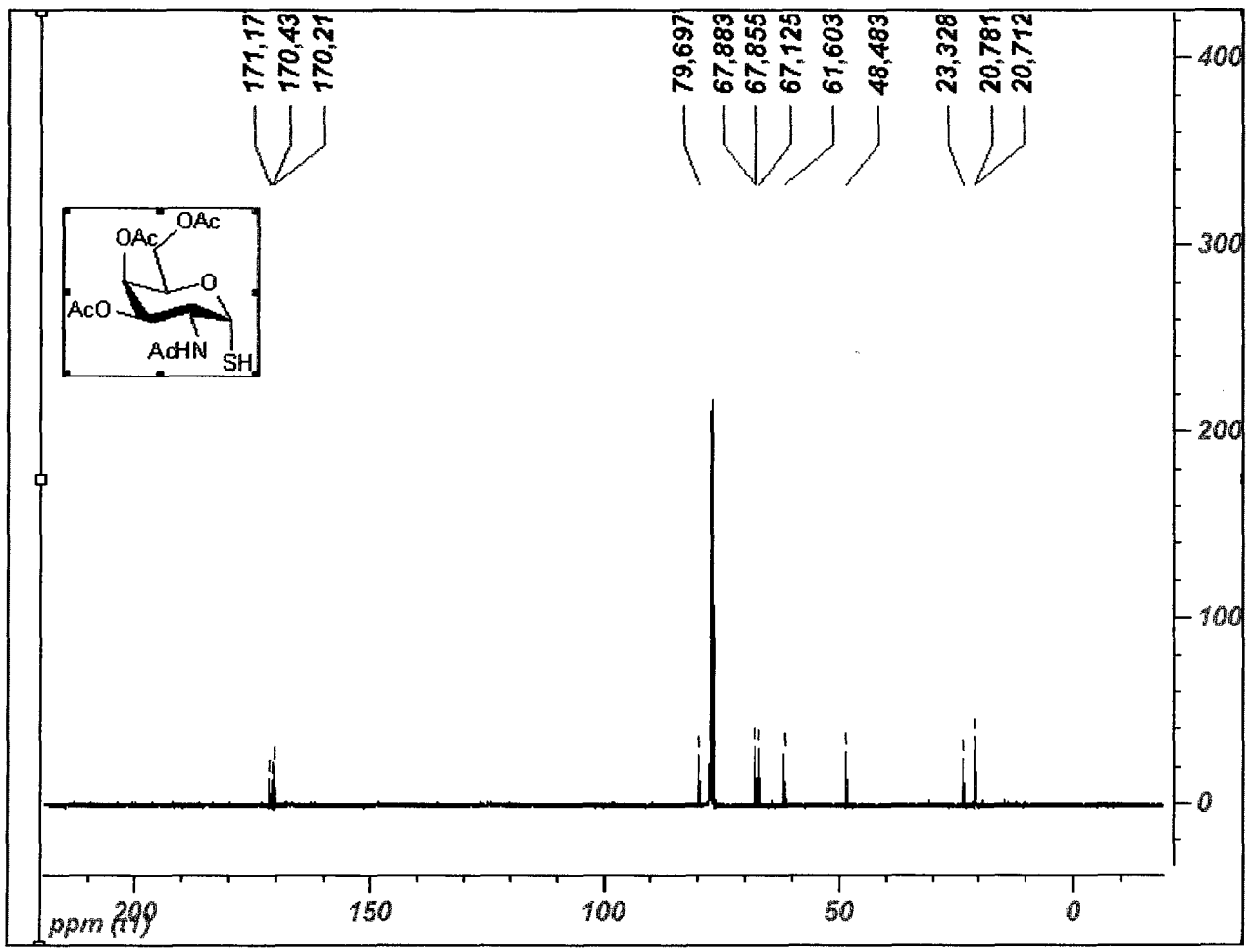
171,17
170,43
170,21
79,697
67,883
67,855
67,125
61,603
48,483
23,328
20,781
20,712
OAc
OAc
O
AcO
AcHN
SH
400
300
200
100
0
ppm (f1)
200
150
100
50
0

XXX

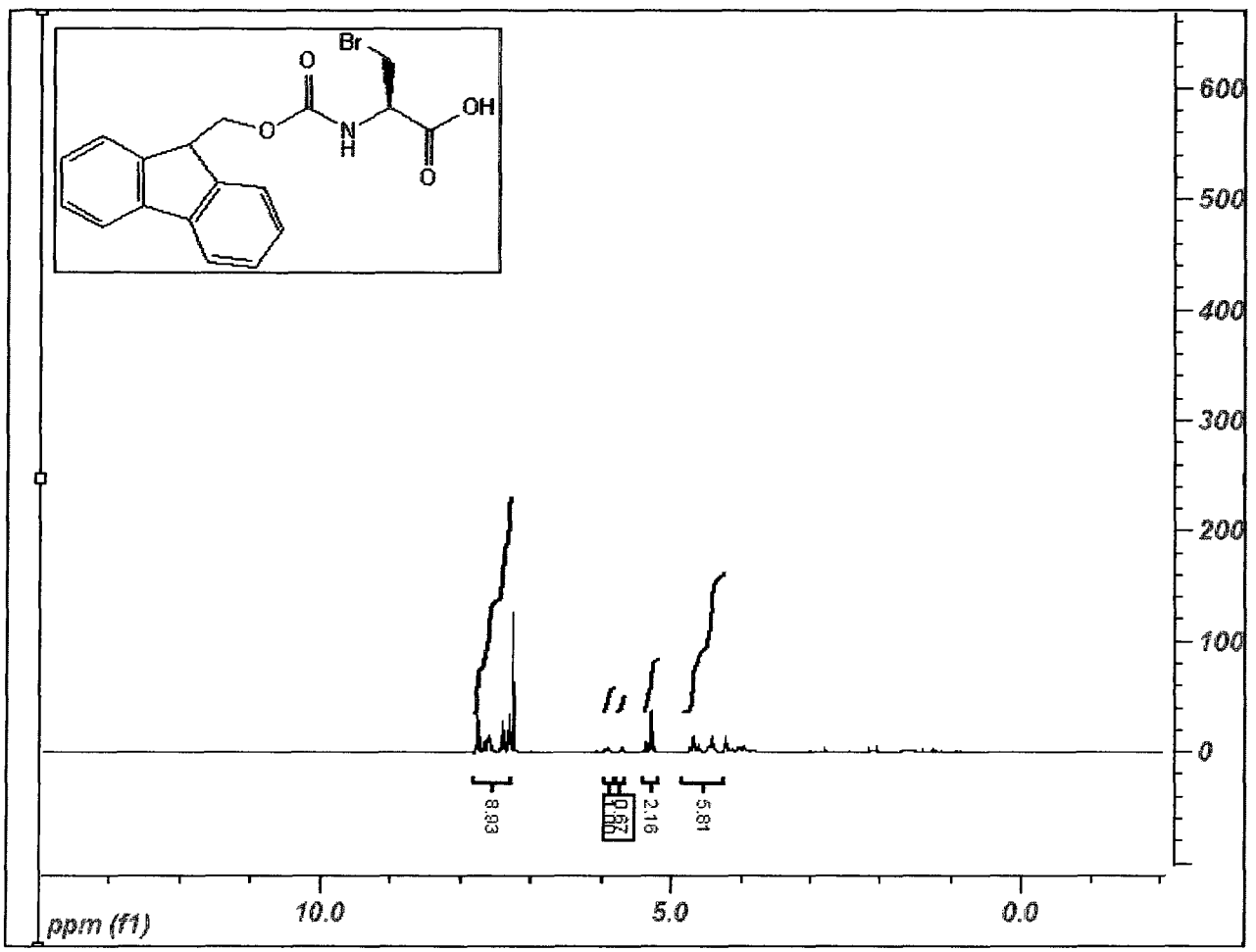
Br
O
O
N
H
OH
O
600
500
400
300
200
100
0
8.93
0.87
2.16
5.81
ppm (f1)
10.0
5.0
0.0

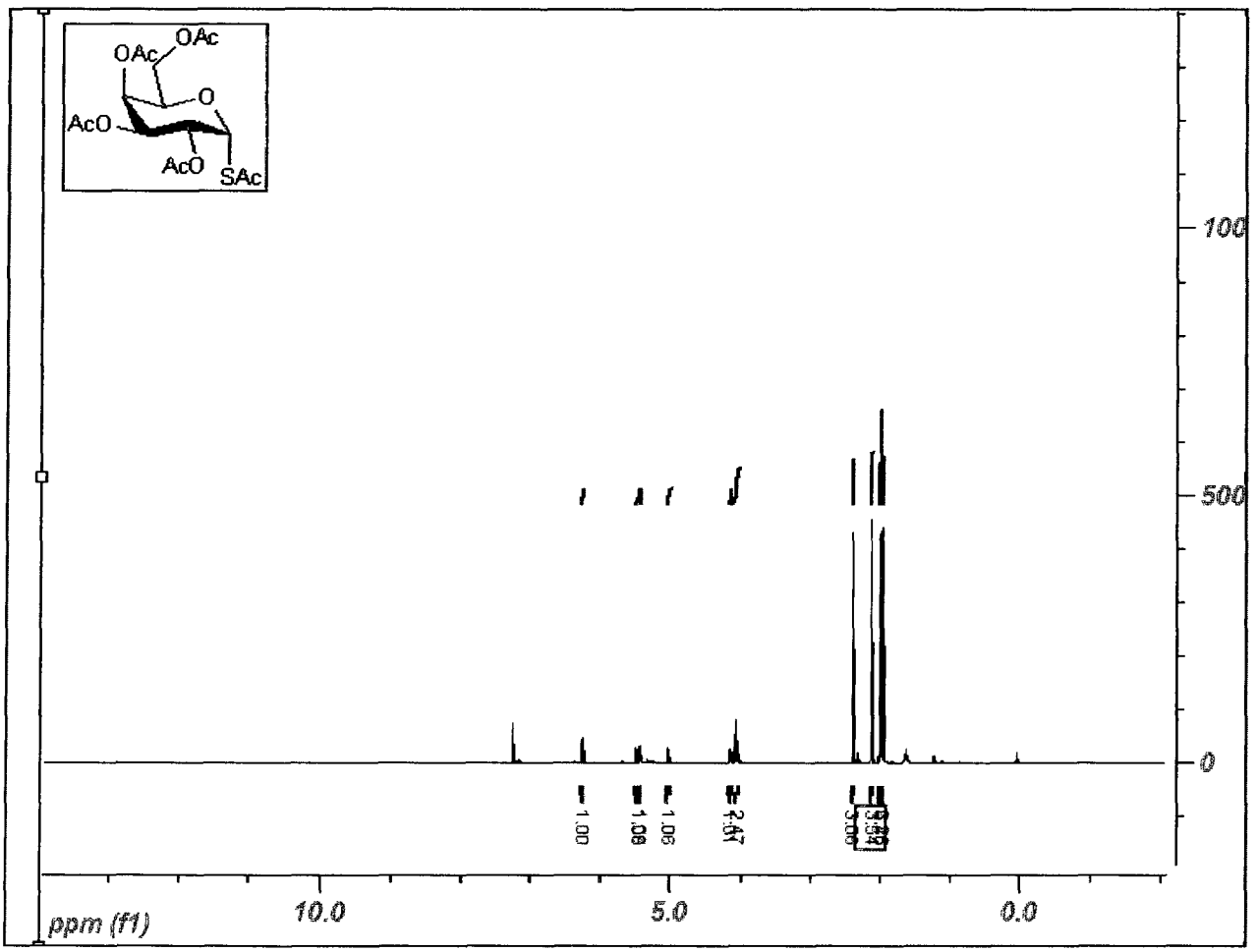
OAc
OAc
O
AcO
AcO
SAc
100
500
0
1.00
1.08
1.06
4.67
3.00
ppm (f1)
10.0
5.0
0.0

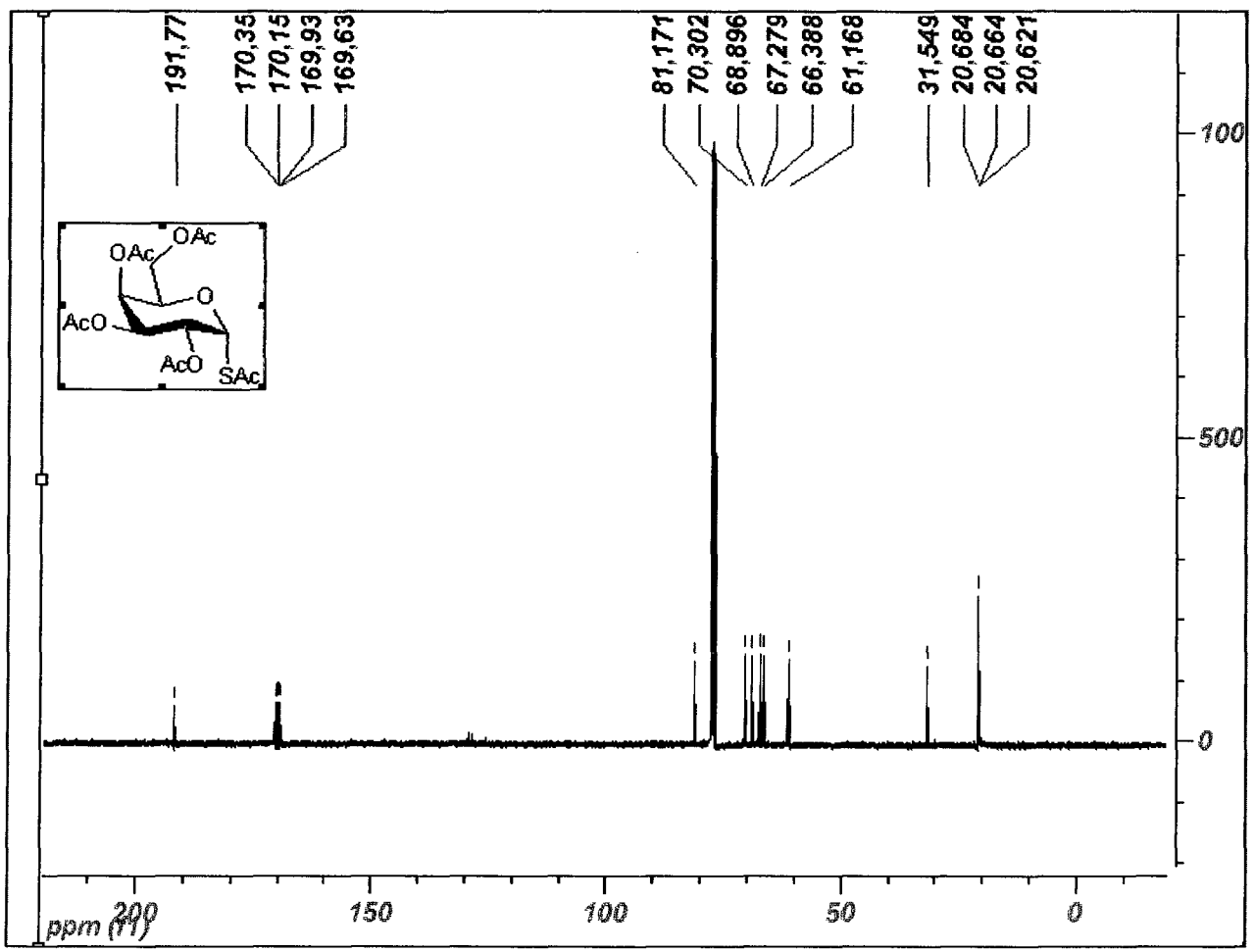
191,77
170,35
170,15
169,93
169,63
81,171
70,302
68,896
67,279
66,388
61,168
31,549
20,684
20,664
20,621
OAc
OAc
O
AcO
AcO
SAc
100
500
0
ppm (f1)
200
150
100
50
0

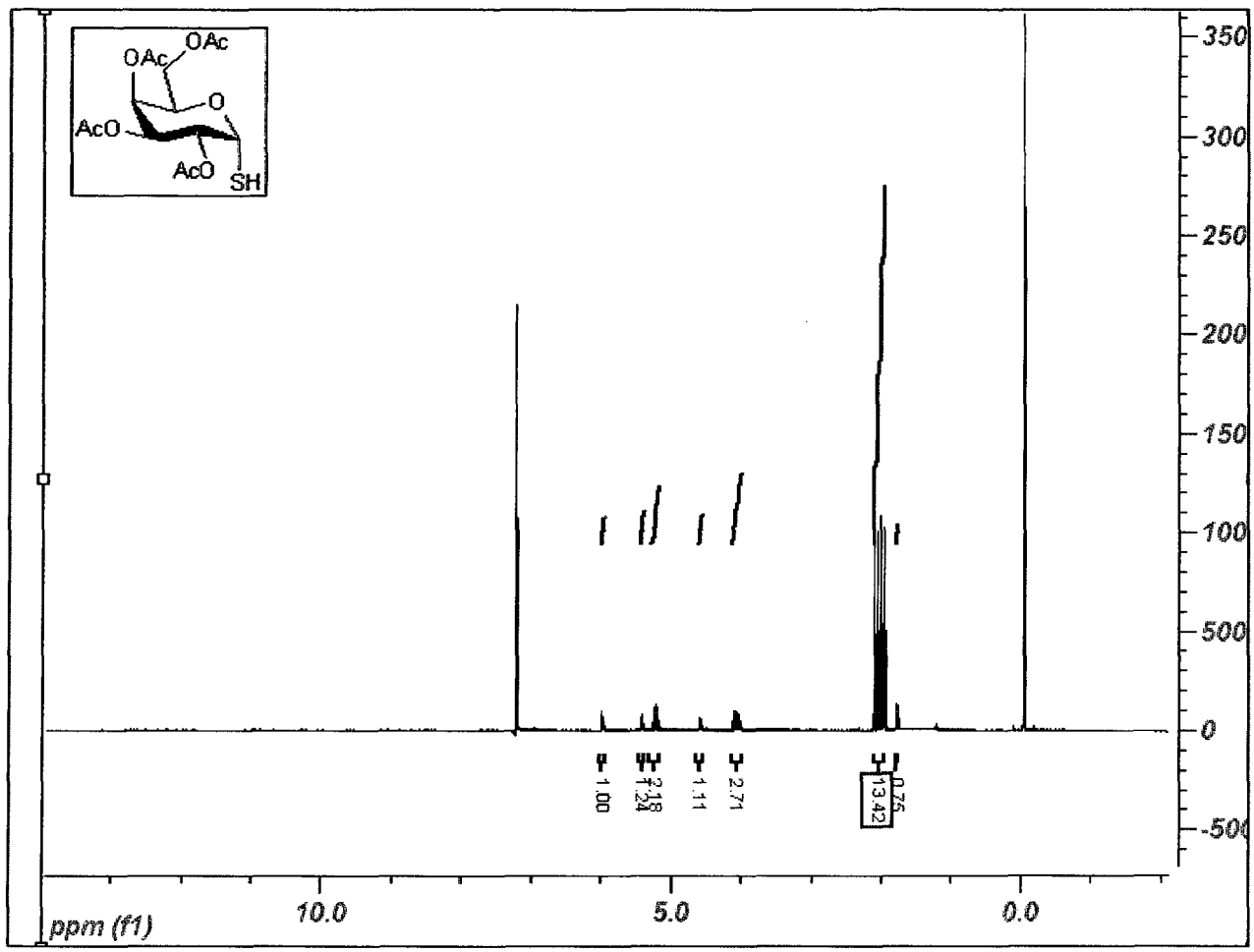
OAc
OAc
O
AcO
AcO
SH
350
300
250
200
150
100
500
0
-500
1.00
2.18
1.24
1.11
2.71
13.42
0.75
ppm (f1)
10.0
5.0
0.0

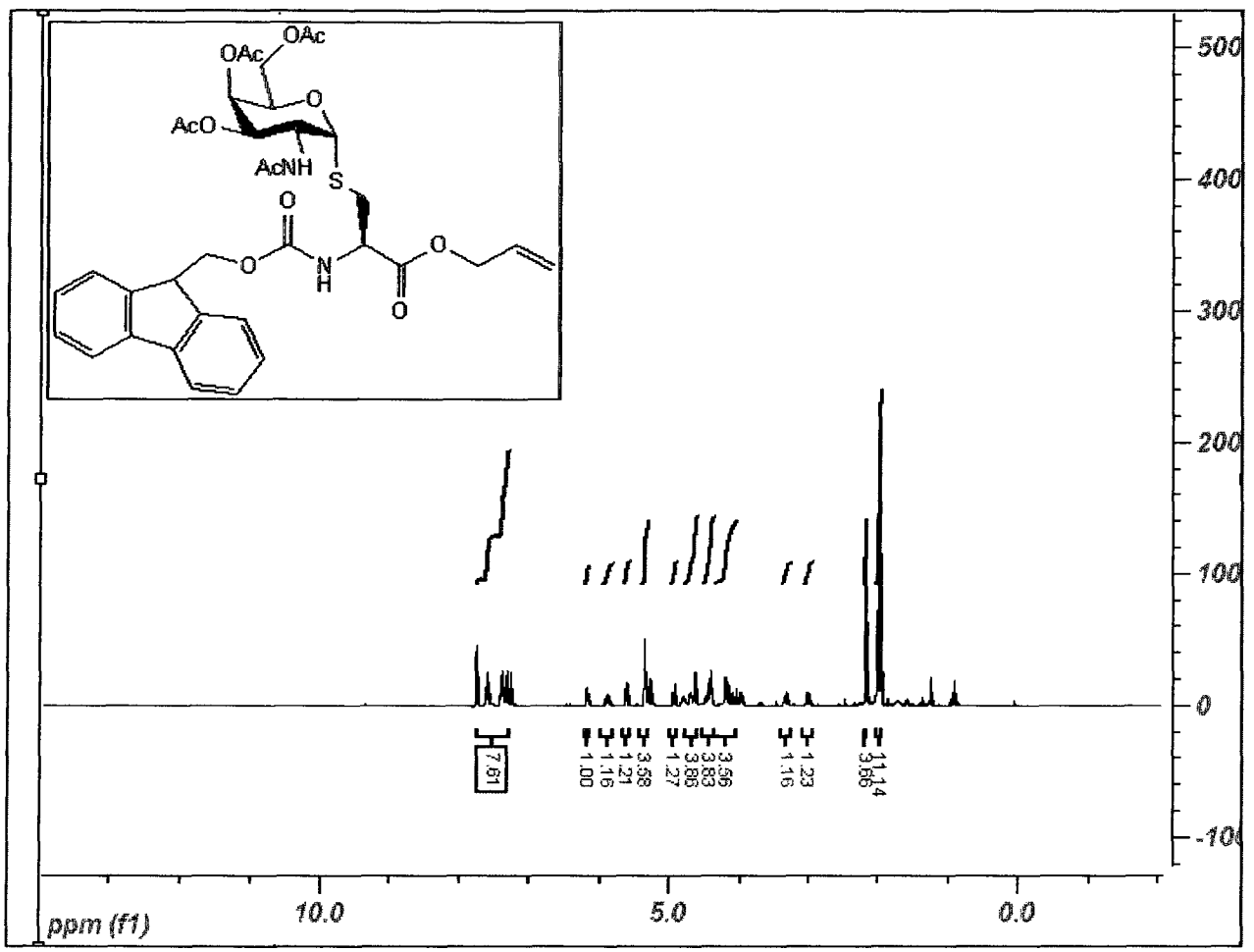
OAc
OAc
AcO
AcNH
O
S
O
N
H
O
O
O
O
500
400
300
200
100
0
-10
7.61
1.00
1.16
1.21
3.58
1.27
3.86
3.83
3.56
1.16
1.23
3.66
11.14
ppm (f1)
10.0
5.0
0.0

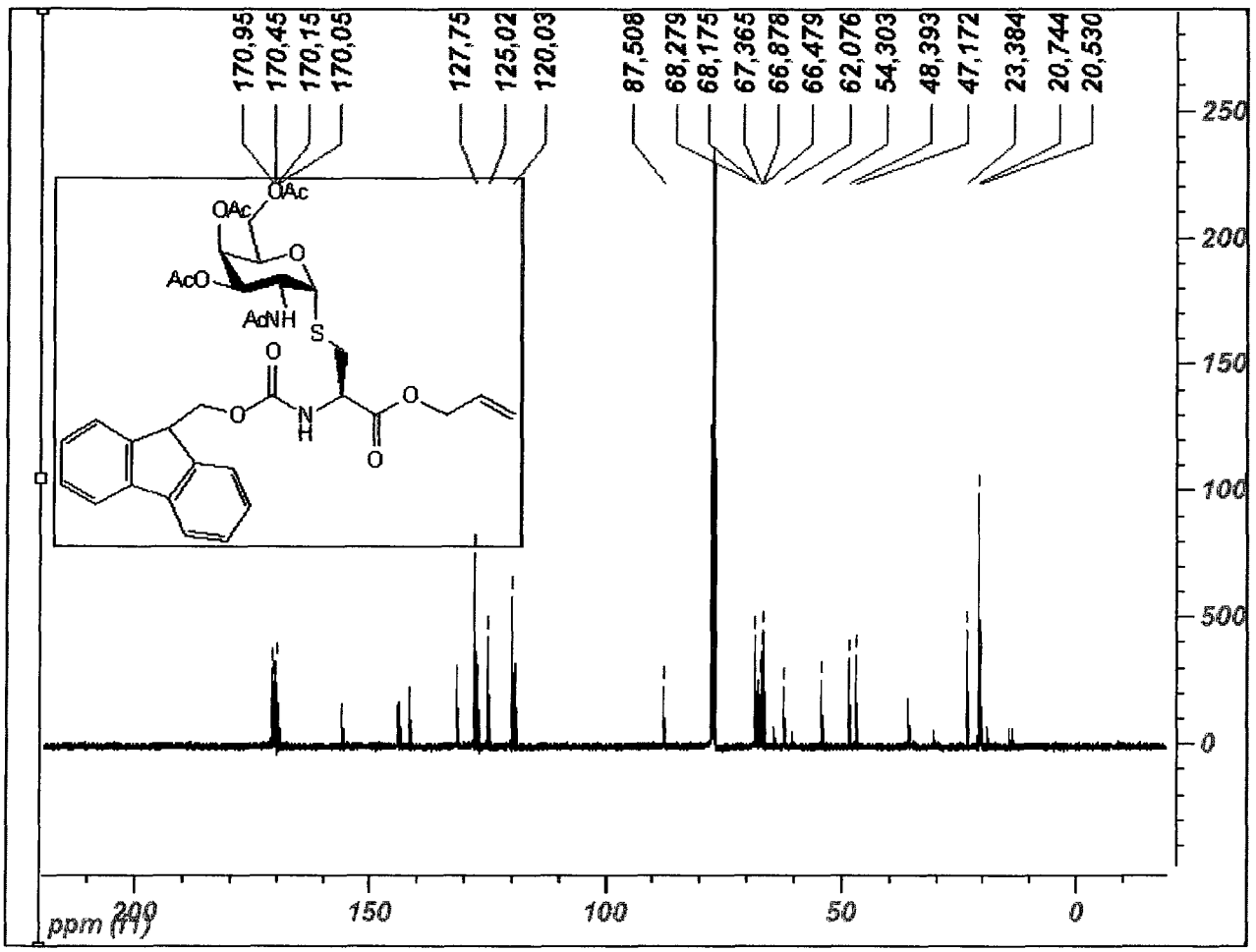
170,95
170,45
170,15
170,05
127,75
125,02
120,03
87,508
68,279
68,175
67,365
66,878
66,479
62,076
54,303
48,393
47,172
23,384
20,744
20,530
OAc
OAc
OAc
O
AcO
AcNH
S
O
O
N
H
O
O
O
250
200
150
100
500
0
ppm (f1)
200
150
100
50
0

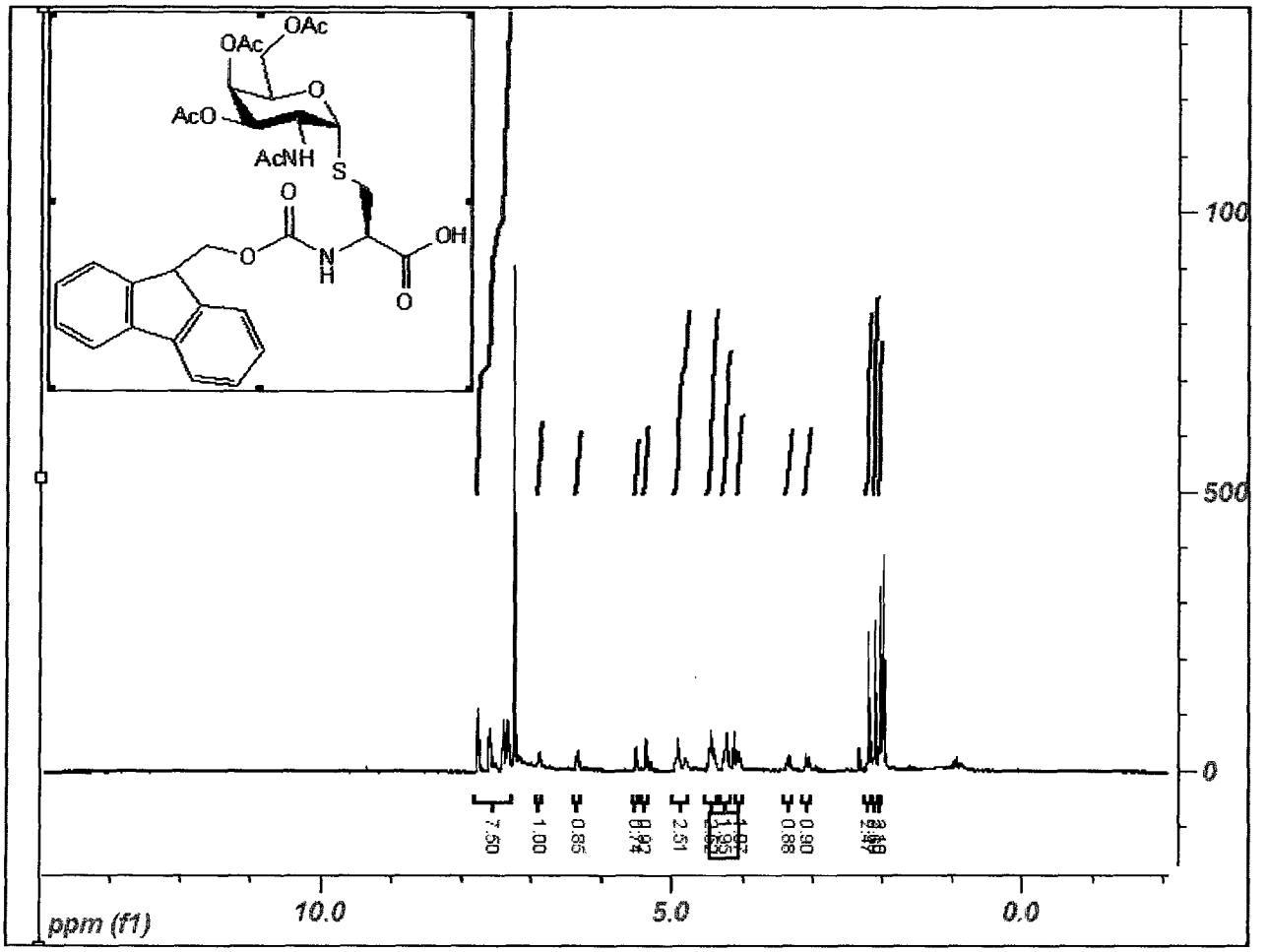
OAc
OAc
O
AcO
AcNH
S
O
O
N
H
OH
O
100
500
0
7.50
1.00
0.85
0.92
2.51
1.07
0.90
0.88
ppm (f1)
10.0
5.0
0.0

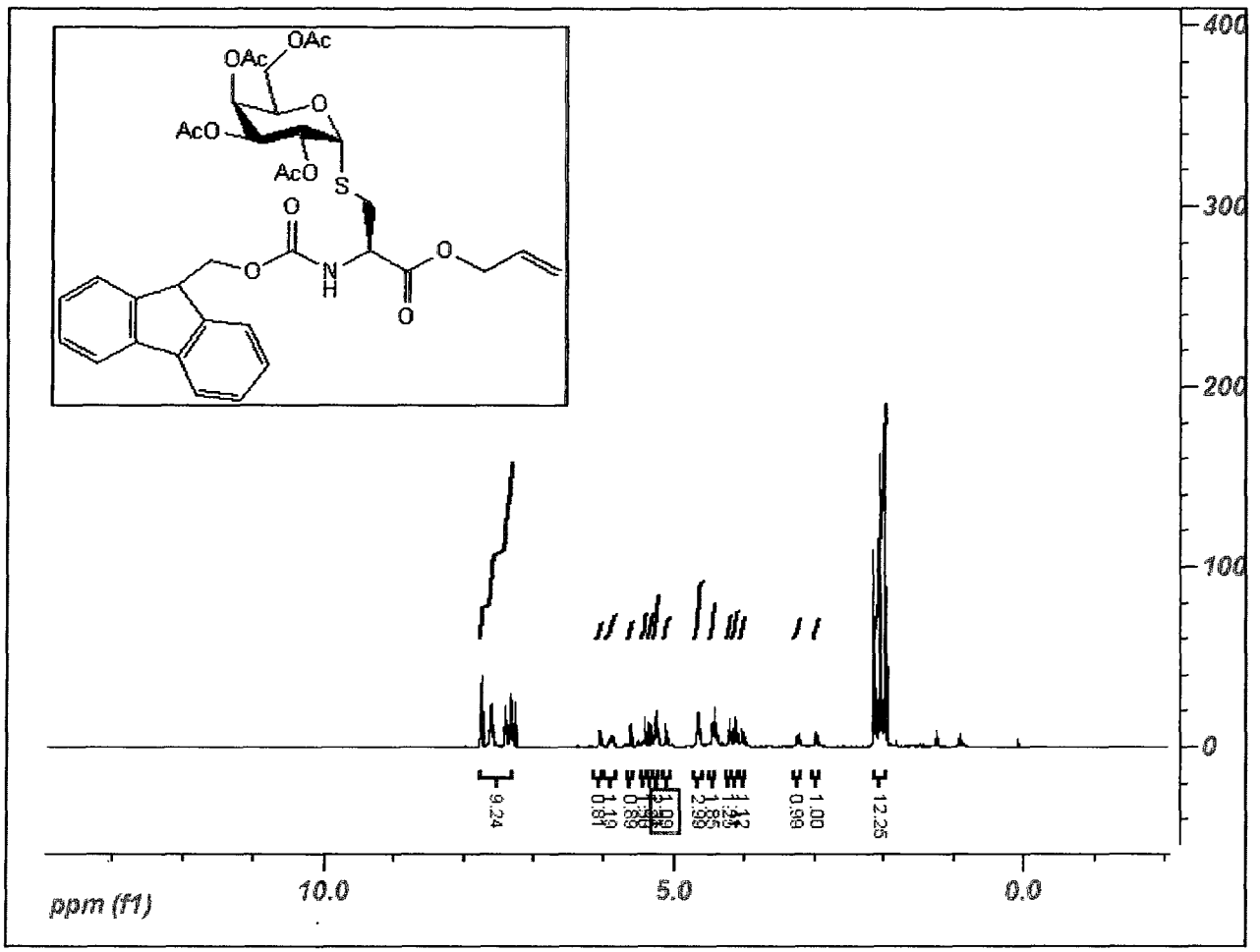
OAc
OAc
AcO
AcO
O
S
O
O
N
H
O
O
O
400
300
200
100
0
9.24
0.81
1.00
0.99
12.25
ppm (f1)
10.0
5.0
0.0

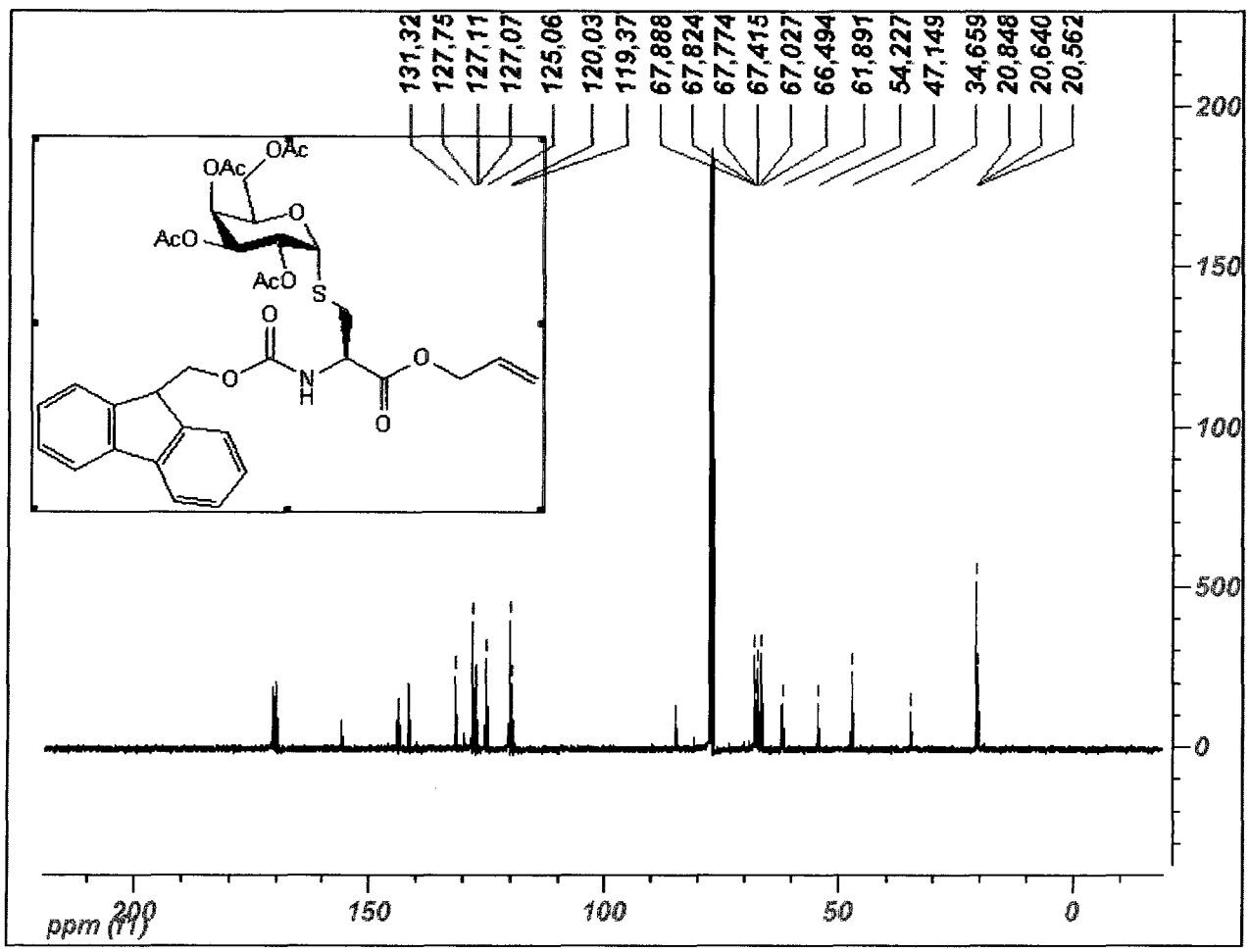
131,32
127,75
127,11
127,07
125,06
120,03
119,37
67,888
67,824
67,774
67,415
67,027
66,494
61,891
54,227
47,149
34,659
20,848
20,640
20,562
OAc
OAc
AcO
AcO
O
S
N
H
200
150
100
500
0
ppm (f1)
200
150
100
50
0

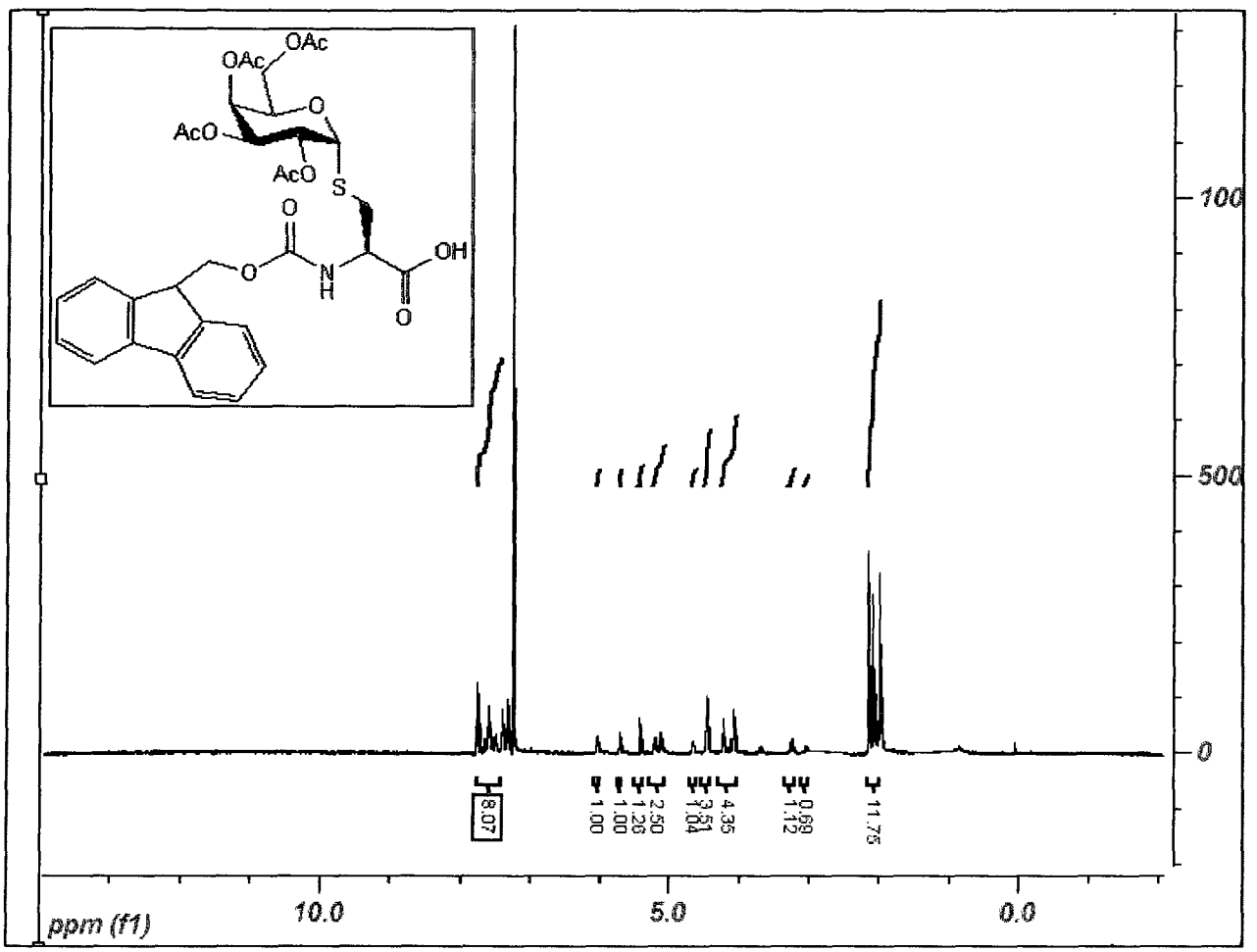
OAc
OAc
AcO
AcO
O
S
O
O
N
H
OH
O
100
500
0
8.07
1.00
1.00
1.26
2.50
3.51
3.64
4.35
0.69
1.12
11.75
ppm (f1)
10.0
5.0
0.0

XL

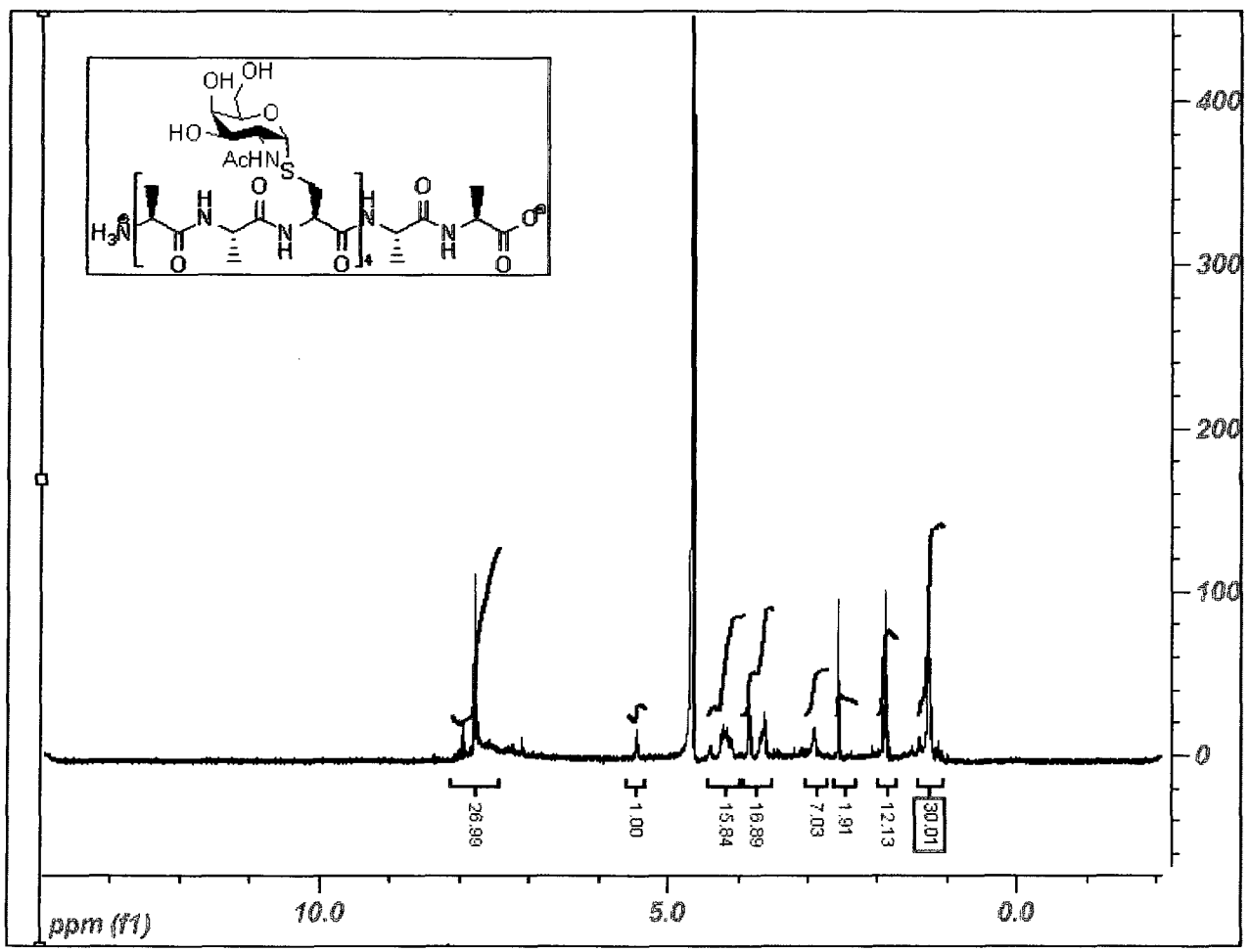
OH
OH
O
HO
AcHN
S
H3N
HN
O
NH
O
4
O
O
400
300
200
100
0
26.89
1.00
15.84
16.89
7.03
1.91
12.13
30.01
ppm (f1)
10.0
5.0
0.0

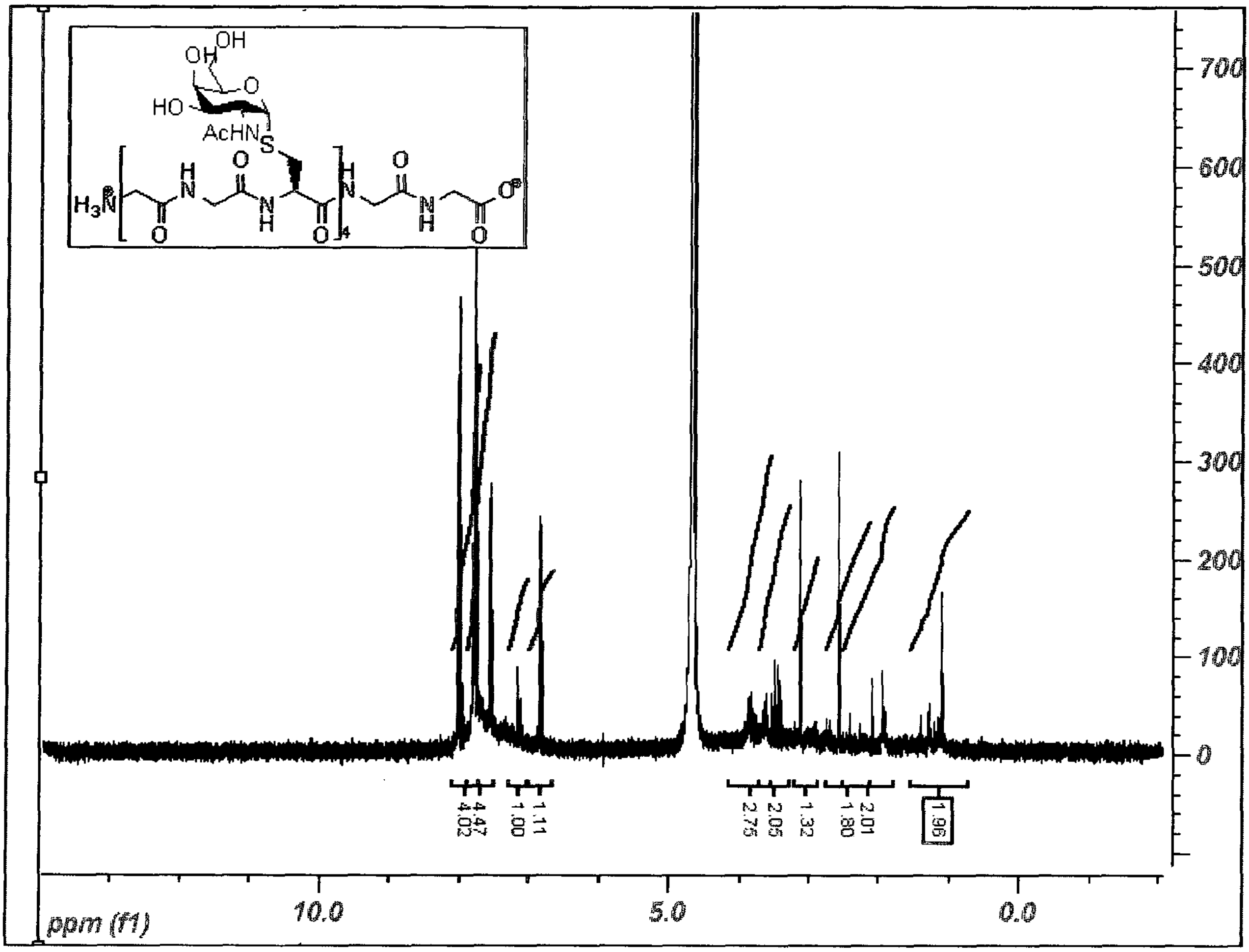

H3N
AcHN
HO
OH
OH
O
S
4
700
600
500
400
300
200
100
0
4.02
4.47
1.00
1.11
2.75
2.05
1.32
1.80
2.01
1.96
ppm (f1)
10.0
5.0
0.0

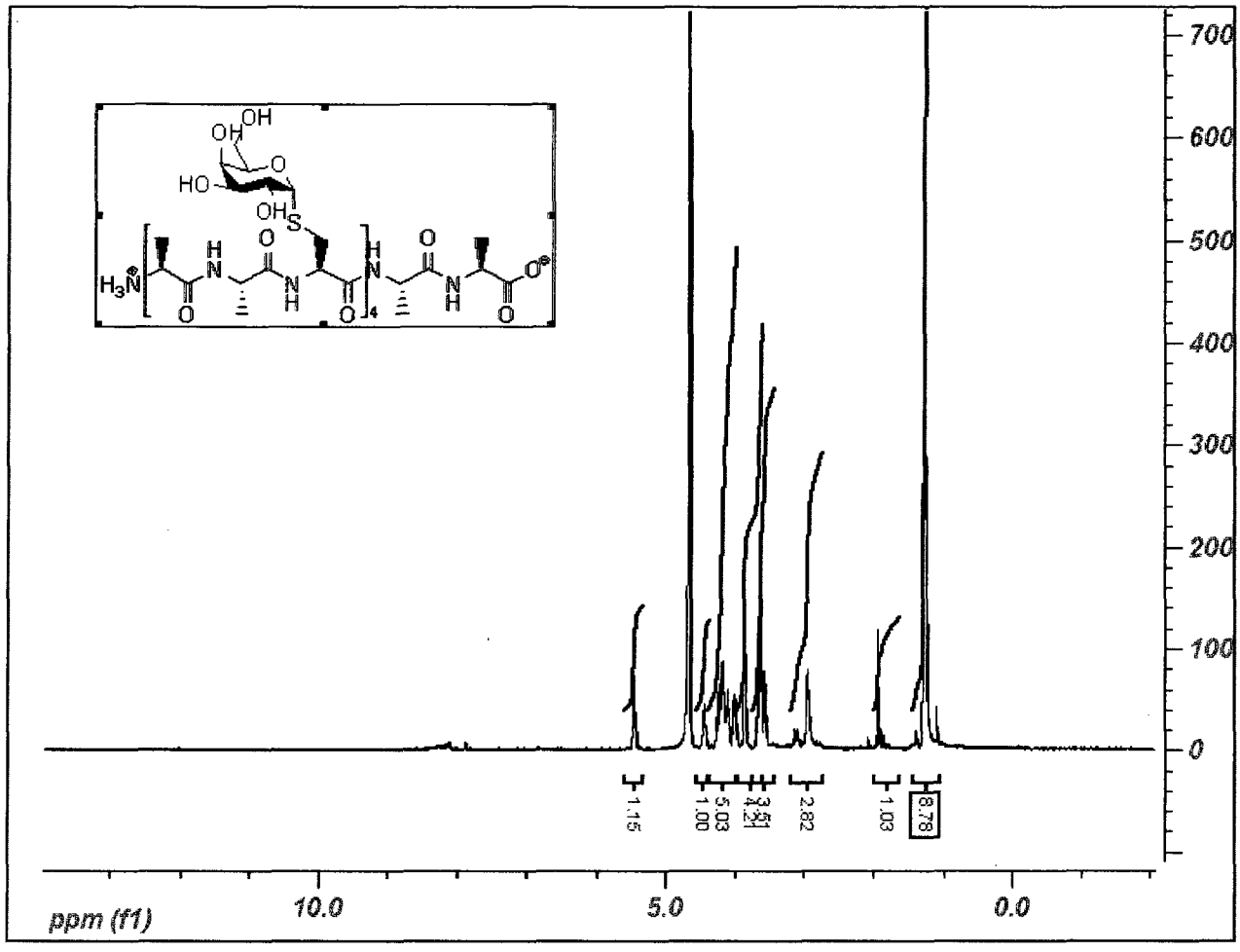
700
600
500
400
300
200
100
0
1.15
1.00
5.03
4.21
3.51
2.82
1.03
8.78
ppm (f1)
10.0
5.0
0.0

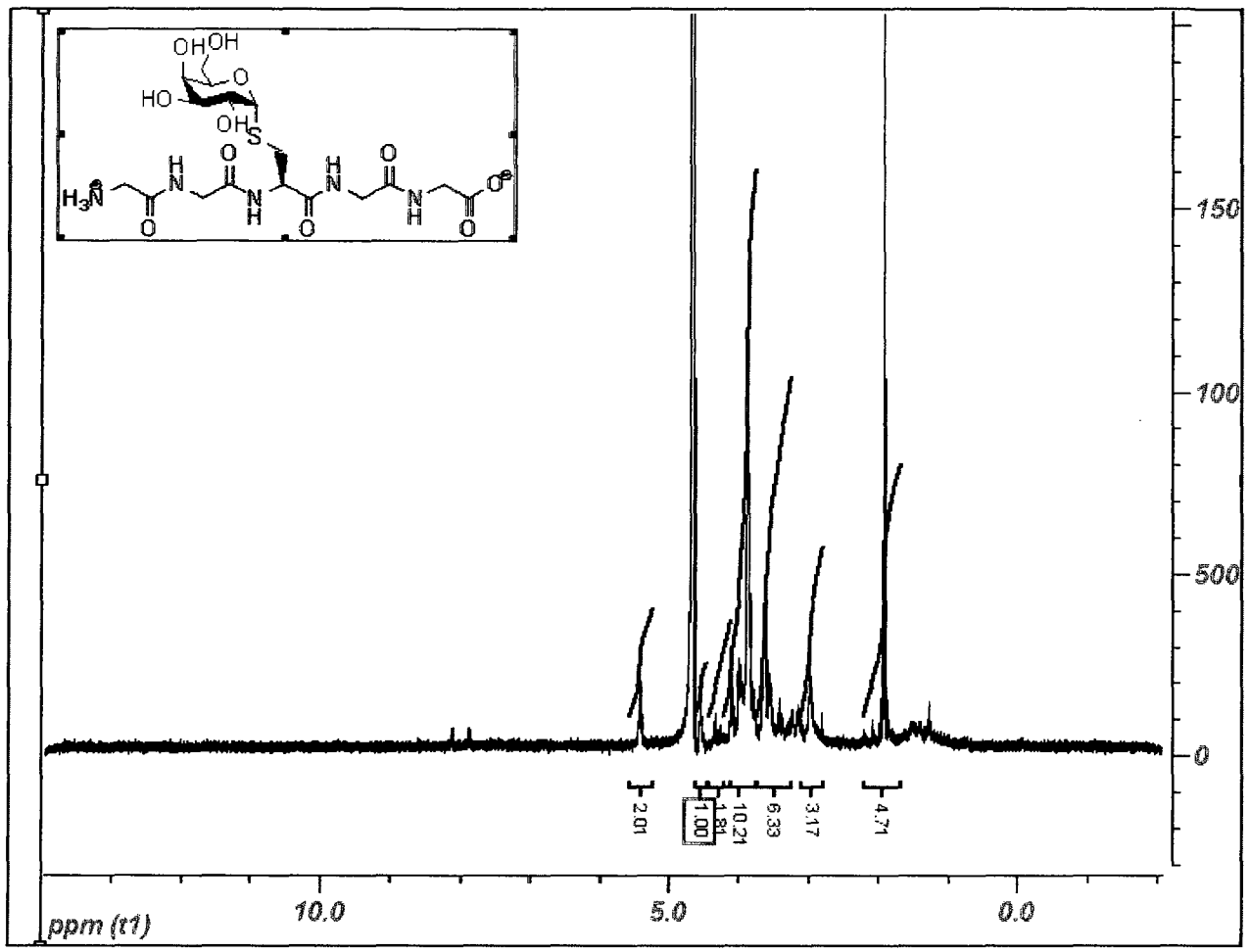
OH
OH
O
HO
OH
S
H3N
HN
O
N
H
O
HN
O
N
H
O
O
O
150
100
500
0
2.01
1.00
1.84
10.21
6.33
3.17
4.71
ppm (t1)
10.0
5.0
0.0